European Society
ESGAR
Gastrointestinal and Abdominal Radiology

Insights into Imaging

Education and strategies in European radiology

ESGAR 2016 Book of Abstracts / Volume 7 / Supplement 2 / June 2016

ESGAR 2016 / June 14 – 17 / Prague, Czech Republic
27th Annual Meeting and Postgraduate Course

ESR
European Society of Radiology

European Society
ESGAR
Gastrointestinal and Abdominal Radiology

JUNE 14 - 17

ESGAR 2016

PRAGUE
CZECH REPUBLIC

European Society of Gastrointestinal and Abdominal Radiology

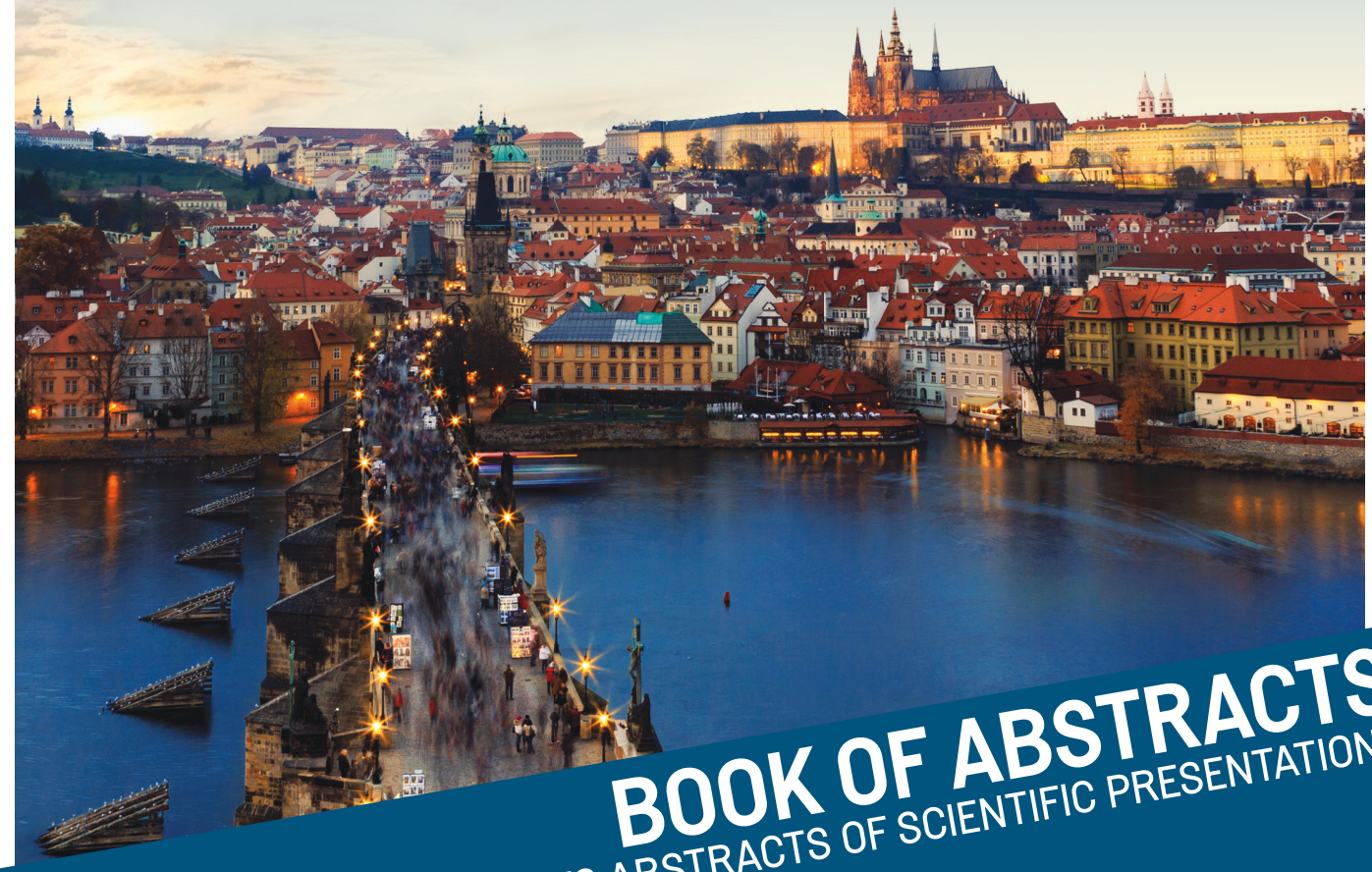

BOOK OF ABSTRACTS

INCLUDES ABSTRACTS OF SCIENTIFIC PRESENTATIONS

IMPORTANT ADDRESSES

ORGANISING SECRETARIAT

Central ESGAR Office
Neutorgasse 9
AT – 1010 Vienna, Austria
Phone: +43 1 535 89 27
Fax: +43 1 535 89 27 -15
E-Mail: office@esgar.org

WEBSITE

www.esgar.org

CONFERENCE VENUE

Prague Congress Centre PCC
5. Kvetna 65
CZ – 140 21 Prague, Czech Republic

CME CREDITS

The 'ESGAR - THE EUROPEAN SOCIETY OF GASTROINTESTINAL AND ABDOMINAL RADIOLOGY' (or) 'ESGAR 2016 - 27th ESGAR Annual Meeting and Postgraduate Course' is accredited by the European Accreditation Council for Continuing Medical Education (EACCME) to provide the following CME activity for medical specialists. The EACCME is an institution of the European Union of Medical Specialists (UEMS), www.uems.net.

The 'ESGAR 2016 - 27th ESGAR Annual Meeting and Postgraduate Course' is designated for a maximum of (or 'for up to') 24 hours of European external CME credits. Each medical specialist should claim only those hours of credit that he/she actually spent in the educational activity.

JOINT SESSION

European Society of Urogenital Radiology

SPONSORS

ESGAR wishes to gratefully acknowledge the support of its Corporate Members:

The Final Programme of ESGAR 2016 is available on the ESGAR Website www.esgar.org

Date of publishing: June 2016

DOI 10.1007/s13244-016-0502-9

TABLE OF CONTENTS

ESGAR EXECUTIVE COMMITTEE

PRESIDENT
C. Matos (Lisbon/PT)

PRESIDENT-ELECT
S. Halligan (London/GB)

VICE PRESIDENT
R.G.H. Beets-Tan (Amsterdam/NL)

SECRETARY
A. Palkó (Szeged/HU)

TREASURER
S.A. Jackson (Plymouth/GB)

PAST PRESIDENT
L. Martí-Bonmatí (Valencia/ES)

EDUCATION COMMITTEE
R.G.H. Beets-Tan (Amsterdam/NL)

MEMBERSHIP COMMITTEE
T. Helmberger (Munich/DE)

WORKSHOP COMMITTEE
G. Brancatelli (Palermo/IT)

MEETING PRESIDENT
V. Valek (Brno/CZ)

PRE-MEETING PRESIDENT
P. Prassopoulos (Alexandroupolis/GR)

PRE-PRE-MEETING PRESIDENT
H. Fenlon (Dublin/IE)

PAST MEETING PRESIDENT
Y. Menu (Paris/FR)

MEMBERS AT LARGE
A. Laghi (Latina/IT)
J. Stoker (Amsterdam/NL)
M. Zins (Paris/FR)

ESGAR EXECUTIVE DIRECTOR
B. Lindlbauer (Vienna/AT)

LANGUAGE ABSTRACT EDITOR

S.A. Jackson (Plymouth/GB)

ESGAR 2016 MEETING PRESIDENT

Prof. Vlastimil Valek
Masaryk University
University Hospital Brno and Medical Faculty
Department of Radiology
Jihlavská 20
CZ – 639 00 Brno, Czech Republic

ESGAR 2016 PROGRAMME COMMITTEE

CHAIRMAN
L. Martí-Bonmatí (Valencia/ES)

MEMBERS
R.G.H. Beets-Tan (Amsterdam/NL)
G. Brancatelli (Palermo/IT)
H. Fenlon (Dublin/IE)
S. Halligan (London/GB)
T. Helmberger (Munich/DE)
S.A. Jackson (Plymouth/GB)
A. Laghi (Latina/IT)
C. Matos (Lisbon/PT)
Y. Menu (Paris/FR)
A. Palkó (Szeged/HU)
P. Prassopoulos (Alexandroupolis/GR)
J. Stoker (Amsterdam/NL)
V. Valek (Brno/CZ)
M. Zins (Paris/FR)

ESGAR 2016 LOCAL ORGANISING COMMITTEE

T. Andrašina (Brno/CZ)
P. Dvořák (Hradec Králové/CZ)
H. Dvořáková (Prague/CZ)
J. Ferda (Plzeň/CZ)
M. Hazlinger (Olomouc/CZ)
J. Hořejš (Prague/CZ)
V. Lehotská (Bratislava/SK)
J. Křístek (Brno/CZ)
H. Petrášová (Brno/CZ)
J. Votrubová (Prague/CZ)
J. Weichet (Prague/CZ)

D. Akata (Ankara/TR)
O. Akhan (Ankara/TR)
C. Aubé (Angers/FR)
C. Ayuso (Barcelona/ES)
M. Bali (London/GB)
I. Bargellini (Pisa/IT)
T.V. Bartolotta (Palermo/IT)
A. Ba-Ssalamah (Vienna/AT)
R.G.H. Beets-Tan (Amsterdam/NL)
E. Biscaldi (Genova/IT)
A. Blachar (Tel Aviv/IL)
L. Blomqvist (Stockholm/SE)
P. Boraschi (Pisa/IT)
R. Bouzas (Vigo/ES)
G. Brancatelli (Palermo/IT)
D. Breen (Southampton/GB)
D. Burling (Harrow/GB)
V. Cantisani (Rome/IT)
F. Caseiro Alves (Coimbra/PT)
C. Catalano (Rome/IT)
J. Cazejust (Paris/FR)
N. Courcoutsakis (Alexandroupolis/GR)
L. Crocetti (Pisa/IT)
L. Curvo-Semedo (Coimbra/PT)
C.N. De Cecco (Latina/IT)
E. Delabrousse (Besançon/FR)
R. Dondelinger (Liège/BE)
M. D'Onofrio (Verona/IT)
N. Elmas (Izmir/TR)
H. Fenlon (Dublin/IE)
A. Filippone (Chieti/IT)
N. Flor (Milan/IT)
B. Fox (Plymouth/GB)
A.H. Freeman (Cambridge/GB)
A. Furlan (Pittsburgh, PA/US)
B. Gallix (Montpellier/FR)
Y. Gandon (Rennes/FR)
V. Goh (London/GB)
M. Gollub (New York, NY/US)
S. Gourtsoyianni (London/GB)
S. Gryspeerdt (Roeselare/BE)
L. Guimaraes (Porto/PT)
J.A. Guthrie (Leeds/GB)
S. Halligan (London/GB)
A. Hatzidakis (Heraklion/GR)
T. Helmberger (Munich/DE)
R.-T. Hoffmann (Dresden/DE)
P. Huppert (Darmstadt/DE)
F. Iafrate (Rome/IT)
S.A. Jackson (Plymouth/GB)
M. Karcaaltincaba (Ankara/TR)
N. Kartalis (Stockholm/SE)
S. Kim (Busan/KR)
M. Krokidis (Cambridge/GB)
H.-U. Laasch (Manchester/GB)
A. Laghi (Latina/IT)
D. Lambregts (Amsterdam/NL)
J. Lameris (Amsterdam/NL)
M. Laniado (Dresden/DE)
T. Lauenstein (Essen/DE)
J.M. Lee (Seoul/KR)
P. Lefere (Roeselare/BE)
M. Lewin (Paris/FR)
D.J. Lomas (Cambridge/GB)
A. Luciani (Creteil/FR)
O. Lucidarme (Paris/FR)
M. Maas (Maastricht/NL)
F. Maccioni (Rome/IT)
A.J. Madureira (Porto/PT)
M. Maher (Cork/IE)
D. Malone (Dublin/IE)
R. Manfredi (Verona/IT)
T. Mang (Vienna/AT)
V. Maniatis (Aabenraa/DK)
D. Marin (Durham, NC/US)
B. Marincek (Cleveland, OH/US)
L. Martí-Bonmatí (Valencia/ES)
D.F. Martin (Manchester/GB)
C. Matos (Lisbon/PT)
R.M. Mendelson (Perth, WA/AU)
Y. Menu (Paris/FR)
G. Morana (Treviso/IT)
M. Morrin (Dublin/IE)
G.H. Mostbeck (Vienna/AT)
E. Neri (Pisa/IT)
B. Op De Beeck (Edegem/BE)
A. Palkó (Szeged/HU)
P. Paolantonio (Rome/IT)
N. Papanikolaou (Stockholm/SE)
P. Pereira (Heilbronn/DE)
P. Pokieser (Vienna/AT)
R. Pozzi Mucelli (Verona/IT)
P. Prassopoulos (Alexandroupolis/GR)
M. Puckett (Torquay/GB)
J. Puig Domingo (Sabadell/ES)
E. Quaia (Trieste/IT)
M. Rengo (Latina/IT)
C. Ridereau-Zins (Angers/FR)
G.A. Rollandi (Genova/IT)
S. Romano (Naples/IT)
M. Ronot (Clichy/FR)
L.H. Ros Mendoza (Zaragoza/ES)
E.J. Rummeny (Munich/DE)
W. Schima (Vienna/AT)
S. Schmidt (Lausanne/CH)
A.G. Schreyer (Regensburg/DE)
O. Seror (Bondy/FR)
S. Skehan (Dublin/IE)

S. Somers (Dundas, ON/CA)
M. Staunton (Cork/IE)
S. Stojanovic (Novi Sad/RS)
J. Stoker (Amsterdam/NL)
C. Stroszczynski (Regensburg/DE)
Z. Tarjan (Coventry/GB)
J.-P. Tasu (Poitiers/FR)
S.A. Taylor (London/GB)
S. Terraz (Geneva/CH)
D. Tolan (Leeds/GB)
A. Torregrosa Andres (Valencia/ES)
C. Triantopoulou (Athens/GR)
V. Valek (Brno/CZ)
B. Van Beers (Clichy/FR)
V. Vilgrain (Clichy/FR)
J. Votrubová (Prague/CZ)
M.-P. Vullierme (Clichy/FR)
D. Weishaupt (Zurich/CH)
S.D. Yarmenitis (Athens/GR)
G. Zamboni (Verona/IT)
C.J. Zech (Basel/CH)
M. Zins (Paris/FR)


European Society
ESGAR
Gastrointestinal and Abdominal Radiology

11:00 - 12:30 **Congress Hall**

Scientific Session SS 1

Pancreas: technical advances in tumour imaging

SS 1.1

Prediction of pancreatic neuroendocrine tumor grade with MR imaging features: added value of diffusion-weighted imaging

M. Ronot[1], E. Lotfalizadeh[1], M. Wagner[2], W. Allaham[1], M.-P. Vullierme[1], V. Vilgrain[1]; [1]Clichy/FR, [2]Paris/FR

Purpose: To evaluate the value of MRI including diffusion-weighted imaging (DWI) for the grading of pancreatic neuroendocrine tumors (pNET).

Material and methods: Between 2006 and 2014, all patients with resected pNETs with preoperative MRI including DWI were included. Tumor grading was based on the 2010 WHO classification (G1-3). MRI features including size, T1w and T2w signal intensity, enhancement pattern, apparent (ADC) and true diffusion (D) coefficients were reported.

Results: 108 pNETs (mean 40±33mm) were evaluated in 94 patients (48 women, 51%, mean 52±12yo). Fifty-five (51%), 42 (39%), and 11 (10%) tumors were G1, G2 and G3, respectively. Mean ADC and D values were significantly lower as grade increased (ADC: 2.13±0.70, 1.78±0.72, and 0.86±0.22 10-3 mm^2/s for G1, G2 and G3; D: 1.92±0.70, 1.75±0.74, and 0.82±0.19 10-3 mm^2/s for G1, G2 and G3, all $p<0.01$). pNETs with hypo/iso-signal intensity on arterial ($p<0.001$), portal venous ($p<0.001$), and delayed phase images ($p=0.005$), and larger size ($p<0.001$) were more likely to be G3. The area under the curve of ADC and D to differentiation between G3 and G1-2 were 0.96±0.02 and 0.95±0.02 ($p<0.001$). The best cutoff values for ADC and D for the identification of G3 were 1.19 10-3mm2/s (sensitivity 100%, specificity 92%), and 1.04 10-3mm2/s (sensitivity 82%, specificity 92%), respectively.

Conclusion: Morphological and functional MRI features of pNETS depend on tumor grade. DWI is useful for the identification of high-grade tumors.

SS 1.2

Advanced pancreatic adenocarcinoma: CT evaluation before and after neoadjuvant treatment with fluorouracil, leucovorin, oxaliplatin and irinotecan and correlation with histopathology

E. Boninsegna[1], B. Sureka[2], R. Negrelli[1], V. Di Paola[1], G. Avesani[1], S. Mehrabi[1], R. Manfredi[1], R.M. Pozzi Mucelli[1]; [1]Verona/IT, [2]New Delhi/IN

Purpose: Majority of patients with pancreatic cancer present with metastatic and locally advanced disease at the time of initial diagnosis. The action to control cardiovascular risk in diabetes trial demonstrated that the survival in pancreatic adenocarcinoma treated with neoadjuvant FOLFIRINOX (fluorouracil, leucovorin, oxaliplatin, and irinotecan) is improved when compared with gemcitabine-based regime. We evaluated CT examinations of patients with adenocarcinoma before and after FOLFIRINOX to assess neoplasm modifications; we also compared imaging findings with histopathological results given by surgery or biopsy.

Material and methods: Twenty-two patients with pancreatic adenocarcinoma treated with FOLFIRINOX were enrolled; we evaluated: longest dimension and volume of the neoplasm, density of the lesion, vessels involvement, metastatic lymphnodes, perineural invasion and resectability (according to Americas hepato-pancreato-biliary association guidelines). After FOLFIRINOX every patient underwent exploratory laparotomy with multiple biopsies of peritumoral tissue.

Results: After FOLFIRINOX treatment we observed significant reduction of tumor volume and longest dimension ($p<0,01$); increase of density and vascularisation; reduction of cases with major vessels involvement. In 6/22 patients (27.3%) CT showed vessels encasement but biopsy results were only fibrosis. CT sensitivity and specificity to assess perineural invasion were, respectively, 22% and 86%; CT sensitivity and specificity to evaluate resectability were 92% and 60%. CT did not recognize metastatic lymphnodes.

Conclusion: FOLFIRINOX is a highly effective treatment for advanced pancreatic adenocarcinoma; CT is indicated to evaluate tumor response, but it might underestimate the percentage of successfully resectable patients.

SS 1.3

Correlation between appearance of the retroportal fat plane at preoperative CT and pathology findings in resected adenocarcinoma of the pancreatic head

F. Lombardo, G.A. Zamboni, M.C. Ambrosetti, M. Chincarini, G. Malleo, G. Marchegiani, R.M. Pozzi Mucelli; Verona/IT

Purpose: To correlate the CT and pathology findings in resected adenocarcinomas of the pancreatic head (PDAC).

Material and methods: We included 41 patients with resected PDAC of the pancreatic head (25M, 16F, mean age 65 years). All patients had a multiphasic preoperative MDCT. All cases were re-evaluated at pathology for the state of the retroportal lamina, lymphnode and perineural invasion. CT images were reviewed in consensus by two radiologists for assessment of the fat plane between the pancreatic head and the mesenteric artery and vein: this was graded in 3 categories (clear, effaced, infiltrated). Fisher's test was used to assess the correlation between CT and pathology findings.

Results: A clear fat plane between the pancreatic head and the mesenteric vessels was significantly associated with a negative retroportal lamina at pathology ($p=0.0266$). This was also observed for the plane between the head and the superior mesenteric artery ($p=0.0011$) and the superior mesenteric vein ($p=0.0327$). No different results were observed between effaced and clearly infiltrated fat. No association was observed between the appearance of the fat planes at CT and the presence of lymphnode or perineural invasion (p=n.s.).

Conclusion: A clear fat plane between the pancreatic head and the mesenteric vessels is significantly associated with negative retroportal lamina at pathology. CT is not accurate in predicting perineural or nodal invasion.

SS 1.4

Pancreatic neuroendocrine tumor: prediction of the tumor grade using CT findings and computerized texture analysis

J.H. Kim, T.W. Choi, S.J. Park, J.K. Han; Seoul/KR

Purpose: To investigate the important CT findings and computerized CT texture variables for prediction of grade of pancreatic neuroendocrine tumor (PNET).

Material and methods: 66 patients with pathologically confirmed PNETs (G1=45, G2/3=21) underwent preoperative contrast-enhanced CT. Two reviewers determined the presence of predefined CT findings. Computerized CT texture was also analyzed on arterial (AP) and portal phase (PP) using both 2D and 3D analysis. Multivariate logistic regression analysis was performed to identify significant predictors for tumor grade.

Results: Among CT findings and CT texture variables, the significant predictors for grade 2/3 tumor were an ill-defined margin (OR, 7.273), lower sphericity (OR, 0.491) and lower grey level co-occurrence matrices moments (OR, 0.563) on AP-2D analysis, higher skewness (OR, 1.972) and lower sphericity (OR, 0.408) on AP-3D analysis, lower kurtosis (OR, 0.436) and lower sphericity (OR, 0.420) on PP-2D analysis, and larger surface area (OR, 2.007) and lower sphericity (OR, 0.503) on PP-3D analysis ($P<0.05$).

Conclusion: CT is useful for predicting grade 2/3 PNET using not only the imaging findings including an ill-defined margin, but also the CT texture variables such as lower sphericity, higher skewness, and lower kurtosis.

SS 1.5

Pancreatic neuroendocrine neoplasms: MRI features and correlation with their histological grade

R. De Robertis[1], M. D'Onofrio[2], S. Ortolani[2], P. Tinazzi Martini[1], S. Cingarlini[2], G. Butturini[1], S. Gobbo[1], P. Capelli[2], R. Girelli[1], P. Regi[1], G. Tortora[2], P. Pederzoli[1], A. Scarpa[2]; [1]Peschiera del Garda/IT, [2]Verona/IT

Purpose: To describe MRI features including diffusion-weighted imaging (DWI) of pancreatic neuroendocrine neoplasms (PanNENs) according to their histological grade.

Material and methods: Preoperative MR examinations of 50 PanNEN patients were retrospectively reviewed. Qualitative and quantitative MR features were evaluated by two radiologists. All MR features were compared between histological grades using Chi-square/Fisher's exact test and Student's T/ANOVA test. P values <0.05 were considered statistically significant.

Results: Ill-defined margins, local infiltration, vascular involvement and liver metastases were significantly more common among G2-3 PanNENs compared to G1 tumors. G1 tumors were significantly smaller than G2-3 tumors (22.8 vs 38.1 mm, $p=0.016$); the mean ADC value was significantly lower among G2-3 tumors as compared to G1 tumors (1.03±0.3 vs 1.38±0.6, $p=0.010$).

Conclusion: MR features of PanNENs vary according to their histological grade; MRI including DWI can differentiate G1 from G2-3 PanNENs.

11:00 - 12:30 **Forum Hall**

Scientific Session SS 2

HCC: imaging and assessment

SS 2.1

MRI features of hepatocellular carcinoma capsule appearance in cirrhotic liver: comparison of gadoxetic acid and gadobenate dimeglumine

M. Dioguardi Burgio, D. Picone, G. Cabibbo, M. Midiri, R. Lagalla, G. Brancatelli; Palermo/IT

Purpose: To compare the MRI features of HCC capsule appearance on gadoxetic acid and gadobenate dimeglumine-enhanced MRI.

Material and methods: Gadoxetic acid and gadobenate dimeglumine-enhanced MRI of 51 patients with 71 HCCs were reviewed. Three readers graded in consensus, using a five-point scale, the presence (score 4-5) of capsule appearance on images obtained during T1-weighted GRE portal venous phase (PVP), three minutes phase and hepatobiliary phase (HBP).

Results: A hyperintense capsule appearance was present either on PVP or three minutes phase in 11/46 and in 24/25 HCCs imaged with gadoxetic acid and gadobenate dimeglumine-enhanced MRI, respectively (24% vs 96% p<0.0001). A hypointense capsule appearance was present on HBP in 8/46 and 0/22 HCCs evaluated with gadoxetic acid and gadobenate dimeglumine-enhanced MR imaging, respectively (17% vs 0% p=0.046). A capsule appearance was detected either on PVP, three minutes phase or HBP in 17/46 (37%) HCCs after gadoxetic acid injection and in 24/25 (96%) HCCs after gadobenate dimeglumine injection (p<0.0001).

Conclusion: A capsule appearance was more frequently seen on gadobenate dimeglumine-enhanced MRI when compared to gadoxetic acid-enhanced MRI.

SS 2.2

Comparing the results of intravoxel incoherent motion diffusion-weighted imaging calculated by different estimation methods: discrimination of histological grade of HCC

S. Ichikawa[1], U. Motosugi[1], D. Hernando[2], H. Morisaka[3], H. Onishi[1]; [1]Yamanashi/JP, [2]Madison, WI/US, [3]Saitama/JP

Purpose: To compare the measurement repeatability of intravoxel incoherent motion (IVIM) imaging using 3 different approximation methods for discriminating the histological grade of HCC.

Material and methods: Fifty-eight patients (60 HCCs) underwent IVIM imaging with 11 b values (0–1000s/mm2). Slow (D) and fast diffusion coefficients (D*) and the perfusion fraction (f) were calculated for HCCs using regions of interest placed individually by two radiologists. The following approximation methods were used during calculation. First, all 3 parameters were obtained simultaneously, using non-linear fitting (method A). Second, D was first obtained using linear fitting (b = 500 and 1000), followed by non-linear fitting for D* and *ƒ* (method B). Third, D was obtained by linear fitting, after which, *ƒ* was obtained using the regression line intersection and signals (b = 0) and non-linear fitting was used for D* only (method C).

Results: Methods B and C (Az-value, 0.707–0.881) yielded better HCC grade discrimination ability, compared with method A (Az-value, 0.537–0.583). The ICCs of D and f were good-to-excellent (0.639–0.835) with all methods. The ICCs of D* were moderate with method B (0.580) and C (0.463), and good with method A (0.705).

Conclusion: Compared with partial linear fitting, complete non-linear fitting, although reproducible, exhibited worse discrimination ability.

SS 2.3

Evolution of indeterminate hepatocellular nodules at initial gadolinium-ethoxybenzyl-diethylenetriamine pentaacetic acid-enhanced MRI in cirrhotic patients

F. Agnello, M. Galia, R. Cannella, F. Midiri, G. Lo Re, L. La Grutta, T.V. Bartolotta, G. Brancatelli; Palermo/IT

Purpose: To retrospectively evaluate the evolution of indeterminate hepatic nodules at initial gadolinium-ethoxybenzyl-diethylenetriamine pentaacetic acid (Gd-EOB-DTPA)-enhanced MRI in cirrhotic patients.

Material and methods: 33 cirrhotic patients (24 males; mean age, 64.9 years) with 69 indeterminate nodules (mean diameter, 1.1 cm; range, 0.5-2) at initial Gd-EOB-DPTA-enhanced MRI and a Gd-EOB-DPTA-enhanced MRI follow-up of at least 2 years (mean, 805 days; range, 745-2440) were evaluated. Indeterminate hepatocellular nodules were defined as nodules that cannot be diagnosed as HCC according to ASSLD 2010 criteria. Based on signal intensity at initial MRI, each nodule was classified into 6 groups: A) hyperintense on precontrast T1 phase (12/69); B) hyperintense on precontrast T1 and hepatobiliary phase (4/69); C) hyperintense on hepatobiliary phase (23/69); D) hypointense on hepatobiliary phase (9/69); E) hypointense on transitional and hepatobiliary phase (20/69); F) hypointense on portal-venous, transitional and hepatobiliary phase (1/69). Changes in size (disappearance, regression, no change, growth) and rate of progression to HCC were compared among groups using Chi-square test. Diagnosis of HCC was done by pathology and ASSLD 2010 criteria.

Results: 5/69 (7%) nodules (3 Group E; 2 group D) become HCC. There was no statistically significant difference in progression to HCC among groups. There was no statistically significant difference in rate of nodule disappearance (6%; 8/69), regression (4%; 7/69), no change (55%; 38/69) and growth (23%; 16/69) among groups.

Conclusion: Indeterminate hepatic nodules at Gd-EOB-DPTA-enhanced MRI in cirrhotic patients rarely progress to HCC.

SS 2.4

Noninvasive biomarker for prediction of treatment response to concurrent chemo-radiotherapy in patients with locally advanced HCC

Y.E. Chung, J. Seong, J.Y. Park, M.-S. Park, M.-J. Kim; Seoul/KR

Purpose: To investigate noninvasive biomarker for prediction of treatment response in patients with locally advanced HCC.

Material and methods: Thirty patients (55.5±10.2 years old, M:F=24:6) who underwent concurrent chemo-radiotherapy (CCRTx) due to advanced HCC were prospectively enrolled. Contrast-enhanced US (CEUS) and perfusion MRI were obtained before and immediately after CCRTx. The third CEUS was obtained 1 month after the end of CCRTx. Response assessment was performed 3 months after the end of CCRTx based on RECIST criteria. Quantitative biomarkers measured by CEUS including peak enhancement (PE), time to peak enhancement (TTP), and mean transit time (MTT) and by perfusion MR including volume transfer constant (Ktrans), reflex constant (Kep), and extravascular-extracellular volume fraction (Ve) were compared with the Mann-Whitney U test. A cutoff value of PE was calculated with ROC analysis and overall survival (OS) was compared by Breslow method.

Results: PE of the first CEUS before CCRTx was significantly lower in responder (median, 18.6%; IQR, 20.9%) than in non-responder (59.1%, 13.5%; P=0.002). There was no significant difference between two groups in other quantitative biomarkers. In receiver operating characteristic analysis, responder could be diagnosed with sensitivity of 90.9% and specificity of 100% with a cutoff value of 42.6% of PE. OS was also significantly longer in patients with PE<42.6% than the others (P=0.014).

Conclusion: Early treatment response and OS could be predicted by PE on CEUS before CCRTx in patients with locally advanced HCC.

SS 2.5

Usefulness of multi-arterial phase for characterization of liver hypervascular focal lesions using gadoxetic acid in liver MRI

R. Faletti[1], L. Grazioli[2], G. Battisti[3], B. Frittoli[2], P. Fonio[1], G. Gandini[1]; [1]Turin/IT, [2]Brescia/IT, [3]Spoleto/IT

Purpose: To evaluate the hypervascular liver lesion studied by a single arterial phase protocol and by a multiarterial phase with CAIPIRINHA (Controlled Aliasing In Parallel Imaging Results IN Higher Acceleration) technique protocol.
Material and methods: MR examinations of 148 patients: 70 with a single phase optimized protocol and 78 with the CAIPIRINHA multi-arterial phase protocol. We analyzed the signal intensities from aorta, portal vein, liver parenchyma and lesions on the pre-contrast phase and on all arterial phase images.
Results: The lesions were 33 in the standard protocol and 50 in the CAIPIRINHA protocol. We identified three groups: A (maximum lesion-to-liver contrast ratios LLCR at 1st phase), B (maximum LLCR at 2nd phase) and C (maximum LLCR at 3rd phase). Group C includes 30% of HCC lesions, and none of benign lesions. The comparison with the standard protocol shows that the aorta enhancement for the latter is significantly higher than the one observed in the 1st arterial phase of the CAIPIRINHA protocol ($p<0.0001$), whereas all other values are midway between the values achieved in the first two arterial phases of the CAIPIRINHA protocol, and significantly inferior ($p=0.0003$) to the values relative to the latest arterial phase.
Conclusion: The existence of three useful phases not only drastically reduces the chance of missing lesions but also allows estimating the lesion enhancement as a function of time.

SS 2.6

Added value of hepatobiliary-phase and T2-weighted images to the liver imgaing reporting and data system for the diagnosis of HCC: preliminary results

G. Rosiak, A. Grodzicka, E. Rosiak, B. Górnicka, O. Rowinski, A. Cieszanowski; Warsaw/PL

Purpose: To retrospectively assess the added value of T2-weighted and hepatobiliary-phase (HP) images in the liver imaging reporting and data system (LI-RADS) for the diagnosis of HCC in patients with chronic liver disease.
Material and methods: 22 patients (18 men, 5 women) in the mean age of 65 years (range, 34-87) with chronic liver disease and 35 histopathologically confirmed HCC (mean diameter of 33 mm, range: 7-138 mm) underwent magnetic resonance imaging (MRI) with hepatobiliary contrast agent (Gd-BOPTA in 15, Gd-EOB-DTPA in 7 patients). Lesions were solitary in 10 patients and multiple in 12 patients. Two abdominal radiologists evaluated dynamic contrast-enhanced images, T2-weighted images and HP images. In case of disagreement between readers, a consensus interpretation was formed. The diagnostic performance of LI-RADS was assessed and compared to T2-weighted and HP images.
Results: Nineteen of 35 HCCs (54.3%) were classified as LI-RADS category 5 lesions, 12 (34.3%) as LI-RADS category 4 lesions and 4 (11.4%) as LI-RADS 3 category lesions. Combining LI-RADS category 4 lesions with hypointensity on HP images and hyperintensity on T2-weighted images for the diagnosis of HCC would improve the sensitivity from 54.3% (for LI-RADS category 5 lesions only) to 80%.
Conclusion: The combined interpretation of T2-weighted and HP images for LI-RADS category 4 lesions significantly improved the sensitivity of MRI for the diagnosis of HCC.

SS 2.7

withdrawn by the authors

SS 2.8

Efficacy of abdominal US surveillance for HCC detection in cirrhotic patients: our experience

F. Agnello, M. Antonucci, F. Midiri, A. Taibbi, T.V. Bartolotta; Palermo/IT

Purpose: To retrospectively evaluate the efficacy of abdominal US surveillance in the detection of HCCs in cirrhotic patients.
Material and methods: In a 24-month period, 224 cirrhotic patients underwent US surveillance. 164/224 (73%) patients (112 men; mean age 64.5 years ± 10; 26-84) underwent subsequent contrast-enhanced CT (n= 56) and Gd-EOB-DTPA-enhanced MRI (n=108). US reports were correlated with CT and MR images. Nodules were classified as true positive (nodules detected by US and confirmed as HCC), false positive (nodules detected by US but not confirmed as HCC) and false negative (HCCs not detected by US). Reference standard for HCC diagnosis was AASLD 2010 criteria and pathology. US sensitivity for HCC detection and agreement among US and CT/MRI were calculated.
Results: Our final study comprised 220 nodules. There were 89/220 (41%) true positive (mean diameter 2.7 cm±1.4; 7-15), 12/220 (5%) false negative (mean diameter 5.7 cm±0.7; 1-4) and 119/220 (54%) false positive (mean diameter 1.3 cm±0.4; 1-3.6). Causes of false-positive were regenerative nodules (n= 20/119), dysplastic nodules (n=16/119), hemangiomas (n=7/119), cysts (n=6/119), other (n=5/119). No explanation for false-positive was found in 65/119 nodules. US sensitivity was 88%. Intermodality agreement was 35.02% (K=0.390).
Conclusion: Abdominal US shows high sensitivity for HCC detection. The agreement among US and CT/MRI for HCC detection is fair.

SS 2.9

MDCT perfusion imaging biomarkers as prognostic indicators of survival in hepatocarcinoma

A. Alberich-Bayarri, A. Torregrosa Andrés, R. Nombela, J. Tomás Cucarella, L. Martí-Bonmatí; Valencia/ES

Purpose: To analyze the relationship of perfusion CT imaging biomarkers in treated hepatocarcinoma with overall survival (OS) to add insights into prognosis evaluation of the disease.
Material and methods: A total of 28 patients with hepatocarcinoma were included in the study (mean age 68±10). Perfusion MDCT acquisitions were performed in a scanner with 256 detectors (Brilliance iCT, Philips Healthcare, The Netherlands). The acquisition had a voxel size of 0.25x0.25x5mm. A mean volumen of 41±5 ml of iodated contrast was administered (IOMERON 400©). Images were pre-processed by a gaussian filtering and a non-linear registration. The parametric maps of arterial perfusion (AP), perfusion index (PI), arterial time-to-peak (TTP) and permeability (P) were calculated. The pre-processing and parametric maps calculation was performed at the IntelliSpace Portal© platform of Philips. Finally, regions of interest (ROI) were placed in the lesions to register the mean values obtained. OS was calculated using the date of the first MR post-treatment.
Results: The values obtained for lesions were of 108.40±38.53 for AP[l/min/100]; 0.61±0.13 for HP; 23.02±8.36 for TTP[s]; 19.07±8.27 for P[l/min/100]. OS was higher in the group with an HP>=0.6 (354 days) vs HP<0.6 (226 days). No differences were observed for the other parameters.
Conclusion: Perfusion CT and especially the hepatic perfusion index is an imaging biomarker with growing applications in HCC prognosis evaluation, as derived from the preliminary evaluation in this study.

SS 2.10

Unenhanced MRI immediately after ablation of liver malignancies to assess treatment efficacy

M. D'Onofrio, N. Cardobi, V. Ciaravino, R. De Robertis, R.M. Pozzi Mucelli; Verona/IT

Purpose: To assess the accuracy of unenhanced MRI immediately after the percutaneous ablation of liver malignancy in predicting the treatment efficacy at CT follow-up.

Material and methods: Percutaneous ablation was prospectively performed in 17 liver malignancies (14 HCCs, 3 METs). After the procedure, on the same day all the lesions were studied with unenhanced MRI. The MRI protocol was essential (T2, FST2, T1, FST1 and DWI) to be performed in short time. The best sequence to detect the coagulative necrosis was established. Sensitivity, specificity, positive predictive value (PPV), negative predictive value (NPV) and accuracy of MRI in predicting the correct centring and the complete treatment of the lesion were calculated with respect to the standard one month follow-up CT.

Results: Coagulative necrosis was hyperintense in T1 sequences in 13/17 (76%). FST1 was the sequence in which the best conspicuity of the ablated area was depicted. With respect to follow-up CT, MRI predicted the correct centring of the lesions in 13/17 (76%) lesions with sensitivity, specificity, PPV, NPV and accuracy of 100%, 75%, 93%, 100% and 94%, respectively. MRI predicted the complete treatment of the lesions in 12/17 lesions with sensitivity, specificity, PPV, NPV and accuracy of 100%.

Conclusion: MRI with the single T1FS weighted sequence was highly accurate in predicting the treatment efficacy of percutaneous ablation of liver malignancies as shown at CT follow-up. Unnecessary CT in case of incomplete treatment can be, therefore, easily avoided.

11:00 - 12:30 **Meeting Hall V**

Scientific Session SS 3

Percutaneous HPB intervention: novel advances

SS 3.1

Percutaneous electrochemotherapy of malignant main portal veins thrombosis: a prospective case series

L. Tarantino[1], G. Busto[1], A. Nasto[1], R. Fristachi[1], L. Cacace[1], M. Talamo[1], P. Ambrosino[2], P. Gallo[3], P. Tarantino[2], C. Accardo[1]; [1]Pagani/IT, [2]Naples/IT, [3]Rome/IT

Purpose: We report our experience in thrombosis of portal vein and/or first-order branches (Vp3-4PVTT) from HCC treated with percutaneous electrochemotherapy (ECT).

Material and methods: Six cirrhotics (5 males; 61–85 years, 4 in Child-Pugh A, 2 in Child-Pugh B class) prevously studied with three-phase CT, contrast-enhanced ultrasound (CEUS) and US-guided percutaneous biopsy of the thrombus, underwent ECT (Cliniporator Vitae - IGEA, Carpi, Italy) of Vp3-4PVTT and the associated HCC nodule in the same session, under general anesthesia.

Results: 24-hour posttreatment CEUS showed complete absence of enhancement of the treated trhombus in all cases. Post-treatment biopsy showed apoptosis and necrosis of tumor cells in all cases. The follow-up ranges from 3 to 12 months (median: 8 months). In 1 patient, the 3-6-9-12 months CEUS and CT demonstrate complete recanalization of the treated PVTT; in another patient, 3-6-9 months CEUS and CT show a partially patent portal vein; other 3 patients (8, 4 and 3 month follow-up, respectively) show avascular complete thrombosis at CEUS and CT. In all 5 patients, CEUS and CT show absence of abnormal intravascular or perivascular enhancement consistent with residual tumor or local recurrence. One patient, was lost to follow-up because of death from gastrointestinal hemorrhage 5 weeks after ECT.

Conclusion: ECT seems effective and safe for curative treatment of Vp3-Vp4 PVTT from HCC.

SS 3.2

Microwave ablation of large HCCs by simultaneous multiple antennae insertion: long-term follow-up

L. Tarantino[1], P. Ambrosino[2], P. Gallo[3], P. Tarantino[2], A. Nasto[1]; [1]Pagani/IT, [2]Naples/IT, [3]Rome/IT

Purpose: We report long-term results of microwawe (MW) ablation with simultaneous insertion of multiple antennae in the treatment of large HCC.

Material and methods: Between 2008 and 2013, 36 cirrhotics with a single HCC nodule >3 cm (3.2-7.0 cm; mean: 4.4 cm) underwent MW ablation in a single session by simultaneous insertion of multiple 13-gauge-MW-antennae (Viva-Wave, Covidien, USA). After intraoperative contrast-enhanced ultrasound (CEUS), residual viable tumor was treated in the same session by reinsertion of 2-3 MW antennae.

Results: According to the tumor size, 10 and 18 patients were treated with a single insertion of 2-3 synchronous antennae, respectively. 8 patients were treated with 2 insertions of 3 antennae in the same session. Intraoperative CEUS showed residual tumor in 12 patients and these patients underwent an additional insertion of 2 or 3 antennae. Intraoperative CEUS at the end of the procedure showed complete necrosis in all patients. 1-month CT showed complete necrosis in 33/36 patients. Only a severe hemoperitoneum occurred in one patient after treatment. Local recurrence occurred in 7 patients. Recurrences in other liver segments occurred in 35/36 patients within 6 to 24 months (mean: 15 months). 20 patients were alive at 18-78 months follow-up (mean: 42 months).

Conclusion: Aggressive ablation of large HCC by simultaneous insertion of multiple MW antennae is safe and seems to result in patients' survival comparing with surgery and small HCC ablation.

SS 3.3

Tumor seeding after percutaneous US-guided FNA of solid pancreatic neoplasms

R. De Robertis[1], C. Sozzi[2], M. D'Onofrio[2], E. Barbi[1], E. Manfrin[2], S. Gobbo[1], G. Butturini[1], S. Ortolani[2], G. Tortora[2], C. Bassi[2], P. Pederzoli[1]; [1]Peschiera del Garda/IT, [2]Verona/IT

Purpose: To determine the frequency of tumor seeding after percutaneous US-guided FNA of solid pancreatic neoplasms.
Material and methods: Follow-up examinations (CT or MR) of 124 patients with solid pancreatic neoplasms who underwent US-FNAs were retrospectively evaluated. Two radiologists evaluated the presence of imaging features suggesting tumor seeding as peritoneal/subcutaneous solid nodules or ascites.
Results: Median follow-up length was 197 days. Subcutaneous nodules along the needle track were found in 1/124 cases (0.8%). Ascites without local or systemic disease progression was found in 7/124 patients (5.6%), after a median time interval of 210 days after FNA.
Conclusion: Tumor seeding is uncommon after percutaneous US-FNA of solid pancreatic neoplasms. Ascites without any sign of local/systemic disease progression can develop after US-FNA and may suggest microscopic peritoneal tumor seeding; nevertheless, as the time interval to the development of ascites is comparable to the disease-specific time to progression, ascites may also be the consequence of disease progression unrelated to the procedure.

SS 3.4

Microwave ablation of large HCCs using a new device: a case series

L. Tarantino[1], P. Ambrosino[2], P. Gallo[3], P. Tarantino[2], A. Nasto[1]; [1]Pagani/IT, [2]Naples/IT, [3]Rome/IT

Purpose: We evaluated a device designed to achieve large volumes of necrosis in HCC by synchronous activation of multiple microwave (MW) antennae.
Material and methods: 10 consecutive patients with a single large HCC nodule (3.5-6.5 cm; mean: 4.6 cm) underwent US-guided percutaneous MW ablation by synchronous insertion of multiple MW antennae (SynchroWave 915 MHz antennas - MicroThermX® microwave ablation system, Terumo, Belgium, Europe). A single insertion of 2 antennae (3 cases), and 3 antennae (5 cases) was performed. 2 insertions of 3 antennae in the same session were performed in 2 cases. Treatment efficacy was assessed by CT and bimonthly US follow-up.
Results: Post-treatment CT showed complete necrosis in 8/10 HCC nodules (80%). 2 patients with incomplete ablation underwent an additional MW ablation session. CT showed complete necrosis in both of them. Several major complications (recovered with medical treatment) occurred: anaerobic infection of the treated necrotic area in 2 cases, severe right pleural effusion in one case, jaundice from transient liver failure. All patients are still alive (follow-up 12-20 months). In 6/10 (60%) cases, intrahepatic recurrence occurred within 6-14 months (mean 10 months) and it could be successfully treated with ablation in 3 cases. The other 3 patients underwent chemotherapy with sorafenib and/or best supportive care.
Conclusion: The MicroThermX microwave ablation system seems an effective and relatively safe device for treatment of large HCC.

SS 3.5

withdrawn by the authors

SS 3.6

CT findings of hepatic abscess: predicting the outcome of percutaneous catheter drainage or percutaneous needle aspiration

J. Lee[1], M. Kang[1], S.C. Baek[1], B.S. Cho[1], K.S. Park[1], J.Y. Moon[2]; [1]Cheongju/KR, [2]Seoul/KR

Purpose: To evaluate association between CT findings and outcome of percutaneous catheter drainage (PCD) or percutaneous needle aspiration (PNA) in patients with hepatic abscess.
Material and methods: 93 patients who had undergone PCD or PNA in a 5-year period were included. Clinical data, microbiologic characteristics, and outcome of treatment were reviewed. Three radiologists evaluated CT findings of hepatic abscess including diameter, volume, mean attenuation values, number, location, configuration, presence of cystic component and gas, rim enhancement, wall thickness, and shortest length to hepatic capsule. Patients were divided into two groups: group 1 (≥50%) and group 2 (<50%) according to ratio of initial-drainage volume to CT-determined abscess volume. Univariate and multivariate statistical analyses were used to examine association of CT and clinical findings between two groups. Statistical relationship between mean attenuation values and outcome of PCD or PNA was assessed using Spearman correlation analysis.
Results: There were 32 patients in group 1 and 61 in group 2. Multivariate analysis revealed that cystic appearance (P=.028) and thick wall (P=.002) were significant in group 1, and there was a tendency to shorter hospital stay (P=.061) in group 1. There was negative correlation between mean attenuation values and ratio of initial-drainage volume to CT-determined abscess volume.
Conclusion: CT findings may be useful predicting factors for outcome of PCD or PNA in patients with hepatic abscess.

SS 3.7

Endoluminal radiofrequency ablation of hilar cholangiocarcinoma

T. Andrasina, J. Panek, J. Hlavsa, V. Bernard, V. Valek; Brno/CZ

Purpose: To prove efficacy of endoluminal radiofrequency ablation in palliative treatment of hilar cholangiocarcinoma.
Material and methods: 35 patients with hilar cholangiocarcinoma have been enrolled in a prospective randomised study since 2010. The infiltrative type of cholangiocarcinoma was predominant. 65 non-covered self-expandable metal stents were inserted. In group A (n=18) the endoluminal ablation with a bipolar radiofrequency catheter (EndoHPB; EMcision Ltd., London, UK) was performed 0-48 hours prior to the stent insertion, in group B (n=17) the stent was implanted without a prior ablation. The primary endpoints of the study were to determine the rate of complications, duration of stent patency and survival of patients (Kaplan-Meier analysis).
Results: The rate of biochemical pancreatitis, which was resolved in 3 days after stent insertion, was significantly higher in group A. The average primary stent patency was 5.9 and 5.7 months in groups A and B, respectively; 3-month and 6-month stent failure was 0% and 6.1% in group A and 6.3% and 25% in group B. The median survival from the initial drainage was 12.3 (6.7-20.1) and 12.8 (5.7-14.7) months in groups A and B, respectively.
Conclusion: The effect of an endoluminal ablation on patients survival was not proven in the prospective randomised clinical study. However, in the group of patients undergoing ablation there is a tendency of a lower rate of early stent failure. The intervention should be associated with very mild biochemical pancreatitis.

SS 3.8

Bacterial isolates from biliary cultures obtained during percutaneous biliary intervention. Are we prescribing the right antibiotics?

P.S. Najran, E. Barclay, J. Bell, D. Mullan, H.-U. Laasch; Manchester/GB

Purpose: To identify the most common pathogens isolated from biliary cultures in patients undergoing percutaneous transhepatic intervention and to assess antibiotic sensitivity. To establish the optimal prophylactic antibiotic regime.

Material and methods: All percutaneous transhepatic interventions performed over a two-year period were reviewed retrospectively. Those where no biliary culture was obtained were excluded. Analysis of the culture results including pathogens grown and antibiotic sensitivity was performed.

Results: A total of 58 patients were included in the analysis. No pathogens were grown in 27.6% of cultures (n=16). Of those with positive cultures Enterococci and Pseudomonas were the most common pathogens grown in 59.5% of cases (n=25). Vancomycin was the most effective antimicrobial demonstrating sensitivity in 31% (n=16) of positive cultures followed by ciprofloxacin showing sensitivity in 26.2% (n=11). Gentamycin was the fifth most effective antimicrobial demonstrating sensitivity in only 14% (n=6).

Conclusion: Effective antibiotic prophylaxis requires knowledge of likely pathogens and procedure-specific infection risks, which may vary between hospitals and patient cohorts. In our institution, gentamycin is traditionally administered prophylactically prior to percutaneous biliary intervention; however, this study has demonstrated this is comparably ineffective, necessitating a change in protocol. The choice of antimicrobial requires continued review due to emerging antibiotic resistance.

SS 3.9

Irreversible electroporation of locally advanced pancreatic cancer: case study of a next day post-interventional fluorodeoxyglucose positron emission tomography in one patient

L. Lambert, Z. Meckova, J. Horejs, Z. Krska, D. Hoskovec, L. Petruzelka, V. Cerny, P. Kriz, J. Briza; Prague/CZ

Purpose: To demonstrate the early effect of irreversible electroporation (IRE) on fluorodeoxyglucose (18F-FDG) consumption in locally advanced pancreatic cancer.

Material and methods: We present an 86-year-old female patient with locally advanced pancreatic cancer (stage III) located in the head of pancreas, who was treated by intraoperative IRE. 18F-FDG PET-CT was preformed 2 days prior to IRE and 1 day after IRE.

Results: PET-CT performed prior to IRE confirmed marked accumulation of 18F-FDG within the malignant tissue without involvement of peripancreatic lymph nodes or distant metastatic disease. One day after IRE, PET-CT demonstrated absence of accumulation in the tumoral mass. However, accumulation was present in the duodenal wall, which was infiltrated by remnants of the tumoral tissue. The patient died six months later of pulmonary embolism.

Conclusion: In this case study, we demonstrated nearly complete destruction of the tumoral mass in the pancreatic head by IRE with remnants in the duodenal wall using 18F-FDG PET-CT one day following the intervention.

SS 3.10

Irreversible electroporation of locally advanced pancreatic adenocarcinoma: long-term follow-up

L. Tarantino[1], V. Iovino[1], G. Busto[1], A. Nasto[1], P. Gallo[2], C. Accardo[1], R. Giordano[1]; [1]Pagani/IT, [2]Rome/IT

Purpose: We report our experience and 2 years follow-up in a locally advanced pancreatic adenocarcinoma (LAC) successfully treated with irreversible electroporation (IRE).

Material and methods: In a female patient, 24 years, CT and MR showed a pancreatic mass (diam.=6.5cm) with complete thrombosis of the middle and distal portions of splenic vein and infiltration of the mesenteric and portal vein wall. Biopsy showed pancreatic “aggressive type of solid papillary adenocarcinoma”. Imaging did not show any lymphnode or distant metastasis. The surgical team excluded indication to resection. We offered the patient IRE as alternative treatment, and she was treated with open laparotomy under general anesthesia with IRE. Six insertions of multiple electrodes (up to 4 per insertion) were performed.

Results: The patient left the hospital 5 days after treatment. Post-treatment 1-month CT and MR showed “shrinkage of the tumor, partial bland thrombosis of the splenic vein, patent mesenteric and portal vein, small splenic infarction”. CT follow-up at 6-12-18-24 months, showed complete regression of the mass, patent splenic/mesenteric veins and absence of local recurrence or distant metastasis.

Conclusion: In cases with poor indications for surgical resection, IRE seems to be a safe and highly effective alternative treatment for advanced stage pancreatic solid papillary adenocarcinoma, even in presence of extensive thrombosis of spleno-portal-mesenteric veins.

11:00 - 12:30 **Chamber Hall**

Scientific Session SS 4

Abdominal vasculature: imaging and intervention

SS 4.1

Dual-energy CT angiography of the abdomen: optimization of window/level settings

D. Caruso[1], C.N.N. De Cecco[1], U.J. Schoepf[2], J.L. Wichmann[3], A. Varga-Szemes[2], A. Laghi[1]; [1]Rome/IT, [2]Charleston, SC/US, [3]Frankfurt am Main/DE

Purpose: To evaluate the optimal window settings to display virtual monoenergetic images using third-generation dual-source, DECT angiography.
Material and methods: 45 patients were clinically evaluated with DECT angiography. Standard linear blending (M_0.6), 70 keV standard virtual monoenergetic (M70), and 40 keV advanced virtual monoenergetic (M40+) datasets were reconstructed. Two readers determined the best window settings (width and length, W/L), which were correlated with the aortic attenuation to obtain optimized W/L settings. Subjective image quality was assessed and vessel diameters were measured to determine the influence of different W/L settings. Repeated measures of variance were used to assess differences in image quality and vessel sizing between M_0.6, M70, and M40+.
Results: The best W/L for M70 was 880/280 and 1410/450 for M40+. From the results of the regression analysis, we found an optimized W/L of 850/270 for M70 and 1350/430 for M40+. A significant difference was found between the best and optimized W/L for M40+ ($p<0.001$), as well as between M70 and M40+ for both the best and optimized W/L (all ($p<0.001$). Significant differences were reported in vessel diameters ($p\leq0.04$).
Conclusion: When using virtual monoenergetic imaging both for standard M70 and advanced M40+ reconstructions, adjusting the W/L settings is mandatory. Optimized W/L settings that correlate with aortic attenuation are advisable. We suggest a W/L setting of 850/270 for M70 and 1350/430 for M40+.

SS 4.2

Comparison of image quality of various virtual monoenergetic algorithms for dual-energy CT angiography of thorax and abdomen

S.S. Martin, M.H. Albrecht, J.-E. Scholtz, D. Leithner, S. Fischer, R.W. Bauer, T. Vogl, J.L. Wichmann; Frankfurt am Main/DE

Purpose: To comprehensively compare objective and subjective image quality of traditional and advanced noise-optimized virtual monoenergetic and standard linearly blended image reconstruction algorithms in third-generation dual-source dual-energy CT angiography (DE-CTA) of the thorax and abdomen.
Material and methods: DE-CTA image series of 55 patients were reconstructed using linearly blended M_0.6 (60% low-kV spectrum), traditional monoenergetic (VMI), and advanced noise-optimized monoenergetic (VMI+) algorithms. Monoenergetic image series were calculated with 10 keV increments from 40-120 keV. Attenuation and standard deviation of region-of-interest measurements in various arteries and anatomical landmarks of the thorax and abdomen were taken to calculate contrast-to-noise ratio (CNR) values. Two radiologists assessed subjective image quality, contrast conditions, image noise, and visualization of small arterial branches using 5-point Likert scales.
Results: VMI+ 40-keV series showed the highest CNR for both thoracic and abdominal DE-CTA ($p<0.001$) and were subjectively rated highest for visualization of small arterial branches ($p<0.109$). VMI+ images at 70 keV demonstrated superior subjective image quality ($p<0.031$) except compared to 60 and 80 keV VMI+ series ($p<0.587$). Contrast conditions at 50-keV VMI+ were rated superior compared to 60-100 keV VMI and VMI+ ($p<0.01$) reconstructions. VMI+ images at 100 keV were rated best regarding image noise ($p<0.843$).
Conclusion: Image quality of DE-CTA can be substantially increased and improved contrast and visualization of small arterial branches can be achieved with low-keV VMI+ reconstructions and should be preferred over traditional VMI or standard linearly blended reconstructions.

SS 4.3

Long-term outcome of transjugular intrahepatic portosystemic shunt placement in primary Budd-Chiari syndrome

M. Ronot, G. Hayek, M. Lagadec, C. Garcia-Alba, M. Zappa, A. Sibert, V. Vilgrain; Clichy/FR

Purpose: To evaluate the long-term efficacy of transjugular intrahepatic portosystemic shunt (TIPS) placement for the treatment of primary Budd-Chiari syndrome (BCS).
Material and methods: From 2004 to 2013, all patients with primary BCS referred for TIPS placement were included in the study. The primary and secondary technical success rates, the number and types of early (<day 7) complications were noted. Survival was analyzed.
Results: Fifty-four patients (34 women, 63%), mean age 36±12 years were included. Twenty-eight patients (52%) had myeloproliferative neoplasms. The mean MELD score was 14.5±4. The most frequent indication for TIPS was refractory ascites (50/54, 93%). Primary and secondary technical success rates were 93% and 98%, respectively. Early complications occurred in 17 patients (32%). After a mean follow-up of 56±41 months, 22 patients (42%) experienced at least one episode of TIPS dysfunction (median delay between TIPS and first episode of dysfunction 10.8 months). Cumulative 1-, 2-, 3-, 5-, and 10-year dysfunction-free rates were 64%, 59%, 54%, 45%, and 45%, respectively. Dysfunction was associated with a myeloproliferative disorder (HR=8.18, 95%CI 1.45–46.18, p=0.017), more than two initial stents (HR=3.90, 95%CI 1.16–13.10, p=0.027), and the occurrence of early complications (HR=11.34, 95%CI 1.82–70.69, p=0.009). The 10-year survival rate was 76%.
Conclusion: TIPS placement in patients with primary BCS was associated with a non-negligible rate of early complications, and required endovascular revision(s) in 42% of patients. Nevertheless, secondary permeability was close to 100%, and long-term survival was good.

SS 4.4

Outcome of transhepatic intravascular porto-systemic shunt in older patients

N. Shah, G. Sheiybani, J. Acevedo, N. Gafoor, M.E. Cramp, S.A. Jackson; Plymouth/GB

Purpose: Transhepatic intravascular porto-systemic shunt (TIPS) is a well-established treatment for complications of portal hypertension. Older patients are a challenging group to treat.
Material and methods: Retrospective study reviewing patients undergoing TIPS between 2004 and 2015 and to determine outcomes according to age.
Results: 141 patients underwent TIPS, 132 were performed successfully (5 patients excluded - insufficient data). 63% were male (81/127) and 28% (36/127) >65 years. Indications were variceal bleeding 60% (76/127), refractory ascites 30% (38/127), TIPS restenosis, 3% (4/127) other 7% (9/127). Aetiology - alcohol-related liver disease (ARLD) 62%, non-alcoholic steato-hepatitis (NASH) 25% and other chronic aetiology 13%. The indications and aetiology were similar between patients >65 and <65 years of age. The most common complication post-TIPS was hepatic encephalopathy (HE) in 33% (12/36) >65 years vs 15% (14/91) <65 years. Patients >65 years had an overall mortality of 30% (13/44), with a 30-day (30%) and 3-year (40%) mortality. Patients with MELD >25 were associated with mortality of 75% (6/8) vs 25% (38/119) in patients with MELD <25. MELD was comparable between the groups with median of 14. 69% (9/13) of patients with Child's class C accounted for a high 30-day mortality.
Conclusion: Patients >65 years are at increased risk of mortality and HE. Age is an independent risk factor and older patients warrant careful selection prior to TIPS.

SS 4.5

Dynamic 4D-CT angiography for planning of liver tumor transarterial chemoembolization: effect on contrast material reduction, operator radiation exposure, catheter consumption, and diagnostic confidence

J.L. Wichmann, M.H. Albrecht, T. Vogl, S. Fischer, R. Hammerstingl, M. Harth, A. Thalhammer, S. Zangos, R.W. Bauer; Frankfurt am Main/DE

Purpose: To evaluate the usefulness of 4D computed tomography angiography (4D-CTA) prior to transarterial chemoembolization (TACE) regarding administered volume of contrast media, operator radiation exposure, catheter consumption, and diagnostic confidence.

Material and methods: 4D-CTA examinations prior to initial TACE of 29 patients with malignant liver tumors were analyzed. Multiplanar-reformate (MPR), volume-rendering technique (VRT) and maximum-intensity projection (MIP) series were used to plan a direct selective catheterization of the tumor-supplying artery without prior conventional digital subtraction angiography (DSA) of the abdominal aorta, coeliac trunk, superior mesenteric artery, and indirect portography. 29 patients who underwent traditional TACE served as the control group. The amount of administered contrast media, operator radiation exposure, and catheter consumption were compared between both groups. Diagnostic confidence in the exclusion of portal vein thrombosis was assessed by two radiologists using 5-point Likert scales.

Results: The 4D-CTA TACE group showed a significant overall contrast media reduction of 12.8ml (-13.8%, $p<0.001$) and 61ml less contrast were administered arterially (-66.3%, $p<0.001$) compared to traditional TACE. Operator radiation could be reduced by 50.5% ($p<0.001$). 4D-CTA TACE was performed using on average 0.7 less catheters ($p=0.063$). Diagnostic confidence in the exclusion of portal vein thrombosis was significantly increased using 4D-CTA compared to traditional DSA images (scores, 3.9 and 2.4, respectively; $p<0.001$).

Conclusion: 4D-CTA facilitates TACE with substantially reduced contrast material volume and operator radiation exposure, while increasing diagnostic confidence in the exclusion of portal vein thrombosis.

SS 4.6

Simultaneous trans-hepatic portal and hepatic vein embolization before major hepatectomy: the liver venous deprivation technique

B. Guiu[1], P. Chevallier[2], A. Denys[3], M.-A. Pierredon[1], J. Ramos[1]; [1]Montpellier/FR, [2]Nice/FR, [3]Lausanne/CH

Purpose: To assess feasibility, safety, and efficacy of the liver venous deprivation (LVD) technique that combines both portal and hepatic vein embolization during the same procedure for liver preparation before major hepatectomy.

Material and methods: Seven patients (mean age: 63.6y [42-77y]) underwent trans-hepatic LVD for liver metastases (n=2), HCC (n=1), intrahepatic cholangiocarcinoma (n=3) and Klatskin tumour (n=1). The PVE procedure was conducted using a Lipiodol:n-butyl-cyanoacrylate. The right hepatic vein (HV) was accessed through the liver using a micropuncture set. An Amplatzer Vascular Plug II of 18-22mm was deployed in HV. Then, embolization of distal branches and collaterals of the right HV was conducted using a 1:1 mixture of lipiodol:n-butyl-cyanoacrylate. Assessment of future remnant liver (FRL) volume, liver enzymes and histology was performed.

Results: Technical success was 100%. No complication occurred before surgery. Resection was performed in 6/7 patients. CT scan revealed hepatic congestion in the venous-deprived area (6/7 patients). Twenty-three days (range:13–30days) after LVD, FRL increased from 28.2% (range: 22.4–33.3%) to 40.9% (range:33.6–59.3%). During the first 7 days, venous-deprived liver volume increased (+13.4%) probably reflecting vascular congestion, whereas it strongly decreased (-21.3%) at 3-4 weeks. Histology (embolized lobe) revealed sinusoidal dilatation, hepatocyte necrosis and important atrophy in all patients.

Conclusion: Trans-hepatic LVD technique is feasible, well tolerated and provides fast and important hypertrophy of the FRL. This new technique needs to be further evaluated and compared to portal vein embolization.

SS 4.7

Risks factors for severe pain after selective liver transarterial chemoembolization

M. Ronot, J. Ben Zakoun, M. Lagadec, C. Garcia-Alba, A. Sibert, V. Vilgrain; Clichy/FR

Purpose: To determine the risk factors of severe pain after selective transarterial chemoembolization (TACE) for HCC.

Material and methods: From January 2012 to June 2014, all treatment-naïve patients undergoing a first session of selective TACE for HCC were included. Non-selective TACE were excluded. Risk factors for severe pain, defined as the need for opioid analgesics (grade II-III according to the World Health Organization), were identified by uni- and multivariate analyses.

Results: We analyzed 335 tumours (mean size 47±37mm) in 159 patients (131 men, 82%), mean age 63.4 years old (20-92). Lesions were solitary in 78 patients (49%). Twenty-seven patients (17%) requested opioids. In univariate analysis, opioid intake was associated with young age ($p=0.021$), the dose of doxorubicin received ($p=0.031$), large HCC ($p=0.038$), an absence of chronic liver disease ($p<0.001$), and alphafoetoprotein levels ($p=0.03$). In multivariate analysis, opioid intake was associated with young age ($p=0.048$), an absence of chronic liver disease ($p<0.001$), and the dose of doxorubicin received ($p=0.009$).

Conclusion: In patients with HCC treated with TACE, a selective procedure does not always prevent severe pain. Young patients without chronic liver disease are at a higher risk of severe pain and should systematically receive preventive opioids.

SS 4.8

Uncommon and ancillary vascular findings in common abdominal vascular compression syndromes

B. Öztoprak; Sivas/TR

Purpose: Although defined as rare vascular pathologies in the literature, abdominal vascular compression syndromes are becoming more commonly encountered with the increased use of MDCT and CT angiography (CTA) in the abdomen. The aim of this study is to investigate the vascular alterations secondary to common abdominal compression syndromes.

Material and methods: MDCT and CTA images of 33 patients with nutcracker (NC) and median arcuate ligament syndromes (MALS) were investigated for presence of secondary abnormal vascular appearances. In addition, 186 patients with retroaortic or circumaortic left renal vein were searched for existence of a posterior NC phenomenon.

Results: Dilatation of gonadal (33%), left lumbar (8%), hemiazygos/inferior phrenic (12%) and left suprarenal (9%) veins was identified. Pelvic varices/varicoceles (15%) and pseudothrombosis of the left renal vein (9%) were also depicted. The incidence of having a secondary vascular finding was significantly lower in pediatric age group, that is, none but one of the 13 pediatric patients showed dilated left lumbar vein. 24 (%14.2) patients had a posterior NC phenomenon among 168 patients with a retroaortic left renal vein. 4 (22%) of 18 patients with circumaortic left renal vein showed NC phenomenon.

Conclusion: Secondary vascular alterations are common in abdominal compression syndromes in adults, and may be the first recognized finding on CT. Awareness and recognition of these findings is important, since they, themselves, may be the source of the symptoms, and may guide therapeutic attempts.

SS 4.9

Replaced common hepatic artery from the superior mesenteric artery: MDCT classification focused on pancreatic penetration and the course of travel

H.K. Lim[1], H.I. Ha[2], M.-J. Kim[2]; [1]Seoul/KR, [2]Anyang-si/KR

Purpose: To categorize the subtypes of replaced common hepatic artery (RCHA) and evaluate the clinical implications.

Material and methods: 34 cases of the RCHA were evaluated retrospectively using MDCT. We categorized them into the three subtypes according to pancreatic penetration and the passing routes. The distance between the orifice of the superior mesenteric artery (SMA) and RCHA bifurcation (DSMA-RCHA) was measured using advanced 3D imaging software. Analysis of variance was used to evaluate the difference in DSMA-RCHA according to the RCHA subtype.

Results: Type A (n=17, 50%) referred to RCHA penetrating the pancreatic parenchyma, all crossing the dorsal aspect of the SMV. Among them, three cases were accompanied by the circumportal pancreas. Type B (n=10, 29%) referred to RCHA without penetration of the pancreatic parenchyma and crossing of the dorsal aspect of the MPV or SMV. Type C (n=7, 21%) referred to RCHA without penetration of the pancreas parenchyma and crossing of the ventral aspect of the MPV or SMV. The mean DSMA-RCHA of each subtype was as follows: type A, 3.13 cm (95% CI, 2.70-3.57); type B, 2.04 cm (95% CI, 1.40-2.68); and type C, 2.14 cm (95% CI, 2.23-2.92). The DSMA-RCHA of the penetrating pancreatic parenchyma of the RCHA was significantly longer than that of the non-penetrating pancreatic parenchyma (P=0.007).

Conclusion: Half of RCHA shows penetrating the pancreatic parenchyma and this type A takes off from the SMA more distally than RCHA without intrapancreatic penetration.

SS 4.10

CT angiography protocol for pancreatic cancer essential for surgical resectability

J. Grubor-Pilipovic, T. Kokovic, U. Milosevic, S. Stojanovic; Novi Sad/RS

Purpose: Early tumor detection and accurate radiological staging in patients with pancreatic carcinoma are crucial. The purpose was to review the technical aspects of the CT angiography (CTA) pancreas protocol and the findings relevant to diagnosis and staging of pancreatic carcinoma.

Material and methods: CTA pancreas protocol included: IV spasmolytic and oral contrast agent prior to the study, bolus tracking at the level of the celiac axis using an enhancement threshold of 150HU, triple phase acquisition. Major vessels running within 1cm from the tumor margin were evaluated. CT appearance was graded on a 0–4 scale (0: none, 1: <24%, 2: 25–49%, 3: 50–74%, 4: 75–100%) by circumferential contiguity of tumor to vessels.

Results: In forty-eight patients, CTA had the highest accuracy in assessing extent of primary tumor (73%), locoregional extension (74%), vascular invasion (83%), distant metastases (88%), tumor TNM stage (46%), and tumor resectability (83%). Surgical correlation of CT findings was available in 89 veins and 83 arteries, and both surgical and histologic correlations were available for 42 veins and 29 arteries. At surgical observation, 29 of 35 veins (82.9%) evaluated as CT grade 3 or 4 were found to be involved, whereas only 18 of 30 arteries (60%) evaluated as CTA grade 3 or 4 were proved to be involved.

Conclusion: The key to management in pancreatic carcinoma evaluation is determining resectability. It is, therefore, important that radiologists describe in detail the findings that are relevant for staging of pancreatic carcinoma and have a clear understanding of the implications of these findings.

11:00 - 12:30 **Meeting Hall IV**

Scientific Session SS 5

GI tract: new paradigms in diagnosis and intervention

SS 5.1

Positron emission tomography-defined tumour variables to predict pathological T-stage in patients with oesophageal cancer

K.G. Foley, B. Berthon, C. Parkinson, C. Marshall, W.G. Lewis, E. Spezi, S.A. Roberts; Cardiff/GB

Purpose: Oesophageal cancer (OC) staging involves a combination of imaging techniques, each with strengths and limitations. A single modality that accurately stages local and distant disease simultaneously does not currently exist. Local staging with EUS is an invasive procedure with associated risk of complications. We investigate whether PET-defined tumour variables, including novel texture analysis, can predict pathological T-stage (pT).

Material and methods: Patients undergoing surgical resection were staged with PET/CT prior to neo-adjuvant therapy between October 2010 and December 2014. PET-defined tumour variables were obtained using PET-STAT software and tumours were outlined with ATLAAS, a learning algorithm for optimised automatic segmentation, both developed at Cardiff University. Seventeen variables describing tumour characteristics were analysed. A one-way ANOVA test was used to identify differences in PET-defined tumour variables between pT-stages, confirmed by histopathological examination.

Results: Sixty-three patients were included [median age 64 (range 39-78), 57 adenocarcinoma, HGD=6, pT1=4, pT2=8, pT3=37, PT4a=8]. Nine PET-defined tumour variables including SUVmax (F=3.179, df=4, p=0.020), metabolic tumour volume (F=5.124, df=4, p=0.001), standard deviation (F=3.741, df=4, p=0.013) and intensity variability (F=5.485, df=4, p=0.001) demonstrated significant differences between pT-stages.

Conclusion: Preliminary data on 63 patients have shown that several PET-defined tumour variables have the potential to predict pT, although small group numbers limit the strength of this current study. Texture analysis of PET images is a rapidly evolving field that may improve OC staging.

SS 5.2

Positron emission tomography-defined tumour variables to predict lymph node metastases in patients with oesophageal cancer

K.G. Foley, B. Berthon, C. Parkinson, C. Marshall, E. Spezi, W.G. Lewis, S.A. Roberts; Cardiff/GB

Purpose: The overall survival of oesophageal cancer (OC) is poor and the presence of lymph node metastases (LNMs) is a major prognostic indicator. Texture analysis of medical images enables additional data to be extracted from routine staging investigations, quantifying intra-tumoural characteristics via non-invasive methods. We investigate whether positron emission tomography (PET)-defined variables and texture analysis of the primary tumour can predict LNMs.

Material and methods: Patients undergoing surgical resection were staged with PET/CT prior to neo-adjuvant therapy between October 2010 and December 2014. PET-defined tumour variables were obtained using PET-STAT software and tumours were outlined with ATLAAS, a learning algorithm for optimised automatic segmentation, both developed at Cardiff University. Seventeen variables describing tumour characteristics were analysed. A binary logistic regression model was used to identify independent predictors of LNMs, confirmed by histopathological examination.

Results: Sixty-three patients were included [median age 64 (range 39-78), 57 adenocarcinoma, N0=25, N1-3=38]. Multivariate analysis demonstrated 8 variables that were significantly and independently predictive of LNMs, including SUVmean (HR 0.025, 95% CI 0.001–0.426, p=0.011), dissimilarity [difference compared to adjacent voxel (HR 0.100, 95% CI 0.012–0.832, p=0.0.033)] and intensity variability [variation in intensity values across tumour (HR 1.752, 95% CI 1.032–2.972, p=0.038)].

Conclusion: Although small numbers limit this study, these preliminary results demonstrate texture variables that could predict LNMs, a major prognostic indicator. On-going work at our institution will investigate the added prognostic significance of texture analysis in OC staging.

SS 5.3

Treatment of benign esophageal fistulae by covered biodegradable stents

M. Hazlinger, M. Cerna, M. Kocher, V. Prasil; Olomouc/CZ

Purpose: To evaluate our experience with the treatment of postoperative anastomotic leaks and benign esophageal perforations with covered biodegradable stents.

Material and methods: From 2008 to 2015, we treated 25 patients with either an anastomotic leak or benign esophageal perforation by implanting covered biodegradable Ella-BD stents. The average age of patients was 59 years. Postoperative anastomotic leaks were treated in 14 patients; postdilatation rupture of benign stricture in 2 patients; spontaneous rupture after vomiting in 4 patients; in 2 patients rupture occurred iatrogenically, 1 patient had perforation in postradiation stricture and in 2 patients perforation occurred as a complication after metallic stent implantation.

Results: Thirty-nine covered biodegradable stents were implanted in 25 patients. Primary technical success was 100%. Small leakages were treated in 12 patients, 13 patients had significantly great to massive leakage. Clinical success (leak sealing) was achieved in small leakages in 11 patients (91.7%), 1 patient died after procedure due to circulatory collapse. In significantly great leakages clinical success was achieved in 4 patients (30.8%), 8 patients (61.5%) had proven leakage on control examination and 1 patient died after procedure due to circulatory collapse.

Conclusion: The use of biodegradable covered stents in the treatment of small anastomotic leaks or esophageal perforations is technically feasible and safe with significantly good clinical success. In great or massive leakages, despite worse clinical success, covered biodegradable stents implantation makes subsequent surgery easier.

SS 5.4

CTC versus transvaginal ultrasonography in the diagnosis of rectosigmoid endometriosis: a preliminary experience

E. Biscaldi, S. Ferrero, V. Remorgida, V. Vellone, U. Leone Roberti Maggiore, P.L. Venturini, G.A. Rollandi; Genoa/IT

Purpose: Rectosigmoid form is a severe presentation of deep endometriosis. Many techniques (endoscopy, CTenema, MRI) have been explored for diagnosis, few experiences are available on CTC. We compared the accuracy of CTC and transvaginal ultrasonography (TVS), evaluating the precision in estimating the length of the rectosigmoid nodules and the distance between them and the anal verge.

Material and methods: All patients recruited, scheduled for laparoscopy, had strong suspicion of intestinal endometriosis. TVS was performed contemporary to water distension of the rectum with 200mL of saline solution. CTC was performed with fecal tagging. A standardized CT examination protocol was used: 16-row CT, supine and prone acquisitions, decreasing of radiation dose (ASIR algorithm). CTC and TVS results were compared with surgical and pathologic findings.

Results: 45patients were included (mean age 34.2 (±5.1)). At the time of the study, 14 patients did not use hormonal therapies, 31 used it. 26 (57.1%) had surgical diagnosis of rectosigmoid endometriosis. In 11, endometriosis was located on the rectosigmoid, in 9 on the upper rectum and in 6 on the lower rectum. The mean (±SD) length of the nodules was 25.4(±6.1)mm. Significant difference in the accuracy of the two techniques was detected in the diagnosis (p=0.508). TVS and CTC similarly estimated the length of the endometriotic nodules (p=0.077). CTC was more precise than TVS in estimating the distance from the anal verge (p<0.001).

Conclusion: TVS and CTC have comparable accuracy in the diagnosis, similar precision in estimating the size of nodules; CTC is more precise in estimating the distance from the anal verge. Patients better tolerated TVS than CTC.

SS 5.5

Evaluation of rectal cancer response to therapy: role of MR-tumour regression grade to predict pathological complete response

S. Picchia, M. Rengo, D. Bellini, D. Caruso, D. De Santis, A. Laghi; Latina/IT

Purpose: To determine if a pathological complete response to therapy in rectal cancer can be predicted by tumour regression grade evaluated by MR (MR-TRG).

Material and methods: 65 patients, diagnosed with locally advanced rectal cancer were prospectively enrolled in the study. All patients underwent MRI on a 3-Tesla before, during and after chemoradiotherapy (CRT). All patients underwent total mesorectal excision (TME). MR-TRG was evaluated on T2-weighted fast spin-echo (FSE) multi-planar imaging. The MR-TRG was determined by the fibrosis/tumour ratio and was divided into 4 grades based on the percentage of fibrosis (<25%, <50%, <75%, 100%). Measurements were performed on all axial images including the tumour. MR-TRG evaluated on the second examination (during therapy) was correlated to the pathological finding after surgery, defined as partial response or complete response.

Results: A complete pathological response was observed only in patients with MR-TRG 4 (100% fibrosis) with a negative predictive value of 100%. In lower MR-TRG groups (1, 2 and 3), a partial response was observed.

Conclusion: MR-TRG 4 is an accurate predictor of complete response after CRT. When a lower MR-TRG is observed the persistence of disease should be suspected. This method, applied during therapy, may reduce the time to surgery.

SS 5.6

Long-term follow-up features on rectal MRI during "wait-and-see" in clinical complete responders after chemoradiotherapy: an update of 68 patients

M.M. Van Heeswijk[1], D.M.J. Lambregts[2], B. Hupkens[1], R. Beckers[1], M. Maas[1], M. Van Der Sande[2], G.L. Beets[2], R.G.H. Beets-Tan[2]; [1]Maastricht/NL, [2]Amsterdam/NL

Purpose: Non-operative treatment with stringent follow-up ("wait-and-see") is emerging as an alternative to surgery in clinical complete responders after chemoradiotherapy for rectal cancer. MRI is one of the main follow-up tools. The aim was to describe the long-term evolution in the morphology of the rectal wall during long-term follow-up of these patients.

Material and methods: 68 patients with a sustained complete response during "wait-and-see" follow-up were analysed. Patients underwent MRI 3 monthly (first year) and 6 monthly (second to fifth year). Two readers in consensus analysed the rectal wall morphology on the initial post-CRT scan and the evolution in morphology on the various sequential follow-up MRIs.

Results: Median follow-up was 30 months (range 6-98). 512 MRIs were analysed (median 7, range 3-15/patient). In 7% of patients, the rectal wall completely normalised post-CRT. The other 93% showed a fibrotic remnant (60% minimal fibrosis limited to the bowel wall; 21% thick/mass-like fibrosis and 12% irregular/spicular fibrosis). In 94% the rectal wall morphology remained unchanged during long-term follow-up, in 2% initial fibrosis later developed into a normalised wall, in 3% the fibrosis slightly thickened (without evidence of recurrence).

Conclusion: In the majority of patients with a complete response residual fibrosis is present post-CRT, which remains unchanged during long-term follow-up in almost all patients. A completely normalised wall is observed in 1 in 10-20 patients.

SS 5.7

Assessment of rectal tumour height and length on MRI: effect of using diffusion-weighted MRI instead of T2-weighted MRI

M.M. Van Heeswijk[1], D.M.J. Lambregts[2], L. Den Ouden[1], M. Ageitos Casais[1], M. Maas[1], G.L. Beets[2], R.G.H. Beets-Tan[2]; [1]Maastricht/NL, [2]Amsterdam/NL

Purpose: MRI is used to assess tumour height (distance from anorectal junction) and length, factors that influence treatment planning: large, distal tumours often require neoadjuvant chemoradiotherapy (CRT) and more extensive surgery. Diffusion-weighted MRI (DWI) is known to improve tumour conspicuity and may thus influence the assessment of tumour height/length. The aim was to compare DWI to standard (T2-weighted) MRI for the assessment of tumour height and length.

Material and methods: 72 patients were included: 23 non-locally advanced cases underwent a staging MRI followed by (5x5 Gy+) immediate surgery, 49 locally advanced cases underwent CRT followed by a second restaging MRI post-CRT. The MRI protocol (1.5T) included T2-weighted and DWI (highest b-value b1000) sequences. On each MRI scan, tumour length/height were measured by two readers (1) using T2W-MRI and (2) using b1000-DWI.

Results: Tumour length (averaged for two readers) pre-CRT was 4.8cm on T2W-MRI and 4.5cm on DWI (P=0.01), post-CRT it was 3.1cm on T2W-MRI and 2.2cm on DWI (P<0.001). Tumour height pre-CRT was 5.0cm for both T2W-MRI and DWI (P=0.86), post-CRT it was 5.4cm on T2W-MRI and 5.9cm on DWI (P=0.006).

Conclusion: T2W-MRI may systematically overestimate the distal tumour margin and tumour length, particularly after CRT. Since the tumour length and height influence treatment planning, it may be more appropriate to use DWI to assess these factors for clinical decision making.

SS 5.8

Additional value of diffusion-weighted imaging over standard MRI in the detection of pelvic recurrences

R. Kochhar, B. Carrington, B. Taylor; Manchester/GB

Purpose: To evaluate the additional value of diffusion-weighted imaging (DWI) over standard MRI sequences in the detection of pelvic recurrence in patients with treated pelvic malignancy.

Material and methods: We prospectively recruited 84 patients referred for MRI with clinical suspicion of pelvic recurrence into our study approved by the local ethics committee. Cases were consensus read and any lesions identified were scored on a 5-point scale (1=benign and 5=malignant) firstly on standard sequences (T1W and high-resolution T2W) alone and then scored again using both standard and DWI sequences. The 2 sets of scores were correlated with patient outcome based on histology and/or clinical/imaging follow-up of at least 2 years.

Results: 86 lesions were identified in 76 patients (8 patients excluded due to insufficient follow-up), 55 of these were benign and 31 malignant. The final score after addition of DWI increased in 14%, decreased in 49% and in 37% stayed the same. Standard MRI alone was compared to standard MRI plus DWI as below: sensitivity 71% versus 77%, specificity 62% versus 82% and accuracy 65% versus 80%. The median apparent diffusion coefficient (ADC) was 1.70 (benign lesions) and 0.94 (malignant lesions). A threshold ADC value of ≤1.1 had an accuracy of 88% for diagnosis of malignancy.

Conclusion: The addition of DWI to standard MRI sequences was helpful in assessing patients with suspected recurrence of previously treated pelvic malignancies.

SS 5.9

High-resolution MRI criteria for deferral of surgery trial

S. Balyasnikova[1], J. Bhoday[1], M. Siddiqui[1], S. Chua[1], D. Tait[1], I. Chong[1], B. Heald[2], P. Tekkis[1], A. Wotherspoon[1], G. Brown[1]; [1]Surrey/GB, [2]Basingstoke/GB

Purpose: Pathological complete response (cr) is observed in over 25% of rectal cancer patients treated with neoadjuvant chemoradiotherapy (CRT). Studies have shown that several MRI techniques could help in post-CRT response assessment and identifying imaging cr. We compared: mrVolumetric regression (VR), mrRECIST craniocaudal-length (ccl), DW-MRI against MR tumour-regression-grade system (mrTRG) to determine which method performed best.

Material and methods: We performed a retrospective analysis of 70 mrTRG (1-3) patients with low rectal cancer who had undergone neoadjuvant CRT and deferred surgery. High-resolution pre- and post-CRT MRI scans using standard T2 and DW imaging was performed. Incomplete response was defined for each method: <80% volume tumor regression and <50% ccl regression, presence of hyperintense MR signal on high B-value (>800) DWI and compared against mrTRG1-3 for regrowth rates.

Results: Median follow-up was 2.5 years. There was a lack of regrowth and sustained complete response in 70% of mrTRG1-3 patients. Using ccl, 62% were defined as incomplete response with 44/70 ineligible for deferral, of 26 eligible according to ccl, regrowths occurred in 19%. Using the VR definition, 54% (38/70) were defined ineligible and of the 32 VR eligible patients, 31% showed regrowth. Only 24% (17/70) patients showed no residual tumour on DW-MRI, with a 41% rate of regrowth.

Conclusion: Compared with mrTRG as a selection criterion for deferral-of-surgery, other modalities such as volume reduction and DWI are of insufficient sensitivity or specificity to enable accurate patient selection.

SS 5.10

Comparing MRI with fluoroscopy in defaecating proctography: the patient's perspective

R. Prasad, C. White, R. Wiles; Liverpool/GB

Purpose: Flouroscopy and MRI are currently used to investigate defaecation and pelvic floor problems. Fluoroscopy has advantages of imaging in a physiological sitting position and may better demonstrate intussusception. MRI has advantages of imaging all pelvic compartments and avoiding ionising radiation. Anecdotally it is suspected that MRI, allowing more privacy, may be better tolerated by patients. The authors aimed to evaluate patient experience of both techniques to potentially guide future modality choice.

Material and methods: This prospective study was conducted during June-December 2015 in a large teaching hospital. Patients completed a post-procedure questionnaire rating out of 5 (1=strongly disagree and 5=strongly agree) their satisfaction of each test including staff communication, patient facilities, replication of symptoms and whether it was comfortable, dignified and pain free.

Results: There were 19 and 8 patients in the fluoroscopy and MRI cohorts, respectively. Every question for both modalities scored median 5.0 and mean 4.4 or more, except for ease of replicating symptoms, for which MRI scored less than fluoroscopy at median 4.5 and mean 3.8 (vs 5 and 4.6, respectively).

Conclusion: Overall satisfaction for both tests was very high. Despite the anecdotal suspicion that MRI may be better tolerated by patients, this study did not find this. For ease of replicating symptoms MRI scored less than fluoroscopy. This may be due to the non-physiological positioning, potentially indicating that fluoroscopy may better demonstrate pathology compared to MRI.

11:00 - 12:30 **Congress Hall**

Scientific Session SS 6
HCC: imaging and assessment II

SS 6.1
Comparison of pulsed and oscillating gradient diffusion-weighted MRI for the characterization of hepatocellular nodules in liver cirrhosis: ex-vivo study in a rat model

M. Wagner, M. Ronot, S. Doblas, N. Pote, S. Lambert, V. Vilgrain, V. Paradis, B. Van Beers; Clichy/FR

Purpose: To compare the performance of pulsed-gradient-spin-echo (PGSE) and oscillating-gradient-spin-echo (OGSE) diffusion-weighted imaging for characterization of hepatocellular nodules in liver cirrhosis.
Material and methods: Twenty-four Wistar rats were included. Cirrhosis was induced by weekly intra-peritoneal injection of diethylnitrosamine (50mg/kg) during 16 weeks. After sacrifice, a cylindrical liver sample was resected and imaged in a 7T MR scanner. The protocol included T1-weighted/T2-weighted/PGSE/OGSE images (b=0/150/300/500s.mm-2). For precise radio-pathological correlations, only 80 nodules identified on T1/T2-weighted images and on pathological examination were analysed. Apparent diffusion coefficient (ADC) was calculated with a monoexponential fit. Two pathologists classified the nodules in regenerative (RN), low (LGDN) or high (HGDN) grade dysplastic nodules, early or progressed HCC. ADC were compared in group 1 (RN+LGDN), group 2 (HGDN+HCCearly) and group 3 (HCCprogressed) with Kruskal-Wallis test and areas under the receiver operating characteristic curves (AUROCs).
Results: ADCPGSE and ADCOGSE differed between the 3 groups (P=0.047/P=0.002). ADC increased in group 2 (ADCPGSE=0.753±0.255 in group 2 versus 0.812±0.198 in group 1; ADCOGSE=0.638±0.066 versus 0.654±0.125) and decreased in group 3 (ADCPGSE=0.601±0.080/ADCOGSE=0.682±0.083). AUROC for differentiating groups 1 and 2 was higher for ADCOGSE(0.77) than for ADCPGSE(0.68). AUROCs for differentiating groups 2 and 3 were similar for ADCPGSE(0.77) and ADCOGSE(0.72).
Conclusion: In this study, ADC during hepatocarcinogenesis had a complex behaviour and increased before decreasing. Our results suggest that OGSE seems to be more sensitive than PGSE to the first step of carcinogenesis.

SS 6.2
Comparison of gadoxetic acid-enhanced MRI and non-specific extracellular gadolinium contrast-enhanced MRI for the assessment of HCC response to loco-regional treatment

J. Rimola[1], M. Davenport[2], P.S. Liu[2], T. Brown[2], N. Parikh[2], B. Mckenna[2], J. Marrero[2], H.K. Hussain[2]; [1]Barcelona/ES, [2]Ann Arbor, MI/US

Purpose: Imaging assessment of HCC response to locoregional therapy (LRT) is critical for patient management. The aim was to compare the accuracy of gadoxetic acid-enhanced MRI (EOB-MRI) and non-specific extracellular gadolinium-based contrast-enhanced MRI (Gd-MRI) for the assessment HCC response to LRT using explant correlation as the reference standard.
Material and methods: Patients with cirrhosis and HCC treated with LRT who underwent EOB-MRI or Gd-MRI within 90 days of liver transplantation constituted the study population (n=49; 23 EOB-MRI, 26 Gd-MRI). Two radiologists independently reviewed the MR images blinded to histology to determine the percentage of viable residual HCC compared to the pre-treatment tumor volume. Liver explant histology (by lesion) was the reference standard. Sensitivities, specificities, and diagnostic accuracy determined by area under ROC curves were calculated. Agreement with pathology (i.e., percent necrosis) was assessed with intraclass correlation. Numbers in brackets are 95% confidence intervals.
Results: Gd-MRI had significantly greater agreement with histology than EOB-MRI (ICC: 0.98 [0.95-0.99] vs. 0.80 [0.63-0.90]). Sensitivities (EOB-MRI: 58% [28-85%] vs. Gd-MRI: 76% [50-93%]) and specificities (EOB-MRI: 85% [66-96%] vs. Gd-MRI: 84% [60-97%]) were statistically similar with wide confidence intervals. AUROC curves were 0.72 (0.55-0.85, EOB-MRI) and 0.80 (0.63-0.92, Gd-MRI).
Conclusion: Gd-MRI is more accurate than EOB-MRI for the determination of viable HCC following LRT, and therefore the preferred contrast agent to be used for its assessment in patients with cirrhosis. Specificity for Gd-MRI and EOB-MRI is similar.

SS 6.3
Comparison of the efficiency of tenth and twentieth minute delayed gadoxetate disodium (Gd-EOB-DTPA) enhanced MR images for diagnosis of small HCC (less than 2 cm)

A. Gocmez, M.G. Kartal, B. Bakir, B. Acunas; Istanbul/TR

Purpose: To find out whether 10-minute delayed images obtained after the injection of Gd-EOB-DTPA are sufficient to characterize small HCC (<2cm) in comparison to the images obtained at 20-minute delayed images, the recommended optimal image acquisition time.
Material and methods: 63 lesions in 48 patients diagnosed with small-sized (<2 cm) HCC on gadoxetate-enhanced MRI performed at Istanbul Medicine Faculty were retrospectively evaluated. MRI images were divided into 2 sets. 10-minute set contained 10-minute images in addition to T1, T2, DWI, and postcontrast phases and 20-minute set contained 20-minute hepatobiliary image in addition to T1, T2, DWI, and postcontrast phases for qualitative analysis. Two independent observers scored focal lesion signal intensities at 10- and 20-minute images. For the quantitative analysis, signal intensities were measured by placing ROI and calculated as was the contrast ratio.
Results: The quantitative analyses showed significant positive correlation between the 10-minute and 20-minute contrast ratio of the lesions. In qualitative analyses (rs=0.914,p<0.001), there was an excellent concordance between both observers for 10-minute and 20-minute images (Kappa for 10-minute images 0.907±0.053, for 20-minute images 0.930±0.049, p<0.001). There was moderate concordance between 10- and 20-minute images for each observer (Kappa for the first observer 0.523±0.095, for the second observer 0.490±0.095, p<0.001).
Conclusion: Compared to 10-minute images, 20-minute images did not reveal significant differences between HCC-liver signal ratio and diagnostic efficency. Therefore, especially for HCC evaluation in Child A group cirrhotic patients, obtaining only 10-minute images for delayed phase images depending on routine clinical needs will shorten image acquisition time but not affect the accuracy of the technique to a significant degree.

SS 6.4
Computed tomographic perfusion imaging for monitoring of transarterial chemoembolization treatment of HCC

H.P. Marquez Masquiaran[1], O. Karalli[2], H. Haubenreisser[3], H. Alkadhi[1], T. Brismar[2], T. Henzler[3], M.A. Fischer[1]; [1]Zurich/CH, [2]Stockholm/SE, [3]Mannheim/DE

Purpose: To prospectively monitor changes in tumor perfusion of HCC in response to transarterial chemoembolization (TACE) using perfusion-CT (P-CT).
Material and methods: 19 patients (mean age 69±6) undergoing P-CT before and directly after TACE due to multifocal HCC were prospectively included in this dual center study. Two readers determined arterial-liver-perfusion (ALP, in mL/min/100mL), portal-venous-perfusion (PLP, in mL/min/100mL) and hepatic-perfusion-index (HPI, in%) placing circular regions-of-interest covering the maximum diameter of each lesion (N=19) before and after TACE. Imaging follow-up with contrast-enhanced CT or MRI was used to distinguish responders (complete response/partial response) from non-responders (stable disease/progressive disease) following EASL criteria. Diagnostic performance of percentual changes in perfusion parameters before and after treatment (Δ) for early assessment of treatment response was determined using receiver operating characteristics.
Results: Mean ALP, PLP and HPI were 36.5, 16.6 and 75.9 before and 11.9, 23.3 and 46.8 after TACE, resulting in a ΔALP, ΔPLP and ΔHPI of -53%, 17% and -25%. Interreader agreement was fair to excellent for all perfusion parameters (ICC, 0.758-0.978). Before TACE, no significant correlations were found between perfusion parameters and treatment response (all p>0.05). After TACE, PLP was the only parameter to significantly correlate with treatment response (p<0.003) showing high accuracy for identification of TACE non-responders (AUC 0.943, 95% confidence interval 0.808-1.000, p<0.01).
Conclusion: P-CT is useful for monitoring the effects of TACE in HCC patients. Decreased PLP after TACE is a potential biomarker for tumor progression.

SS 6.5

Volumetric analysis versus response evaluation criteria in solid tumors and modified response evaluation criteria in solid tumors in the evaluation of HCC after transarterial chemoembolization

M. Stankova, T. Andrasina, J. Sedmik, V. Valek, L. Ostřížková, S. Tucek; Brno/CZ

Purpose: To compare volumetric analysis with the standard criteria - response evaluation criteria in solid tumors (RECIST) and modified response evaluation criteria in solid tumors (mRECIST) - for the evaluation of HCC and its response to transarterial chemoembolization (TACE).

Material and methods: The total of 40 patients treated in the University Hospital Brno with HCC were included in this study. All of them underwent TACE and their tumor range was evaluated on the CT/MR input and output. The volumetric analysis was performed semiautomatically. The survival of the patients was evaluated since the date of the first chemoembolization. The overall survival was evaluated by the Kaplan-Meier method and the differences in survival by the log-rank test.

Results: The strongest correlation has been proven between the length of survival and determination of the viable part of a tumor using volumetric analysis, and between the length of survival and the ratio viable/nonviable parts of the tumor. The median of survival since the first performed TACE is 15.0 months. RECIST and mRECIST have not been proven as a statistically significant factor of correlation with the overall survival.

Conclusion: Volumetric analysis was statistically proven the strongest factor of the correlation with the length of the survival of the patients, contrary to RECIST and mRECIST. It is a convenient way to evaluate the response of HCC to treatment, particularly in complex tumors after TACE.

11:00 - 12:30 **Forum Hall**

Scientific Session SS 7
Diffuse liver disease: technical update

SS 7.1

US-guided percutaneous liver biopsy: is pathological analysis affected by needle type?

A. Walker, P. Fineron, L. Wong; Edinburgh/GB

Purpose: Quantitative studies have shown that pathological assessment of disease stage is compromised in inadequate biopsies (<25mm in length, fewer than 11 portal tracts, or tissue area less than 22mm2). This study aimed to determine if the liver biopsy sample affected pathological analysis between side-notch and end-cutting needles.

Material and methods: Retrospective analysis of a total of 105 non-targetted US liver biopsies was carried out using either end-cutting and side-notch needles within a 42-month period (2011–2014). Blinded pathological analysis of the samples was performed by a consultant pathologist for adequacy, length and fragmentation. Furthermore, each biopsy was reviewed for associated complications, gauge of needle and number of throws.

Results: 49 biopsies using end-cutting needle and 56 with side-notch needle were analysed. The samples were deemed inadequate from 0% of the end-cutting group vs 24.5% of the side-cutting group. Length yield was higher in the end-cutting group (mean of 26.7mm vs 20.1mm), respectively, with less fragmentation in the end-cutting group (12% v 50%). Total number of portal tracts was also higher in the end-cutting group (mean 11.25 vs 7.3). The difference in length and number of portal tracts was statistically significant with p values of 0.0009 and 0.0263, respectively.

Conclusion: End-cutting needle performed better with regard to sample adequacy, specifically the number of portal tracts, length yield and degree of fragmentation.

SS 7.2

Evaluation of 3D VIBE-DIXON imaging sequence for quantification of hepatic iron overload at 3T

A. Kiani, E. Bannier, G. D'Assignies, G. Gambarota, H. Saint-Jalmes, Y. Gandon; Rennes/FR

Purpose: To assess at 3T the ability of 3D gradient echo (GRE) imaging to quantify liver iron concentration (LIC).

Material and methods: After IRB approval and written consent from all participants, 202 patients suspected of hepatic iron overload were included. Examinations were performed on a 3T MRI (MAGNETOM Verio, Siemens). Our reference 2D 11 echos multi-echo (ME)-GRE sequence (body coil), previously validated versus biopsy, was compared to a prototype 3D ME GRE (VIBE) sequence (surface coil). R2* mapping was computed and compared to R2* of reference sequence. VIBE R2* was converted to LIC according to Wood's formula adapted at 3T and compared to LIC provided by R2* and signal intensity ratio method of reference sequence. The shortest TE was 1.23 ms for both sequences.

Results: According, respectively, to 2D GRE and 3D ME VIBE results, mean R2* were 144±63Hz and 108±44Hz; mean LIC were 58±65µmol/g and 24±10µmol/g ($p<0.001$). Over all patients, correlation coefficients were 0.33 and 0.11 for R2* and LIC. Excluding patients with high LIC (>120 µmol/g), coefficients were 0.74 and 0.66. LIC correlation curve slope was 0.24.

Conclusion: 3D ME VIBE results are well correlated to our reference method for patients with low/medium overloads. Evaluation of major overloads is limited at 3T using only R2* if the first TE is not short enough. 3T extrapolated Wood's formula seems to significantly underestimate LIC with the use of VIBE sequence.

SS 7.3

Assessment of liver, pancreas, spleen and bone marrow iron distribution in patients with diffuse liver diseases using a 3T single breath-hold MR sequence

M. França[1], S. Silva[1], A. Alberich-Bayarri[2], L. Martí-Bonmatí[2], G. Porto[1], J.A. Oliveira[1], H. Pessegueiro-Miranda[1]; [1]Porto/PT, [2]Valencia/ES

Purpose: Multiecho GRE MR imaging is being used to determine liver R2* as an imaging biomarker of iron overload. Our purpose was to determine the R2* of liver, pancreas, spleen and bone marrow in patients with diffuse liver diseases and to evaluate their relationship.

Material and methods: The series included 100 consecutive patients with diffuse liver disorders, liver biopsy and abdominal MR examination (3T, single breath-hold, 12 echoes GRE sequence). Parametric iron R2* quantification was performed with a dedicated software selecting ROIs in liver, pancreas, spleen and vertebral bone marrow. Liver biopsy was used as gold standard for liver iron deposits grading (0-4).

Results: Regarding liver histologic iron grading, patients were distributed into none (49 cases), grade 1 (26), grade 2 (15), grade 3 (4) and grade 4 (6). Median (IQR) R2* values (s-1) in the liver were 42 (33); in pancreas: 30(10); in spleen: 28 (33); and bone marrow: 167 (66), respectively. Liver R2* was highly correlated with histologic determined siderosis (ρ=0.65, p<0.001). Liver R2* measurements were significantly correlated with pancreatic, splenic and bone marrow R2* measurements (ρ=0.22, ρ=0.55, ρ=0.32, p<0.05).

Conclusion: R2* measurements showed a correlation between liver, pancreas, spleen and bone marrow iron deposits in patients with diffuse liver diseases. These results add insights into liver iron disorders and their relationship with other abdominal organs and tissues.

SS 7.4

Liver iron overload assessment by MRI T2* relaxometry: a systematic review

J.M. Alústiza, J.I. Emparanza, E. Garmendia Lopetegui, E. Inchausti, E. Salvador, M. Ubeda; San Sebastián/ES

Purpose: To systematically review the T2* relaxometry methods used to quantify hepatic iron concentration.

Material and methods: A literature search was conducted in MEDLINE and EMBASE, using the search terms “MRI”, “Liver” and “Iron”, combined with appropriate boolean operators. Were considered relevant those articles that: (1) used T2* relaxometry to determine hepatic iron concentration and (2) included acquisition parameter specifications. Four radiologists agreed on the parameters to be considered in each article and designed a data collection sheet.

Results: From all retrieved papers (357) only 61 were judged to be relevant for our purpose. Reference T2* values used to differentiate between normal and iron overload (n=16) varied from 6.3 to 21 ms. First echo time (TE) varied from 0.8 to 4.7 ms. Only 14 articles compared the MRI results with direct biopsy measurement of hepatic iron. The threshold to differentiate normal from iron overload varied from 4.6 to 14.5 ms. Eighteen articles gave not only T2* values, but also its transformation into mg/ Fe/gr. Eight of them used the same mathematical formula but with different acquisition parameters.

Conclusion: There is no standard method. There is no standardised acquisition protocol. Results are not reproducible. Thus, T2* relaxometry is not yet a valid method for standardised assessment of hepatic iron concentration.

SS 7.5

Failure of liver MR elastography: what are the predictive factors?

M. Wagner, I. Corcuera-Solano, G. Lo, S. Esses, J. Liao, C. Besa, B. Taouli; New York, NY/US

Purpose: To determine the failure rate of liver magnetic resonance elastography (MRE) and to assess predictive factors for failure.

Material and methods: 781 consecutive patients (mean age 58 y, 63% male) including 650 (83%) with chronic liver disease who underwent liver MRE between 6/2013 and 8/2014 were retrospectively evaluated. MRE was acquired either on a 3T [GE750, n=443(57%)] or 1.5T system [GE HDX n=338(43%)], using a 2D-gradient-recalled-echo MRE sequence (4 axial slices) with 60Hz frequency. Image analysis was performed by 2 observers. A failure was defined as either no pixel with a confidence index higher than 95% on the confidence map or no wave propagation. The following parameters were noted: presence of cirrhosis, degree of ascites, steatosis, iron deposition and subcutaneous fat thickness.

Results: Failure occurred in 80 cases (10%). The rate of failure was significantly higher at 3T than 1.5T (n=68,15% vs. n=12,4%, P<0.0001). High weight, high BMI, presence of massive ascites, significant iron deposition, alcoholic liver disease and cirrhosis were all associated with a high failure rate (P<0.008). On multivariate analysis, only presence of iron, massive ascites and 3T were significantly associated with MRE failure (P<0.0001). Presence of steatosis and subcutaneous fat had no significant impact on failure rate (P>0.05).

Conclusion: Massive ascites, iron deposition and use of 3.0T were all independent factors associated with liver MRE failure. Alternate sequences should be developed and used in these scenarios.

SS 7.6

MR elastography of the liver: qualitative and quantitative comparison of gradient echo and spin echo echoplanar imaging sequences

M. Wagner[1], C. Besa[1], J. Bou Ayache[1], O. Bane[1], T.K. Yasar[1], M. Fung[1], R. Ehman[2], B. Taouli[1]; [1]New York, NY/US, [2]Rochester, NY/US

Purpose: To compare 2D gradient recalled echo (GRE) and 2D spin echo echoplanar imaging (SE-EPI) magnetic resonance elastography (MRE) sequences of the liver in terms of image quality and quantitative liver stiffness (LS) measurement.

Material and methods: This prospective study involved 50 consecutive subjects (M/F=33/17, mean age 58 y) who underwent liver MRI at 3.0T including two MRE sequences, 2D GRE and 2D SE-EPI (acquisition time 56s/16s). Image quality scores were assessed by two independent observers based on wave propagation and organ coverage on the confidence map (range 0-15). A third observer measured LS on stiffness maps (kPa). Mean LS values, ROI size (based on confidence map) and image quality scores between SE-EPI and GRE-MRE were compared using paired nonparametric Wilcoxon test. Reproducibility of LS values between the two sequences was assessed using intraclass coefficient correlation (ICC), coefficient of variability (CV) and Bland-Altman limits of agreement (BALA).

Results: There were 4 cases of failure with GRE-MRE and none with SE-EPI-MRE. Image quality scores and ROI size were significantly higher using SE-EPI-MRE vs. GRE-MRE (p<0.0001). LS measurements were not significantly different between the two sequences (3.75±1.87 vs. 3.51±1.53 kPa, p=0.062), were significantly correlated (ICC=0.909) with high reproducibility (CV=10.2%, bias=0.023, BALA=[-1.19; 1.66kPa]).

Conclusion: SE-EPI-MRE provided better image quality, larger confidence maps and faster acquisition time compared to standard 2D-GRE acquisition, with equivalent LS values.

SS 7.7

MR elastography and dynamic contrast-enhanced MRI for the non-invasive prediction of portal hypertension

M. Wagner, S. Hectors, O. Bane, T. Schiano, A. Fischman, B. Taouli; New York, NY/US

Purpose: To assess the diagnostic performance of MR elastography (MRE) and dynamic contrast-enhanced MRI (DCE-MRI) of liver and spleen for prediction of portal pressures.

Material and methods: This prospective study included 26 patients (M/F: 11/15, mean age 50y) who underwent hepatic venous pressure gradient (HVPG) measurement. MRI examination (1.5T/3.0T) was performed within 3 months of HVPG and included 2D-GRE-MRE of liver and spleen (n=25) and DCE-MRI using 3D-FLASH (n=20). Liver (LS) and spleen (SS) stiffness were determined from stiffness maps. DCE-MRI data were analysed using model-free parameters and pharmacokinetic modeling (liver: dual-input single compartment model, spleen: Tofts model). MRI parameters were correlated with HVPG. ROC and sensitivity/specificity analysis for prediction of HVPG≥5 and ≥10mmHg were performed for individual and combinations of parameters.

Results: Mean HVPG was 8.0±7.5 mmHg. There were significant positive correlations between HVPG and liver time-to-peak (TTP; r=0.712,P<0.001), liver mean transit time (MTT; r=0.514,P=0.020) and LS (r=0.478,P=0.016), while liver upslope was negatively correlated with HVPG (r=-0.548,P=0.01). ROC analysis provided significant AUCs for HVPG≥5mmHg (LS:0.786/SS:0.752) and HVPG≥10mmHg (LS:0.833, SS:0.771, liver MTT:0.786, liver TTP:0.857, liver upslope:0.869, spleen TTP:0.845, spleen upslope:0.786). Sensitivity/specificity of LS for detection of HVPG≥10mmHg were 67%/92%, while LS and spleen TTP in combination yielded the highest sensitivity/specificity (100%/92%).

Conclusion: Liver and spleen perfusion and stiffness metrics correlate with HVPG and can be combined into a multiparametric analysis to maximize diagnostic performance for the prediction of clinically significant portal hypertension.

SS 7.8

Clinical validation of a novel method to measure total liver and hepatic arterial blood flow using phase-contrast MRI in cirrhotic patients

M. Chouhan, A. Bainbridge, N. Davies, R. Jalan, S. Walker-Samuel, M. Lythgoe, S. Punwani, R. Mookerjee, S.A. Taylor; London/GB

Purpose: Non-invasive measurements of total liver blood flow (TLBF) and hepatic arterial flow (HAF) using phase contrast MRI (PCMRI) maybe valuable in evaluating portal hypertension. Direct HAF measurement is time consuming and technically challenging in patients with chronic liver disease, who often struggle to comply with MRI protocols. The purpose of this study was to validate a novel PCMRI technique to estimate TLBF and HAF in cirrhotic patients using inferior vena cava (IVC) and portal vein (PV) measurements alone.

Material and methods: Histologically confirmed cirrhotic patients (n=11) underwent PV, HA, proximal and distal IVC breath-hold, cardiac-gated 2D cine-PCMRI (5 mm slice thickness, α=10°, 256x256(FExPE)) at 3T, with velocity encoding settings of 40,60 and 80cm/s. TLBF was estimated by subtracting proximal IVC flow (above renal but below hepatic venous inlets) from distal IVC flow (above hepatic venous inlets, but below the IVC-right atrial junction). HAF was estimated by subtracting PV flow from estimated TLBF. Estimated flow measurements were compared with direct PCMRI measurements using Bland-Altman limits-of-agreement and Pearson's correlation coefficient.

Results: Estimated and directly measured Bland-Altman 95% limits-of-agreement were ±29.1 ml/min/100g for TLBF and HAF; and ±14.9% for HA fraction. There were significant correlations between estimated TLBF (r=0.9924; p<0.0001), estimated HAF (r=0.8061; p=0.0027), estimated HA fraction (r=0.8102; p=0.0045) and their directly measured counterparts. There were no significant differences between mean estimated and directly measured TLBF (99.1±14.8 vs 106.4±18.8 ml/min/100g; p=0.1328), HAF (24.2±5.15 vs 31.5±7.4ml/min/100g; p=0.1328) and HA fraction (22.±4.0 vs 25.2±3.7%; p=0.2486).

Conclusion: PCMRI IVC and PV flow measurements can successfully estimate TLBF and HAF in cirrhotic patients.

SS 7.9

Diagnosis of sinusoidal obstruction syndrome by contrast-enhanced US

L. Tarantino[1], P. Ambrosino[2], P. Gallo[3], A. Sullo[4]; [1]Pagani/IT, [2]Naples/IT, [3]Rome/IT, [4]Nocera/IT

Purpose: Hepatic sinusoidal obstruction syndrome (SOS) is a rare cause of acute hepatic failure. In this case report, we emphasize the diagnostic value of CEUS in the diagnosis of SOS.

Material and methods: A 62-year-old woman previously in good health conditions was admitted to our hospital for fever, vomiting, hypertension and epistaxis, abdominal pain, abdominal swelling, jaundice. She had received oral antibiotics (ciprofloxacin) for 10 days. Laboratory tests showed the following results: aspartate aminotransferase (AST) 1685 IU/L; alanine aminotransferase (ALT) 404 IU/L; alkaline phosphatase level 1145 IU/L; gamma-glutamyl transpeptidase level 96 IU/L, total bilirubin level 5.08 mg/dL; prothrombin time 30.2 %, platelets 31.000/mmcc; white blood cells 16.170/mmcc. The patient underwent CEUS and CT.

Results: Enhanced CT imaging showed hepatomegaly, massive ascites, multiple parenchymal undefined areas and absence of clear space-occupying lesions. CEUS showed large and completely avascular, irregular areas in the liver, crossed from patent portal, arterial and hepatic vessels. These aspects were highly consistent with massive occlusion of sinusoids without any vascular damage to portal spaces. The patient died because of liver failure 4 days after admission. At autopsy microscopic examination showed markedly dilated sinusoids filled with thrombi and fibrin and hepatic venules lumen obstruction.

Conclusion: Contrast material for CEUS, as blood-pool agent, allows a clear and well-defined detection of thrombosed sinusoids. CT and MR contrast materials could miss these aspects due to their interstitial diffusion.

SS 7.10

Hepatic enhancement of gadolinium-ethoxybenzyl-diethylenetriamine pentaacetic acid-enhanced 3-T MRI predicts the severity of liver cirrhosis

S. Lee; Seoul/KR

Purpose: To evaluate the effectiveness of gadolinium-ethoxybenzyl-diethylenetriamine pentaacetic acid (Gd-EOB-DTPA)-enhanced MR in the assessment for the severity of liver cirrhosis and quantitative liver function.

Material and methods: This retrospective study consists of 120 patients who underwent Gd-EOB-DTPA-enhanced 3-T MR (normal liver, n=30; Child-Pugh class A, n=30; B, n=30; C, n=30), using matching method by underlying disease, age (±5 years), gender, and creatinine (±0.05 mg/dL). Contrast enhancement index (CEI) was calculated and compared between normal liver and each cirrhotic group. We analyzed the correlation between hepatic function parameters and CEI on 20-min hepatobiliary phase (HP). The diagnostic performance of CEI on HP for the severity of cirrhosis was evaluated by area under curve analysis.

Results: The degree and time course of hepatic enhancement differed significantly between normal and each cirrhotic group (P<0.001). The mean CEI on HP constantly and significantly decreased as severity of liver cirrhosis progressed (P<0.001). Total bilirubin (P=0.022), albumin (P<0.001), platelet count (P=0.04) and model for end stage liver disease (MELD) score (P=0.01) were independent predictors of hepatic enhancement on HP. The CEI on HP showed good discriminatory ability in the severity of cirrhosis (AUC ≥ 0.94).

Conclusion: The degree of hepatic enhancement with Gd-EOB-DTPA indicates the severity of liver cirrhosis and correlates with hepatic function parameters.

11:00 - 12:30 **Meeting Hall V**

Scientific Session SS 8

Pancreas: solid and cystic tumours

SS 8.1

What is the optimal interval between abdominal CT and surgery for pancreatic adenocarcinoma? A review using evidence-based medicine methods

G.M. Healy, A.G. Carroll, D. Malone, E.R. Ryan; Dublin/IE

Purpose: Complete (R0) resection is the only curative therapy for pancreatic adenocarcinoma. Up to 21% of candidates may have unexpected disease progression found at surgery, not identified on pre-operative imaging.

Material and methods: A literature review was performed using evidence-based medicine (Oxford/McMaster) methodology. An answerable question was created using the population, intervention, comparison and outcome (PICO) format and used to perform a systematic search of international guidelines, information systems, Cochrane and Trip databases and Pubmed from 2005 to 2015. Reverse citation analysis was performed. Studies were appraised using the Oxford centre for evidence-based medicine (CEBM) tools for diagnostic studies.

Results: There are no international guidelines or secondary literature addressing this topic. Two retrospective cohort studies were identified and appraised as CEBM level of evidence level 2B and 3B. Both articles focused on liver and peritoneal metastasis, excluding local progression. Negative predictive values were reported for the 2B study and derived from provided data for the 3B study. Each paper shows a deterioration in negative predictive values with an increasing interval between imaging and surgery, dropping below 80% at 25 and 27 days, respectively.

Conclusion: Current best evidence (level 2B) directs that surgery for pancreatic adenocarcinoma should be performed within 25 days of the last CT scan.

SS 8.2

Differentiation of mass-forming focal pancreatitis from pancreatic ductal adenocarcinoma: value of characterizing dynamic enhancement patterns on contrast-enhanced MR images with adding signal intensity color mapping

Y.A. Choi, K.M. Jang, D.I. Cha, M. Kim, J.H. Min; Seoul/KR

Purpose: To evaluate the value of dynamic enhancement patterns on contrast-enhanced MR images with adding signal intensity color mapping (SICM) for the differentiation of mass-forming focal pancreatitis (MFFP) from pancreatic ductal adenocarcinoma (PDAC).

Material and methods: Clinicopathologically proven 41 MFFPs and surgically confirmed 144 PDACs were enrolled. Laboratory and MR imaging parameters were used to differentiate MFFP from PDAC. In particular, enhancement patterns on MR images with adding SICM were evaluated. Using classification tree analysis (CTA), we determined the predictors for the differentiation of MFFP from PDAC.

Results: In the CTA with all parameters except enhancement pattern on SICM images, ductal obstruction grade and T1 hypointensity grade of the pancreatic lesion were the first and second splitting predictors for differentiation of MFFP from PDAC in order. With adding enhancement pattern on SICM images to CTA, enhancement pattern was the only splitting predictor for the differentiation of MFFP from PDAC. The CTA model including enhancement pattern on SICM images has sensitivity at 78.1%, specificity at 99.3%, and accuracy at 94.5% for the differentiation of MFFP from PDAC.

Conclusion: The characterization of enhancement pattern for pancreatic lesions on contrast-enhanced MR images with adding SICM would be helpful to differentiate MFFP from PDAC.

SS 8.3

Pancreatic MRI for the surveillance of cystic neoplasms: comparison of a short with a comprehensive imaging protocol

R.M. Pozzi Mucelli[1], I. Rinta-Kiikka[2], K. Wünsche[3], J. Laukkarinen[2], K.J. Labori[4], K. Ånonsen[4], C. Verbeke[1], M. Del Chiaro[1], N. Kartalis[1]; [1]Stockholm/SE, [2]Tampere/FI, [3]Trondheim/NO, [4]Oslo/NO

Purpose: Pancreatic cystic neoplasms (PCN) are increasingly identified and multiple MRI controls are often recommended. This results to increased healthcare costs for the society. The study aims were, therefore, to evaluate: (i) whether a short-protocol (SP) MRI for the surveillance of PCN provides equivalent clinical information as a comprehensive-protocol (CP) and (ii) the cost reduction from substituting CP with SP for patient surveillance.

Material and methods: This retrospective study included 154 consecutive patients (median age: 66, 52% men) with working diagnosis of PCN and available contrast-enhanced MRI/MRCP. Three radiologists evaluated independently two imaging sets (SP/CP) per patient. The CP included: T2-weighted (HASTE/MRCP), DWI and T1-weighted (chemical-shift/pre-/post-contrast) images [acquisition time (AT)≈35 min], whereas the SP included: T2-weighted HASTE and T1-weighted pre-contrast images (AT≈8 min). Mean values of largest cyst/main pancreatic duct diameter (DC/DMPD) were compared. Agreement regarding presence/absence of cystic/MPD mural nodules (MNC/MNMPD), inter-observer agreement and cost differences between SP/CP were calculated.

Results: For DC and DMPD, mean values with SP/CP were 21.4/21.7 mm and 3.52/3.58 mm, while mean differences SP-CP were 0.3 mm (P=0.02) and 0.06 mm (P=0.12), respectively. For presence/absence of MNC and MNMPD, SP/CP coincided in 93% and 98% of cases, respectively. Inter-observer agreement was strong for SP/CP. SP cost was 25% of CP cost.

Conclusion: For the surveillance of PCN, short-protocol MRI provides information equivalent to the more time-consuming and costly comprehensive protocol.

SS 8.4

Usefulness of DWI combined with MRCP in detection of pancreatic cancer and secondary liver lesions

E. Kasatkina[1], T. Rieden[2], H.U. Kauczor[1], M. Klauß[1], V. Sinitsyn[2]; [1]Heidelberg/DE, [2]Moscow/RU

Purpose: To compare the performance of DWI combined with MRCP and contrast-enhanced (CE) MDCT with emphasis of isodense pancreatic cancer (PC) and liver metastases.

Material and methods: DWI (b values 0,50,400,800s/mm2) with MRCP and CEMDCT were performed in 64 patients with PC, the interval between studies did not exceed 10 days. All patients underwent surgery, in 38 patients carcinoma was resected. Images were analyzed in consensus by two radiologists blinded to clinical data. Results were correlated with intraoperative surgical and pathologic analysis.

Results: In seven patients (11%) the tumor was isodense to pancreatic parenchyma in CEMDCT, in all cases DWI/MRCP showed a superior performance to CEMDCT with mass identifiability at DWI and duct interruption at MRCP. In detection of liver metastases, CEMDCT and MRI results were discrepant in 13 patients (20%), in these cases lesions were smaller than 1-1.5cm. In two patients, metastases were missed both in CEMDCT and MRI. Sensitivity and specificity in detection of PC were 83% and 93% for CEMDCT and 81% and 88% for DWI/MRCP; in detection of liver metastases 54% and 76% for CEMDCT and 87% and 96% for DWI/MRCP.

Conclusion: DWI combined with MCRP was useful and preferable to CEMDCT in cases of isodense PC, showed equivocal performance to CEMDCT in cases of typical PC without need of i.v. contrast agent. DWI showed superiority in assessment of liver status in patients with PC, which is crucial for treatment strategy.

SS 8.5

Pancreas serous cystadenoma operated on by mistake: how to avoid it?

M.-P. Vullierme, N. Bessaoud, M. Lagadec, M. Ronot, V. Vilgrain; Clichy/FR

Purpose: To study misdiagnosis of pancreas serous cystadenoma, comparing MRI and MDCT of two series of serous cystadenoma, patients with typical pattern and patients operated on for erroneous diagnosis of other diseases.

Material and methods: Monocentric study, by two radiologists, retrospective over 10 years, of 77 patients with MRI (n=64) and or MDCT (n=63) (out of 126 patients), of n=85 serous cystadenoma diagnosed by resection (n=14), biopsy (n=8), endoscopic ultrasound (n=61). Criteria were: shape, presence of microcysts, presence of central scare, enhancement of peripheral wall, enhancement of internal cystic wall. Same criteria were studied upon n=14 patients operated on for erroneous diagnosis of NET n=6, and branch duct IPMN n=8.

Results: Microcysts were seen in 75% MRI and 45 % MDCT, and diagnosed with kappa=0.74 at MRI. Central scar had k=0.821. The 6 false NET were pseudo solid serous cystadenoma. This subtype contains microcyst at pathology. It has liquid pattern with T2, but microcyst were less diagnosed (p=0.034). The 2/6 cases ADC available were high (2.9). No true solid serous cystadenoma was present. The 8 false branch-duct-IPMN were of small size (mean 2 cm) and misdiagnosed with endoscopic US.

Conclusion: Pseudo solid serous cystadenomas could be diagnosed by mean of MRI with MRCP and DW-MRI. True solid serous cystadenoma is highly infrequent. Small branch-duct IPMN is difficult to differentiate from serous cystadenoma.

SS 8.6

Factors affecting transabdominal US detection rate of focal pancreatic lesion detected by endoscopic US

J.H. Kim[1], S.-Y. Choi[2], H.W. Eun[1], J.K. Han[1]; [1]Seoul/KR, [2]Bucheon/KR

Purpose: To assess the factors affecting detection rate of transabdominal ultrasound (TAUS) for focal pancreatic lesion detected by endoscopic ultrasound (EUS).

Material and methods: 338 consecutive patients with focal pancreatic lesions (cyst, n=253; adenocarcinoma, n=54; PNET, n=24; SPN, n=4; IPAS, n=1; metastasis, n=1; and lymphoma, n=1) detected by EUS and who underwent TAUS were included in our study. We reviewed formal report and assessed the presence or absence of focal lesion, single or multiple, size, and location on TAUS. We also assessed the same parameters for only cystic and solid lesions. Statistical analyses were performed using Chi-square tests, Student t test, and multivariable logistic regression analysis.

Results: The overall detection rate of TAUS was 61.5 % (208/338). Solid lesion, located in the body, and larger size (15.5+10.1mm vs 23.1+12.9mm) showed significantly higher detection rate than others (p<0.05). In multivariable analysis, body lesion (OR=2.337, 95% CI, 1.39- 3.92) and solid (OR=1.745, 95% CI, 1.02- 2.99) were significant variables (p<0.05). For cystic lesion, detection rate of TAUS was 58.5 % (148/253). In multivariable analysis, only body lesion (OR=2.435, 95% CI, 1.36- 4.36) was significant variable (p=0.003). On the contrary, for solid lesion, detection rate of TAUS was 70.6 % (60/85). However, in multivariable analysis, there was no significant variable.

Conclusion: Transabdominal US is useful for detection of focal pancreatic lesion detected by EUS, especially, located in body and solid lesion.

SS 8.7

Diagnostic value of contrast-enhanced transabdominal US and contrast-enhanced endoscopic US in pancreatic cystic tumors

X. Yu, Y. Sun, F. Zhou, P. Liang, F. Liu, E. Linghu, Z. Wang; Beijing/CN

Purpose: Pancreatic cystic tumors account for approximately 1-2% of pancreatic tumors. Contrast-enhanced US has now been used for the differential diagnosis of pancreatic cancer. This research aimed to investigate the diagnostic value of contrast-enhanced transabdominal ultrasound (CEUS) and contrast-enhanced endoscopic ultrasound (CE-EUS) in pancreatic cystic tumors.

Material and methods: We prospectively reviewed database of patients diagnosed with pancreatic cystic tumors between April 2015 and October 2015 in our institute. The inclusion criteria were as follows: patients who underwent conventional ultrasonography, CEUS, CE-EUS, CT/MRI, endoscopic US guided-FNA and were pathologically diagnosed with pancreatic cystic tumor. One radiologist with more than 20 years' experience in contrast-enhanced US read all the patients' imaging and made diagnosis. We compared the diagnostic results from CEUS and CE-EUS with that of histopathology and made comparisons between the diagnostic efficacy of CEUS and CE-EUS.

Results: A total of 55 patients were enrolled in this study. Diagnosis included pancreatic cystadenoma (n=36), pancreatic pseudocyst (n=6), intraductal papillary mucinous neoplasm of pancreas (n=5), solid-pseudopallary tumor of pancreas (n=3), pancreatic cyst (n=3), and pancreatic cystadenocarcinoma (n=2). The diagnostic accuracy of CE-EUS was significantly higher than that of CEUS (78.2% vs 85.5%, P =0.004). For 36 cases with pancreatic cystadenoma, CEUS and CE-EUS showed comparable diagnostic accuracy of 80.6 % and 88.9% (P=0.25).

Conclusion: CE-EUS is more effective in the diagnosis of pancreatic cystic tumor than CEUS.

SS 8.8

CT patterns of recurrence of pancreatic adenocarcinoma after surgery: is there a correlation with resection margin involvement?

F. Lombardo[1], G.A. Zamboni[1], M. Bonatti[2], G. Marchegiani[1], R.M. Pozzi Mucelli[1]; [1]Verona/IT, [2]Bolzano/IT

Purpose: To correlate CT pattern of recurrence of pancreatic adenocarcinoma with surgical margins status.

Material and methods: We retrospectively reviewed the multiphasic MDCTs performed on 43 patients (22 M, 21 F; mean age 66,6 years) with pancreatic adenocarcinoma recurrence after major pancreatic resection. Presence of local recurrence, metastatic disease or peritoneal carcinomatosis was noted and correlated with surgical margins status (R status) after resection. CT findings were confirmed by subsequent follow-up examinations, by increasing levels of CA 19-9 or by both.

Results: 31 patients underwent pancreaticoduodenectomy, 10 patients underwent spleno-pancreatectomy and 2 patients underwent total pancreatectomy. 31 patients had R0 resections and 12 patients had R1 or R2 resections. 18 patients presented local recurrence with solid tissue formation along the surgical margins and/or surrounding the main splanchnic vessels; of these, 14 had R0 resections and 4 had R1-2 resections. 26 patients had hepatic/pulmonary metastases; of these, 17 had R0 resections and 9 had R1 or R2 resections. 7 patients presented peritoneal carcinomatosis; of these, 5 had R0 resections and 2 had R1 or R2 resections. No association was observed between R+ status after resection and the presence of local recurrence and/or metastases (p=n.s.).

Conclusion: Metastatic disease is the most frequent pattern of recurrence of pancreatic adenocarcinoma after surgery, followed by local recurrence and peritoneal carcinomatosis. These patterns of recurrence do not appear to be associated with a specific surgical margins status.

SS 8.9

Low-dose CT perfusion in the evaluation of the pancreatic neuroendocrine tumors grading

Y. Nerestyuk, G.G. Karmazanovsky, A. Smirnov; Moscow/RU

Purpose: To evaluate CT perfusion values for pancreatic neuroendocrine tumors.

Material and methods: 8 patients with known pancreatic neuroendocrine tumor (4 patients - well-differentiated tumors (G1) and 4 patients - moderately differentiated tumors (G2)) underwent whole pancreas perfusion by a 256-slice CT (Brilliance iCT; Philips). 80-kVp/100mAs (low-dose) image data were reconstructed with iDose5 iterative reconstruction. Perfusion parameters were calculated with maximum-slope and dual-input one-compartment model methods. The parameters generated included the blood flow (BF, ml/min/100 ml tissue), blood volume (BV, ml/100 ml tissue), arterial blood flow (AF, ml/min/100 ml tissue), portal blood flow (PF, ml/min/100 ml tissue) and perfusion index (%) [PI = AF/(AF + PF) x 100].

Results: CT-perfusion characteristics of the healthy pancreatic parenchyma were: BF - 72±32.2 ml/min/100ml, BV - 26.2±10.7 ml/100ml, AF - 58.9±17.5 ml/min/100ml, PF - 30.3±28.8 ml/min/100ml. There was a significant difference in neuroendocrine pancreatic tumors between G1 and G2 for PI ($p<0.05$). TTP for G1 tumor decreases, for G2 maybe not changed in comparison with the parenchyma. TTP for the healthy pancreatic parenchyma was 16±6.4 sec. The radiation dose was 7.4±0.4mZv.

Conclusion: Low-dose whole pancreas CT perfusion values can be used as an additional parameter to differentiate the neuroendocrine tumors grading.

SS 8.10

Non-enhanced MRI versus contrast-enhanced MDCT in detection of pancreatic neuroendocrine tumors: does DWI add additional information?

K. Lomovtseva, D. Babaeva, N. Karel'Skaya, G.G. Karmazanovsky; Moscow/RU

Purpose: To compare non-enhanced MRI with contrast-enhanced MDCT in detection of pancreatic neuroendocrine tumors (NET) and evaluate the role of diffusion-weighted imaging (DWI) in detection of NETs.

Material and methods: 18 patients with 19 histologically proved solid pancreatic NETs were included in this study. The three imaging sets (I – arterial and portal phases of MDCT, II - T1-weighted image (WI) + T2WI with fat suppression, III - T1WI +T2WI with fat suppression+DWI (b value 600 s/mm2)) were retrospectively evaluated. The presence of tumor on all three sets was graded on a three-point scale (1 – definitely present, 2 – probably present, 3 – absent) by consensus of two radiologists. Grade 1 and 2 were considered as the presence of a tumor and relative sensitivity value was calculated.

Results: Tumor size varied from 3 to 41mm (mean value 18.5mm+-10.4mm). The presence of tumor was graded with MDCT: (1)-13, (2)-4, (3)-2; T1WI+T2WI: (1)-13, (2)-4, (3)-2; T1WI+T2WI+DWI: (1)-15, (2)-3, (3)-1. Relative sensitivity for sets I and II was 89.5%, for set III 94.7%.

Conclusion: DWI improves MRI sensitivity in detection of pancreatic NETs. MRI sensitivity with added DWI may be even higher than MDCT sensitivity.

11:00 - 12:30 **Chamber Hall**

Scientific Session SS 9

Appendix, mesentery and peritoneum: what's new?

SS 9.1

The diagnostic performance of CT in detecting colorectal peritoneal metastases

W.J. Van Eden, M.J. Lahaye, D.M.J. Lambregts, N.F.M. Kok, G.L. Beets, R.G.H. Beets-Tan, A.G.J. Aalbers; Amsterdam/NL

Purpose: Staging of tumor burden is essential in patients with colorectal peritoneal carcinomatosis (PC) who are eligible for cytoreductive surgery (CRS) and hyperthermic intraperitoneal chemotherapy (HIPEC). CRS-HIPEC is not advised in patients with more than 5 affected regions, according to 7-point Dutch region count. This study aims to compare the extent of PC on CT with the peroperative findings of PC and long-term survival.

Material and methods: Preoperative abdominal CT scans, for patients who underwent CRS-HIPEC, were performed between January 2005 and March 2007. An experienced radiologist evaluated all scans and scored the extent of PC according to the Dutch region count. A region count up to 5 was used as cutoff value for a good prognosis. Peroperative region count was the reference standard. Diagnostic performance of CT imaging was calculated. Survival analyses were performed.

Results: Forty-nine patients were included. The accuracy for selecting PC patients with a good or bad prognosis with CT was 86%. Disease-free survival (median 21.9; 19.0-24.7 months) and overall survival (median 39.5; 25.8-53.2 months) showed significant lower survival rates for patients with more affected abdominal regions on CT imaging ($p=0.041$ and $p=0.014$).

Conclusion: These results show that CT has a high accuracy in selecting patients who could benefit from CRS-HIPEC. Survival rates decreased when more abdominal regions on CT were affected.

SS 9.2

Diagnostic value of imaging for the detection of peritoneal metastases: a meta-analysis

M.J. Lahaye[1], D.M.J. Lambregts[1], I. Bekkers[2], A.G.J. Aalbers[1], W. Van Driel[1], R.G.H. Beets-Tan[1]; [1]Amsterdam/NL, [2]Maastricht/NL

Purpose: To determine the diagnostic value of pre-operative imaging in detecting peritoneal carcinomatosis (PC) in staging cancer patients.

Material and methods: A literature search of Ovid, Embase and Pubmed was performed to identify studies reporting on the accuracy of imaging for the detection of PC for colorectal, gastric and gynaecological cancers. Data extraction was performed by two observers in consensus. The sensitivity, specificity, and diagnostic odds ratio (DOR) were calculated using a bivariate random effects model and hierarchical summary operating curves (HSROC) were generated.

Results: The search resulted in 4165 articles. Thirty-five relevant studies fulfilled all the required inclusion criteria of >15 patients and surgery/histology/clinical follow-up as reference standard. From these articles 42 datasets could be extracted for analysis; 21 for CT, 5 for MRI, 5 for PET and 11 for CTPET. The pooled sensitivity, specificity, DOR for detection of PC were 73% (CI: 60-83%); 90% (CI: 84-94%); 25.6 (CI: 13.3-49.1) for CT and for MRI 78% (CI: 69-85%); 88% (CI: 83-92%); 26.6 (CI: 14.7-48.4). For PET these values were 53% (CI: 32-75%); 98% (CI: 94-99%); 55.7 (CI: 19.4-159.9) and CTPET: 87% (CI: 74-94%); 87% (CI: 69-95%); 46.0 (CI: 16.2-130.4).

Conclusion: This meta-analysis shows that CTPET is the most optimal imaging modality for the detection of PC. CT and MRI demonstrate similar results in detecting PC with a lower pooled sensitivity than CTPET.

SS 9.3

Prediction of complete resections after cytoreductive surgery based on the extent of colorectal peritoneal carcinomatosis

W.J. Van Eden, M.J. Lahaye, D.M.J. Lambregts, N.F.M. Kok, G.L. Beets, R.G.H. Beets-Tan, A.G.J. Aalbers; Amsterdam/NL

Purpose: Cytoreductive surgery (CRS) and hyperthermic intraperitoneal chemotherapy (HIPEC) are the treatments of choice for colorectal peritoneal carcinomatosis (PC). Prior to surgery abdominal CT was performed to gain insight into the extent of PC and the presence of distant metastases. Our objective was to evaluate the relation between the completeness of cytoreduction and the Dutch 7 region count evaluated with CT and during surgery.
Material and methods: Patients who underwent abdominal CT imaging for PC prior to CRS-HIPEC were eligible. The 7-point region count was assessed with CT by an experienced radiologist and peroperative by the operating surgeon, based on the Dutch region count. The completeness of cytoreduction was scored after CRS. Survival analyses were performed.
Results: Forty-nine patients were included. Patients who had an incomplete resection had more often PC in 5 to 7 regions during surgery (p=0.05). This result was not found using the CT assessment of the region score (p=0.60). Regarding disease-free and overall survival no differences were found between patients with complete and incomplete resections (p=0.39 and p=0.70).
Conclusion: Patients with four or less involved abdominal regions with PC peroperative were more likely to have a complete resection. CT assessment of the region score could not accurately predict a complete resection. No survival differences were seen between complete and incomplete resections.

SS 9.4

Role of elastosonography and diffusion-weighted MRI for the assessment of mesentery in patients with Crohn's Disease: preliminary results

D. Picone, R. Cannella, F. Vernuccio, C. Tudisca, M. Costanzo, A. Di Piazza, S. Serraino, G. La Tona, S. Salerno, A. Lo Casto, T.V. Bartolotta, G. Lo Re; Palermo/IT

Purpose: To evaluate the diagnostic role of elastosonography (USE) and the apparent diffusion coefficient (ADC) in differentiating oedematous and fibrotic change of mesentery of patients affected by Crohn's disease (CD).
Material and methods: In our department, twenty-five patients (mean age 33,12 ± 7,32) with CD underwent MR enterography and in the same time a real-time USE from July 2014 to October 2015. ADC values were calculated in the mesentery of pathological ileum (study group) and of normal ileum (control group) and were compared with the USE colour images in the same location. These results were statistically analysed.
Results: In the study group, the USE colour-scale coding showed a colour change from blue to red in the fibrotic change of mesentery, and blue-green in the oedematous change, 10 and 15 patients, respectively. Moreover, there was a significant (p<0,05) restriction of the diffusion in 13 patients with CD in the active phase (mean ADC values for the fibrotic mesentery: 2,83 ± 0,21 x 10-3, mean ADC values for oedematous mesentery: 2,17 ± 0,33 x 10-3). However, there was a significant difference between the control and the study group.
Conclusion: Evaluation of CD through USE and DWI is a more and more growing field, and many tools are available. USE also gives a confirmation of the nonsolid nature of the mesenteric mass because the tumor appeared almost entirely green (soft) on hardness colorimetric scale.

SS 9.5

withdrawn by the authors

SS 9.6

A clinical scoring system to discriminate between infected and non-infected postoperative abdominal fluid collections

C.G. Radosa[1], J.C. Radosa[2], D. Seppelt[1], A. Volk[1], R.-T. Hoffmann[1], V. Plodeck[1], M. Laniado[1]; [1]Dresden/DE, [2]Homburg/DE

Purpose: The aim of this retrospective study was to introduce and validate a CT-scoring system to discriminate between infected and non-infected postoperative abdominal fluid collections.
Material and methods: Between May and November 2015, all patients with portal-venous CT within 24 hours before CT-guided intervention were included. CTs were independently reviewed by two radiologists. Imaging signs (Hounsfield units - HU, wall enhancement, entrapped gas) and C-reactive protein ≤ 24h before CT were retrospectively correlated with results of microbiology (CT-guided intervention).
Results: 50 patients were included. On binary logistic regression analysis, the four parameters were associated with the incidence of infected abdominal fluid collections. A scoring system consisting of nominal categorization of the four variables was selected to develop a clinical scoring from 0 to 11 (C-reactive protein ≥ 150 mg/l: 4 points; HU ≥ 20: 2 points; wall enhancement: 2 points; entrapped gas: 3 points). The model was well calibrated (Hosmer-Lemeshow test). A cut-off of 5 points showed a 83% positive predictive value for the presence of infected fluid and a 74% negative predictive value. The sensitivity was 73% and the specificity was 83%.
Conclusion: This study provides a validation of a newly developed scoring system and cut-off values for the discrimination between infected and non-infected postoperative abdominal fluid collections. These findings might help to prevent unnecessary interventions.

SS 9.7

Abdominal fungal ball sign for invasive fungal infection in immunocompromised patients

S. Hur, M.H. Lee, S.-Y. Choi, B.H. Yi, H.K. Lee, S. Chin; Bucheon/KR

Purpose: To retrospectively review abdominal CT findings of patients with leukemia who suffered from suspected invasive fungal infections.
Material and methods: Medical records of 343 consecutive patients who were treated for leukemia in our hospital from March 2004 to February 2014 were reviewed. Two abdominal radiologists reviewed medical records and CT images of all patients. A total 155 patients took abdominal CT scan and we excluded 124 patients who had only lymphadenopathy or organomegaly due to leukemic involvement, or didn't have any abdominal lesion, who hadn't undergone any chemotherapy. Consequently, 31 leukemic patients who underwent CT examination for their abdominal symptoms were included in this study and they were divided into two groups. The first group was the fungal ball group consisting of 8 patients who had poorly enhancing ball-shaped lesion involving bowel or liver and the second group consisted of other patients. We compared ANC, duration between chemotherapy induction and CT scan, and clinical diagnosis for two groups.
Results: The result showed ANC was significantly low and the duration was significantly short for the fungal ball group. Clinical diagnosis of invasive fungal infection was significantly high for the fungal ball group.
Conclusion: Poorly enhancing ball-shaped lesion involving the liver or intestine of immunocompromised patients may suggest invasive fungal infection. The CT findings are not pathognomonic but are helpful in narrowing the differential diagnosis and early treatment in an immunocompromised patient.

SS 9.8

Suspected acute appendicitis (AA) in adults: influence of experience and intravenous (IV) contrast on diagnostic accuracy of multidetector computed tomography (CT)

Q. Monzani, S. Beranger-Gibert, M. Gavrel, L. Corno, S. Gerber, J. Gregory, H. Beaussier, M. Zins; Paris/FR

Purpose: To assess the influence of IV enhancement at CT for suspected AA depending on the reader's experience.

Material and methods: Over 14 months, patients from our emergency department who underwent CT for suspected AA were retrospectively included. The CT protocol included both unenhanced (UCT) and IV-enhanced CT (IVCT) scans. Four readers (two residents, one senior abdominal radiologist, one senior non abdominal radiologist (SNAR)) read each patient scans: UCT first then IVCT. At each reading, they were asked to confirm or rule out AA, to record their level of confidence and to propose an alternative diagnosis. The reference standard was pathologic specimen when available or a composite reference standard with other tests and follow-up when the patient did not undergo surgery.

Results: 62/175 patients included were finally diagnosed as AA. Diagnostic performances were not significantly superior with IVCT. Sensitivities for the four readers were, respectively, 95.6, 92.9, 91.1 and 93.8 with UCT and 98.2, 95.6, 97.3 and 97.3 with IVCT. Specificities were, respectively, 91.9, 96.8, 96.8, 80.7 and 95.2, 100, 96.8, 90.3. The SNAR had lower diagnostic performances. For the 113 non-AA remaining patients, an accurate alternative diagnosis was more frequently proposed with IVCT for all readers ($p<0.001$).

Conclusion: Regardless of the reader's experience, diagnostic performances of IVCT for the diagnosis of AA were not significantly superior to UCT. IV contrast administration improves CT performances in establishing an accurate alternative diagnosis.

SS 9.9

Contribution of diffusion-weighted MR imaging in follow-up of inflammatory appendiceal mass

Y. Metin, N. Orhan Metin, O. Özdemir, E. Özer; Rize/TR

Purpose: The main goal of this prospective study was to assess the added value of DWI in patients with inflammatory appendicial mass, who were decided a conservative treatment rather than immediate surgery. We also aimed to reveal alternative diagnoses such as tumors of cecum and appendix. This paper hypothesizes that DWI has the ability show the morphological and inflammatory changes of IAM to monitor the treatment response and show alternative diagnoses.

Material and methods: A total of 19 consecutive patients (mean age, 37+-13.1; range, 19-69; F/M: 9/10) with a clinical diagnosis of IAM followed-up with conservative treatment with or without interval appendectomy, were enrolled in this prospective study during a period of 19 months. All the diagnoses of IAM were made with contrast enhanced CT. After the CT diagnosis of IAM, only those patients who were decided a follow-up period of conservative treatment were included to our study. For follow-up period, DWI was chosen as the modality of imaging.

Results: It provided statistical confirmation that ADC values increase as CRP and WBC drop towards their normal level. Additionally, we assessed the size of IAM that the decrement also corresponded to increase of ADC value.

Conclusion: The study revealed that DWI has the ability to show the morphological and inflammatory changes of IAM to monitor the treatment response and show alternative diagnoses.

SS 9.10

Reliability of Alvarado score in acute appendicitis and establishment of a compound sonographic score

M. Mannil, C. Polysopoulos, D. Weishaupt, A. Hansmann; Zurich/CH

Purpose: The purpose of this clinical retrospective study is to improve the diagnosis of acute appendicitis using the established Alvardo score in its modified version [1.2] combined with sonographic criteria.

Material and methods: 132 patients with clinical suspicion of acute appendicitis received an abdominal US between 2012 and 2014. Sonographic criteria included appendix found, appendix diameter, appendix stone, compressibility, free fluid, mesenteric lymph nodes, inflamed mesenteric fatty tissue, perforation, abscess formation, small/large bowel affection and gynecological/urological pathologies. 100 patients had a surgically and pathologically confirmed acute appendicitis. The remaining 32 patients served as controls. Two models were computed in case the appendix was found (n=93) and when it was not (n=39) using logistic regression.

Results: The modified Alvarado score shows already excellent correlation with acute appendicitis with a cutoff value of 8. However, the diameter of the appendix adds significant information to this already strong predictor ($p = 0.003$). Adding the appendix diameter to the Alvarado score improves its sensitivity (~100%) and specificity (91.4%), resulting in the formula: modified Alvarado score + appendix diameter [mm] ≥13 is highly suggestive of an acute appendicitis, while 1 point/per mm is subtracted in case the appendix shows a diameter of <8 mm and 1 point/per mm is added if the diameter is >8 mm.

Conclusion: The modified Alvarado score shows excellent correlation with acute appendicitis. However, the diameter of the appendix adds significant additional information.

11:00 - 12:30 **Meeting Hall IV**

Scientific Session SS 10

Small bowel: technical update

SS 10.1

Early changes in MRI-measured segmental small bowel motility after initial anti-TNF treatment may predict longer term outcome

M. Almarashi, A. Plumb, A. Menys, E. Russo, T. Orchard, S. Halligan, S.A. Taylor; London/GB

Purpose: To determine if early changes in MRI-measured small bowel (SB) motility, occurring after initiation of anti-TNF treatment, are associated with longer-term response to therapy.

Material and methods: 11 patients were recruited prospectively; 20 patients were identified retrospectively. All completed a standard SB-MRI protocol pre- and post- initiation of anti-TNF therapy. Patients ingested mannitol orally and underwent 8-12 breath-hold coronal TruFISP/BTFE imaging at a frame rate of 1/second, encompassing the entire SB. Two radiologists independently segmented diseased ileum and motility was measured using a validated optic-flow algorithm. Subsequently, patients were followed-up for a mean of 10.3 months, with response to therapy being judged via a physician global assessment (PGA). Motility changes in responders vs. non-responders were compared via the Wilcoxon rank sum test. The sensitivity and specificity of improved motility for response to therapy was calculated.

Results: Mean time between initiation of anti-TNF therapy and follow-up SB-MRI was 16 weeks (range = 8-28 weeks). Patients who were durable responders (i.e. sustained response to anti-TNF therapy at a mean of 10.3 months) had significantly greater motility changes (median=83.3% rise from baseline) than non-responders (median=22.7% reduction from baseline, p<0.001). Improved motility at mean 16 weeks had 93% Sn and 83% Sp for predicting longer term response.

Conclusion: Early changes in segmental SB motility measured by MRI may be able to predict longer-term durable response to anti-TNF therapy.

SS 10.2

Elevated fecal calprotectin (FCP) is associated with correlation between restricted diffusion (RD) and mucosal inflammation (MI) in patients with quiescent Crohn's disease (CD)

E. Klang, U. Kopylov, S. Ben-Horin, A. Eliakim, M.-M. Amitai; Ramat Gan/IL

Purpose: Elevated fecal calprotectin (FCP) is associated with correlation between restricted diffusion (RD) and mucosal inflammation (MI) in patients with quiescent Crohn's disease (CD).

Material and methods: The study was partially sponsored by a generous grant from the Helmsley Charitable Trust. 52 quiescent CD patients prospectively underwent MRE, video capsule endoscopy (VCE), FCP and CRP. RD was assessed in the terminal ileum qualitatively (absence/presence) and quantitatively (ADC). The VCE Lewis score (LS) was calculated for the distal small bowel. MI was defined as LS>135. ADC's correlation to biomarkers was calculated. RD's sensitivity and specificity for MI and ADC's correlation to LS were assessed for elevated FCP (>100 µg/g) and normal FCP patients. ROC curve assessed ADC's prediction of patients that had both MI and elevated FCP.

Results: 26/52 (50%) patients had elevated FCP. ADC correlated with FCP (r=-0.527, p<0.0001), but not CRP. RD's sensitivity and specificity for MI and ADC's correlation to LS were high in elevated FCP patients (76.1%,100%; r=-0.5, p=0.009, respectively) but insignificant in normal FCP patients (15.4%, 76.9%; r=0.146, p=0.496, respectively). ADC's prediction in patients with both MI and elevated FCP was high (AUC=0.832). ADC of 1.92X103 mm2/s had 89.7% sensitivity and 71.4% specificity for these patients.

Conclusion: In quiescent CD patients, RD significantly associates with MI in elevated FCP patients, but not in normal FCP patients. RD represents a more severe inflammation and shows low sensitivity for MI in normal FCP patients.

SS 10.3

Diffusion-weighted imaging in the assessment of the small bowel in patients with inflammatory bowel disease: a comparative study using standard magnetic resonance imaging, diffusion-weighted imaging and capsule endoscopy

M.L. Hahnemann[1], A. Dechene[2], S. Kathemann[2], S. Sirin[2], G. Gerken[2], T. Lauenstein[2], S. Kinner[2]; [1]Muenster/DE, [2]Essen/DE

Purpose: To investigate diffusion-weighted imaging (DWI) compared to standard MRI (sMRI) in the assessment of inflammatory lesions of the small bowel using small bowel capsule endoscopy (CE) and ileocolonoscopy (ICS) as standard of reference.

Material and methods: MRI of the small bowel including DWI followed by CE and ICS were retrospectively analyzed in thirty consecutive patients with suspected or established diagnosis of IBD. Inflammatory lesions of the small bowel detected in endoscopy (CE and ICS) were compared with findings in 1.) standard MRI alone (sMRI = MRI without DWI), 2.) DWI alone and 3.) sMRI in combination with DWI (sMRI + DWI). Sensitivity, specificity and accuracy were calculated.

Results: DWI alone showed slightly superior results in sensitivity compared to sMRI alone (60.0% vs. 55.2%). DWI alone and sMRI alone revealed lower results in sensitivity than sMRI + DWI in combination (60.0% and 55.2% vs. 70%). Specificity and accuracy of different readouts showed no differences (specificity/accuracy; sMRI alone 99.5%/94.2%, DWI alone 99.0%/94.2%, sMRI + DWI 99.0%/95.4%). Missed lesions in sMRI and DWI were located in the proximal bowel segments.

Conclusion: DWI can be recommended as additional sequence for the detection of inflammatory small bowel lesions.

SS 10.4

Prelesionary bowel dilatation and morphological signs of inflammatory bowel disease correlation in children with Crohn's disease

J. Podgorska, R. Pacho, P. Albrecht, I. Lazowska; Warsaw/PL

Purpose: To determine if prelesionary bowel dilatation correlates with morphological signs of inflammatory bowel disease in children with Crohn's disease.

Material and methods: MRE examinations of 77 consecutive paediatric patients (36 female, mean age 14, range 7-17), with confirmed Crohn's disease were retrospectively reviewed. The 'cine' imaging (coronal, Fiesta sequence, TR 3.5 ms, TE 1.5ms, slice thickness 5mm, 22 sec. breath hold) was performed through the small bowel. The bowel segment proximal to the terminal ileum (TI) was identified, and its maximal diameter measured. Other MRE sequences were used to evaluate Crohn's disease activity characteristics in TI: bowel wall thickening, T2 hyperintensity, relative contrast enhancement (RCE), deep ulcerations and mesenteric hyperaemia. ROC curve analysis was performed.

Results: Strongest correlation was found between the dilatation and presence of bowel wall thickening (OR=1.17, p<0.02, area under ROC curve (AUC) 0.72), RCE (OR=1,1, p<0.006, AUC=0,72), T2 hyperintensity (OR=1,05, p<0,125, AUC=0,72) and mesenteric hyperaemia (OR=1,09, p<0.03, AUC=0.76). Strong correlation was found between these inflammatory signs and prelesionary dilatation greater than 22,5mm. There was no correlation between the length of inflammatory segment nor presence of deep ulcerations and prelesionary dilatation.

Conclusion: This retrospective study showed that prelesionary dilatation is related to signs of inflammatory activity and is not related to the length of the inflamed bowel segment. Cut-off value in adolescents should be considered as 22,5mm.

SS 10.5

The assessment of usability of the ADC as a biomarker of the inflammatory process activity in the Leśniowski-Crohn's disease

O. Kozak, A.M. Szymańska-Dubowik, D. Gałąska, K. Markiet, E. Szurowska; Gdańsk/PL

Purpose: The aim of the study is to assess the usability of the ADC as a biomarker of the inflammatory process activity in the CLC disease.

Material and methods: We analyzed the MRI scans of 43 patients, performed on 1.5T scanner. A standard protocol of MR enterography was performed including the DWI sequence and the following values b (0, 100, 300, 500, 800 s/mm2), the ADC maps were generated. The ADC value was obtained by way of a 5-fold measurement and marking a region of interest (ROI) for each of the affected bowel area. The results were averaged and compared with the value of CRP and colonoscopy results and histo-pathological examination.

Results: Based on the colonoscopy and histopathological examination, in 32 of 43 examined patients an active stage of CLC was ascertained, and in 11 people – a chronic stage. The average value of the ADC for the active stage of disease was ~1.411x10-3 mm2/s, and for the chronic stage ~1.750x10-3 mm2/s. 27 patients' CRP was accordant with the clinical stage of the disease activity and the ADC value, low in active stage and high in chronic stage. In 6 cases of the active process, the value of the ADC correlated with disease activity better than the CRP.

Conclusion: The apparent diffusion coefficient (ADC) can be used as a biomarker of active inflammation in Leśniowski-Crohn's disease.

SS 10.6

Role of DWI in MR enterography evaluation of tumoral and inflammatory lesions of small bowel

V. Sobko, A. Karpenko, O. Shchukina, E. Bogdanova, A. Dmitriev; Saint Petersburg/RU

Purpose: DWI analysis of small bowel lesions in the differential diagnosis of neoplasms and inflammation in Crohn's disease at performance of magnetic resonance enterography (MRE).

Material and methods: 49 patients (23 men and 26 women) with long painful syndrome in an abdominal cavity were included in this study. MRE was performed after oral administration of 1000 ml Mannitol-solution (2.5%). The study protocol included sagittal, axial, coronal true-FISP, T2 HASTE sequences and contrast-enhanced T1 VIBE. DWI with b-values 50, 400, 800 s/mm2 and intravenous injections of contrast agent was performed in all cases.

Results: 8 patients (16.3 %) were identified malignant tumors (adenocarcinoma, lymphomas, carcinoid tumors, GIST, metastasis). In all cases the high signal on DWI b=800 s/mm2 with diffusion restriction ranged from 0.45 ±0.1 mm2/s to 0.91 ±0.1 mm2/s . 2 patients (4.1 %) in ileocecal valve benign tumors (lipoma) were found, that characterized by high signal on T1 and T2-weighted images and low signal on T1 and T2. Tumors characterized by low signal on DWI b=800 s/mm2 and ADC ranged from 1.34 ±0.1 mm2/s to 1.45 ±0.1 mm2/s. Wall of small intestine in Crohn's disease show ADC value from 0.90 ±0.1 mm2/s to 1.25 ±0.1 mm2/s.

Conclusion: DWI is good additional tool for performing MRE in differential diagnosis Crohn's disease and neoplasms of small bowel.

SS 10.7

CT characteristics and clinical relevance of the small-bowel faeces sign in patients with small-bowel obstruction: are there different faeces signs?

W. Khaled[1], L. Corno[1], I. Millet[2], A.-M. Chuong[1], M.A. Benadjaoud[3], I. Boulay-Coletta[1], M. Zins[1]; [1]Paris/FR, [2]Montpellier/FR, [3]Villejuif/FR

Purpose: To study CT characteristics of the small-bowel faeces sign (SBFS) and its clinical relevance to predict medical management success and the diagnostic of ischaemia in small-bowel obstruction (SBO) due to matted adhesions or adhesive bands.

Material and methods: Two senior radiologists retrospectively performed blinded and independent review of 237 consecutive CT scans amongst 216 patients with SBO due to matted adhesions or adhesive bands for assessment of the transition zone (TZ) (number, location) and the SBFS characteristics (presence, location related to the TZ, length, density, morphology) between two groups: surgical (n = 108) or medical (n = 129) treatment.

Results: The prevalence of SBFS was 41.4%. SBFS was proximal to the TZ in 82 of 98 CT scans (83.7%). A unique TZ (OR = 0.25; IC95% 0.13-0.46, p < 0.001), an anterior location of the TZ (OR = 0.39; IC95% 0.18-0.86, p = 0.019) or an SBFS >5 cm proximal to the TZ (OR = 0.43; IC95% 0.21-0.89, p = 0.022) were inversely predictive of surgery. More than two TZ (OR = 6.54, IC95% 2.96-14.41, p < 0.001) or an SBFS >5 cm located in a closed loop (OR = 4.00; IC95% 1.11-14.42, p = 0.034) were predictive of ischaemia.

Conclusion: The SBFS is a common and useful sign to locate the TZ. There are multiple types of SBFS and their clinical relevance depends on their length and location.

SS 10.8

The incidence and risk factors of transient bowel angioedema induced by iodinated contrast media

N. Seo, Y.E. Chung, J. Lim, M.-J. Kim, K.W. Kim; Seoul/KR

Purpose: To investigate the incidence and risk factors of iodinated contrast medium (CM)-induced bowel angioedema during CT.

Material and methods: From July 2013 to July 2015, 427 patients with a history of adverse reactions to iodinated CM during CT (group A) and propensity score-matched control group (group B, n=427) without adverse reactions were studied. Age, sex, CM types, CM injection protocols including velocity, total amount and duration, the presence or absence of prophylaxis and accompanying allergic symptoms were compared between patients with angioedema and those without angioedema in group A. In addition, the incidence of bowel angioedema was compared between group A and B using a clustered logistic regression method.

Results: The incidences of CM-induced bowel angioedema in group A were 3.3 % (14/427) in per-patient analysis and 2.6 % (15/578) in per-exam analysis. Angioedema was found in 1 of 14 patients in consecutive CT examinations. None of the patient demographics or CM related factors were different between the patients with and without bowel angioedema (P > 0.05). The incidences of CM-induced bowel angioedema in group B were 1.7 % (8/458) and 1.9 % (8/427) in per-patient and per-exam analyses, and these rates were not significantly different between group A and B (P=0.35 and P=0.37, respectively).

Conclusion: The incidence of CM-induced bowel angioedema during CT was 1.7%-3.3% and none of the studied risk factors was associated with bowel angioedema.

SS 10.9

CT enteroclysis imaging features for diagnosis, treatment and follow-up of small bowel neuroendocrine tumors

D. Maiettini, C. Valloncelli, P. Ferolla, A. Rebonato, M.C. Bellucci; Perugia/IT

Purpose: To analyse the role of CT-enteroclysis (CT-E) in the identification and diagnosis of small-bowel neuroendocrine tumors (SBNET) defining CT-E findings and SBNET features useful in the management of SBNET.
Material and methods: We selected for this retrospective study 75 patients suspected of primary or recurrence SBNET, who underwent to CT-E from 2009 through 2015. Written informed consent was obtained. After the positioning of an 8-French naso-jejunal tube, CT-E acquisition was performed with a double continuous bolus (DCBT) or a single-bolus technique (SBT). SBNET diagnosis was immune-histochemical confirmed after surgery. Imaging features were gathered to evaluate sensitivity and prevalence of each one. Primary tumor densitometric values and the radiation dose were analyzed comparing the two contrast techniques.
Results: Fifty-one cases of primary SBNET were detected and 29 (57%) were multifocal. Tumor densitometry showed a statistical non-significant difference between phases (p>0.05). DCBT did not allow a significant radiation dose reduction (p>0.05). Among all the 75 CT-E in patients with SBNET, 53% had liver metastasis. Desmoplastic reaction was present in 38 (51%) cases, but only in 9 (12%) figured out as “Sun Burst Sign”. In the 57% (43 patients) of cases mesenteric lymph nodes were noticed and a mesenteric mass was present in 41 cases (33 cases presented vascular encasement).
Conclusion: CT-E might be proposed as the main imaging technique in the diagnosis and planning the management of SBNETs.

SS 10.10

Contrast-enhanced computed tomography (CT) assessment of the positioning of a novel intestinal bypass liner device (Endobarrier) for type 2 diabetes: correlation of the degree of metabolic response with the extent of intestinal exclusion

V. Hedayati[1], P. Sen Gupta[1], B.M. Mcgowan[1], R.E. Ryder[2], F. Rubino[1], S.A. Amiel[1], S.M. Ryan[1]; [1]London/GB, [2]Birmingham/GB

Purpose: The Endobarrier is a 60cm duodenal bypass liner placed endoscopically for up to 1-year, improving glucose control and weight in obesity-related diabetes. The aim of this study was to evaluate whether failure of response to Endobarrier relates to chyme leakage around the device’s proximal anchor.
Material and methods: Adults with suboptimally controlled type-2 diabetes and obesity who had undergone minimum 6 months’ treatment were classified as responders (≥3% initial body weight loss; ≥1% HbA1c reduction) and non-responders. They underwent limited CT post oral contrast. Leakage was evaluated (none, mild, moderate, severe) by an independent experienced radiologist, blinded to responder status, and correlated with metabolic response. Anteroposterior, craniocaudal dimensions of the anchor, wall thickness, liver HU were measured.
Results: Twelve patients (53.7±8.7years, 33.3% male, 75% Caucasian, BMI, 115.5±13.8kg, HbA1c 8.9±2.2%) underwent scanning at 8.5 (6.0-11.7) months. There were 6 responders [mean weight loss 15.8±8.9kg (13.4±7.4%) and HbA1c fell 2.0±0.6%] and 6 non-responders [weight fell 10.6±6.2kg (9.7±5.5%) and HbA1c fell 0.4±1.1%], P=NS and P=0.02 respectively, with no baseline differences between groups. One (16.7%) moderate leak was found in non-responders vs none in responders, with no correlation between leakage and responder status (P=0.27). Anteroposterior, craniocaudal dimensions of the anchor, wall thickness and fatty liver status were not significant.
Conclusion: Endobarrier was successful at providing duodenal exclusion with associated weight loss but variable diabetes improvement. Reasons other than peri-Endobarrier leakage must account for failure of glycaemic response.

11:00 - 12:30 **Panorama Hall**

Scientific Session SS 11

Rectum: advances in tumour assessment

SS 11.1

Dynamic contrast enhanced MRI in rectal cancer: tumours with poor prognosis show low vascularity

M. Maas[1], G. Shakirin[2], D.M.J. Lambregts[3], M. Weibrecht[2], M. Perkuhn[2], M.H. Martens[1], R. Dijkhoff[1], G.L. Beets[3], R.G.H. Beets-Tan[3]; [1]Maastricht/NL, [2]Aachen/DE, [3]Amsterdam/NL

Purpose: Dynamic contrast-enhanced (DCE) MRI has shown promise for response evaluation after chemoradiation for rectal cancer. Conflicting results have been reported regarding predictive value of DCE-MRI for tumour aggressiveness. Aim was to explore the value of DCE-MRI with gadofosveset trisodium for the distinction between patients with and without poor prognostic factors.
Material and methods: 19 patients with primary rectal cancer underwent DCE-MRI with gadofosveset trisodium. DCE-MRI was processed using the Intellispace Discovery research platform (Philips Healthcare). One reader delineated whole-tumour volumes. Semi-quantitative DCE-parameters based on the enhancement curve (initial slope, wash-in, wash-out, initial signal excess, wash-in time to peak(TTP), final slope, TTP, maximum enhancement, mean transit time, AUC) were compared between patients with and without prognostic unfavourable factors (primary metastasis, lymphangio-invasion, CEA, cT&cN-stage, cMRF-stage and differentiation grade). P<0.05 was statistically significant.
Results: Patients with metastasis (n=2) had significantly lower peak enhancement, washin-time and AUC60. Patients with high CEA (> 5,n=9) had significantly lower peak enhancement and total AUC. Patients with lymphatic invasion (n=3) had significantly higher maximum slope. A trend to higher washin-time was found in patients with unfavourable characteristics at histopathology (n=12,p=0.076).
Conclusion: Low vascularity at DCE-MRI indicates a risk of poor prognosis. This might reflect a poor vascular organisation/efficiency in patients with metastasis, angio-invasion and high CEA. Possibly this is due to rapid tumour growth. Poor vascularity can be important for treatment decisions with regard to chemotherapy and/or radiotherapy.

SS 11.2

Multiparametric functional MR imaging assessment of primary rectal cancer: correlation between diffusion, perfusion, magnetization transfer and signal intensity measurements

D.M.J. Lambregts[1], J.J.M. Van Griethuysen[1], G. Shakirin[2], M. Maas[3], M. Weibrecht[2], M.J. Lahaye[1], M.M. Van Heeswijk[3], G.L. Beets[1], M. Perkuhn[2], R.G.H. Beets-Tan[1]; [1]Amsterdam/NL, [2]Aachen/DE, [3]Maastricht/NL

Purpose: Different functional MRI-techniques have shown promise in rectal cancer assessment, but limited data exist on how various quantitative measurements correlate. Aim was to evaluate how different components of multiparametric-MRI are related to each other in primary rectal tumours.
Material and methods: 19 primary rectal cancer patients underwent multiparametric-MRI including diffusion-weighted (DWI), dynamic contrast-enhanced (DCE), magnetisation transfer (MT), T2-weighted, and contrast-enhanced 3DT1-weighted imaging (with gadofosveset-trisodium). Sequences were processed using the Intellispace Discovery research platform (Philips Healthcare). One reader delineated whole-tumour volumes on b1000-DWI, which were subdivided into three equal subvolumes (high, intermediate and low DWI-signal). The following parameters were compared between these 3 DWI-signal groups: ADC, MT-ratio, signal intensity on T2W and contrast-enhanced MRI, and various DCE parameters (initial slope, wash-in/wash-out, initial signal excess, wash-in time to peak (TTP), final slope, TTP, max enhancement, mean transit time, AUC).
Results: Significant differences between the 3 DWI-signal groups were found for the DCE-parameters initial slope and initial signal excess (both higher with increasing DWI-signal; P=0.008/0.026). ADC, wash-in TTP, TTP and AUC60 were significantly different for the high vs. low DWI-signal groups with lower ADC and TTP, and higher wash-in TTP and AUC60 in the high DWI-signal group.
Conclusion: Differences in perfusion correlate with differences in DWI signal intensities within rectal tumours. DCE and DWI measurements may thus be of complementary value in the functional multiparametric-MRI assessment of rectal cancer.

SS 11.3

Comparison of the effectiveness of computed tomography and magnetic resonance imaging in the preoperative staging of rectal cancer

D. Oncel; Izmir/TR

Purpose: To compare the effectiveness of computed tomography and magnetic resonance imaging in the preoperative staging of rectal cancer.

Material and methods: The study includes 105 patients who have been operated with the diagnosis of rectal cancer between October 2011 and December 2015. The patients were graded with CT and MRI examinations and the results were compared with the pathologic grading.

Results: Pathologically, 86 patients were graded as T1-2 and 19 patients as T3. With CT 80 patients with in T1-2 grade were correctly graded, 6 patients were graded as T3. Among 19 patients in grade T3, 17 were correctly graded and 2 patients were misgraded as T2. With MRI, 82 patients with in T1-2 grade were correctly graded, 4 patients were graded as T3. 18 was correctly graded as T3 and only one was misgraded as T2. According to those results, the sensitivity and specificity of CT in the preoperative staging of rectal cancer was 86% and 93% and for MRI 94% and 95%, respectively.

Conclusion: According to our study, although MRI has higher sensitivity and specificity values than CT in the preoperative staging of rectal cancer, no statistically significant difference was found between the two methods. The reason for the relatively high sensitivity and specificity of CT compared to the literature data is the thin slice collimation and multiplanar imaging capability of multislice CT imaging.

SS 11.4

Quantifying treatments based on CT versus mandated MRI-based policy for rectal cancer staging: implications for patient care and outcomes

A. Wale, M. Chand, M. Usher, M. Capucci, G. Brown; Surrey/GB

Purpose: MRI is mandatory for staging rectal cancer in the UK due to its ability to identify validated poor prognostic features. However globally MRI has not replaced the CT/EUS staging method. Consequent implications for patient care according to preoperative treatment strategies have not previously been assessed or quantified. This study aims to compare the impact on treatment when rectal cancer is staged by CT compared with MRI within three recognised preoperative strategies; current and future planned USA/global guidelines and local treatment guidelines.

Material and methods: Retrospective case-controlled study of rectal adenocarcinoma patients. MRI is used as the reference. Concordant treatment decisions are those when CT and MRI based treatments are identical, discordant decisions are when treatments differ.

Results: 85 patients were included. When preoperative treatment is decided by CT alone 20-31% of patients receive discordant treatment depending on the treatment strategy followed. More patients are over-treated (12-20%) than under-treated (5-15%). For treatment strategies based on T and N staging, CT T overstaging (13/20, 65%) and N overstaging (12/20, 60%) account for the majority of discordant decisions. When treatment strategy also considers EMVI & CRM status, CT EMVI understaging (36/38, 95%) accounts for most discordant decisions.

Conclusion: Irrespective of treatment strategy local staging of rectal cancer with CT alone is unsafe; up to 31% of patients receive discordant treatment, with both under and over-treatment likely to impact negatively upon morbidity and mortality.

SS 11.5

Limited accuracy of DCE-MRI in identification of pathological complete responders after chemoradiotherapy treatment for rectal cancer

T. Tong[1], M.J. Gollub[2], K. Zakian[2], J. Zheng[2], M. Gonen[2], M. Weiser[2]; [1]Shanghai/CN, [2]New York, NY/US

Purpose: To determine if DCE-MRI can accurately detect patients with pathologic complete response (pCR) to treatment for rectal cancer

Material and methods: From a surgical database between 2007-2014, consecutive patients with stage II/III primary rectal adenocarcinoma; received chemoradiotherapy which terminated within 8 weeks of the index MR;underwent curative intent total mesorectal excision surgery within 6 weeks of the index MRI and had a diagnostic quality rectal MRI with dynamic contrast enhanced (DCE) imaging were included. Two experienced radiologists, in consensus, used image J to draw regions of interest (ROI) on the sagittal DCE image. Data were exported to Matlab for analysis of Ktrans, Kep, vp and ve. Mean values and decile and quartile histogram analysis of Ktrans, Kep, vp and ve were derived to see if post-CRT DCE-MRI could distinguish between patients with and without pCR.

Results: In 49 patients (19 males and 30 females; mean age 53 yrs); using histogram analysis, the 90th percentile Ktrans and Kep values (p=0.025 and 0.048 respectively), were statistically significantly different between patients with and without pCR. Using a cutoff value of Ktrans90 = 0.16 min-1 , the sensitivity, specificity, PPV and NPV were: 0.69, 0.55, 0.42, and 0.78 respectively. The area under the receiver operating characteristic curve (AUC) was 0.73.

Conclusion: The DCE-MRI parameter Ktrans90 could identify patients with complete pathological response to chemoradiotherapy for rectal cancer with an AUC of 0.73.

SS 11.6

Significance of mesorectal vascular lesion on rectal MRI for assessment of metastasis among indeterminate hepatic lesions on CT in patients with rectal cancer

K.A. Kang[1], K.M. Jang[1], S.H. Kim[1], T.W. Kang[2], D.I. Cha[1], S.Y. Heo[1]; [1]Goyang si/KR, [2]Seoul/KR

Purpose: To assess the significance of mesorectal vascular lesion (MVL) on rectal magnetic resonance imaging (MRI) for evaluating metastasis among indeterminate hepatic lesions on CT in patients with rectal cancer.

Material and methods: A total of 210 patients with rectal cancer who underwent preoperative contrast-enhanced abdominopelvic computed tomography (CT), and rectal and liver MRI were included. Univariate analysis and multivariate logistic regression were used to evaluate determining factor for the significance of indeterminate hepatic lesions on CT in patients with rectal cancer.

Results: Hepatic metastases were diagnosed in 29 (20.6%) of 141 patients who had indeterminate hepatic lesions on preoperative CT obtained for rectal cancer. On univariate analysis, carcinoembryonic antigen level, N stage and MVL grade on rectal MRI ($p < 0.05$) were associated with the possibility of metastasis for indeterminate hepatic lesions on CT. On multivariate analysis, MVL grade on rectal MRI was the only independent factor associated with the possibility of metastasis for indeterminate hepatic lesions on CT (p=0.0002).

Conclusion: MVL grade on rectal MRI is an independent factor for estimating hepatic metastasis among indeterminate hepatic lesion on CT in patients with rectal cancer.

SS 11.7

Organ-preservation for clinical complete responders after chemoradiation for rectal cancer: does timing of selection matter?

M. Maas[1], M.H. Martens[2], B. Hupkens[1], M. Van Der Sande[3], M.M. Van Heeswijk[1], R. Beckers[1], D.M.J. Lambregts[3], J. Leijtens[4], C. Hoff[5], L. Heijnen[1], G.L. Beets[3], R.G.H. Beets-Tan[3]; [1]Maastricht/NL, [2]Sittard/NL, [3]Amsterdam/NL, [4]Roermond/NL, [5]Leeuwarden/NL

Purpose: Wait-and-see policy can be offered to clinical complete responders (cCR) after neoadjuvant chemoradiation. Aim was to evaluate whether the timing of selection influences outcome, by comparing patients included for wait-and-see at initial assessment with patients who were selected after a second assessment 3 months later.

Material and methods: 114 eligible patients underwent initial assessment with endoscopy and MRI+DWI ±8 weeks post-CRT. 61 had a typical cCR and were selected for wait-and-see immediately(W&S-1). 24 had residual tumour and underwent TME. The other 29 patients had a near cCR (not meeting 1 or 2 criteria for cCR) and underwent a second assessment after 3 months, after which 24 were included for wait-and-see(W&S-2) and 5 for TME. 3-6 monthly follow-up (with MRI+DWI and endoscopy) was performed.

Results: 2/24 patients that underwent TME after first assessment had a pathologic complete response(pCR). 1/5 that underwent TME after second assessment had pCR. In total 85/114 (75%) were in wait-and-see with 25 months median follow-up. 3-year LRFS was 88% for W&S-1 compared to 77% for W&S-2 (p=0.22), 3-year overall survival was 96% and 96%, respectively (p=0.95). All local regrowths could be easily salvaged with standard TME.

Conclusion: A second response assessment after 3 months can offer wait-and-see to more patients. However, there is a trend towards lower 3-year LRFS in patients included after second assessment, although overall survival is not influenced by the lower LRFS.

SS 11.8

MRI can accurately predict sphincter preservation after CRT

J. Krdzalic[1], M. Maas[2], S. Engelen[2], J.J.M. Van Griethuysen[3], D.M.J. Lambregts[3], G.L. Beets[3], R.G.H. Beets-Tan[3]; [1]Heerlen/NL, [2]Maastricht/NL, [3]Amsterdam/NL

Purpose: It is believed that chemoradiation for low rectal cancer increases sphincter preservation. Aim was to evaluate with MRI whether sphincter preservation is increased by chemoradiation and whether MRI can predict sphincter preservation after chemoradiation.

Material and methods: A radiologist independently evaluated the T2-weighted MRIs (in 3 directions) in 47 patients before and after CRT with tumours <5 cm from the anorectal junction (ARJ) and measured distance of the lower tumour pole to the ARJ. Also, a confidence level score for feasibility of sphincter preservation was scored (CL=0 definitely no sphincter preservation, CL4=sphincter preservation definitely possible). Likelihood for sphincter preservation before and after CRT was compared and receiver operator characteristics(ROC) curves with area under the curve (AUC) were calculated.

Results: Mean distance from ARJ increased significantly during CRT from 21±16mm pre-CRT to and 31±18mm post-CRT (P<0.001). In 42% sphincter preservation was deemed not feasible pre-CRT, which decreased to 23% after CRT. AUC for sphincter preservation based on confidence level score was 0.84(0.72-0.96), with sensitivity of 100% and specificity of 44%. Based on post-CRT height measurement AUC was 0.87(0.76-0.98), with optimal size cut-off at 26 mm (sens: 86%, spec: 71%).

Conclusion: This is the first study to show that CRT increases the distance to the ARJ and thus leads to a higher rate of sphincter preservation. MRI can accurately predict sphincter preservation after CRT.

SS 11.9

Artefacts on diffusion-weighted MRI of the rectum: how often do they hamper our clinical interpretation?

D.M.J. Lambregts, M.J. Lahaye, J.J.M. Van Griethuysen, M. Maas, G.L. Beets, R.G.H. Beets-Tan; Amsterdam/NL

Purpose: Single-shot echo planar imaging (EPI) diffusion-weighted imaging (DWI) is the most commonly used DWI method in the abdomen. DWI-EPI sequences are prone to susceptibility artefacts, which may pose a particular challenge when performing DWI of the bowel. Aim was to quantify in which percentage of rectal DWI-examinations (without bowel preparation) clinical interpretation is hampered by artefacts.

Material and methods: 360 rectal MRI-examinations (at 1.5T) including T2-weighted MRI (in 3 directions) and an axial EPI-DWI (highest b-value b1000) were analyzed. MRIs were obtained in 127 patients undergoing (sequential) follow-up after primary rectal cancer treatment. Two readers visually assessed image quality of each MRI (T2W and DWI) and scored it as [1] sufficient for clinical interpretation or [2] uninterpretable due to artefacts. DW-imaging assessment was performed using the high b-value (b1000) images.

Results: On T2W-MRI, 2/360 (1%) examinations were uninterpretable due to artefacts, the other 358/360 (99%) were of sufficient quality for clinical interpretation. On DWI, 299/360 (83%) examinations were of sufficient quality, the other 61/360 (17%) were uninterpretable due to artefacts. Artefacts were mainly caused by air in the rectal lumen or suboptimal fat-suppression causing band-like artefacts.

Conclusion: In a substantial percentage of rectal EPI-DWI examinations (without bowel preparation), image quality is hampered by artefacts. As such, we need to look for ways to improve image quality, e.g. by means of bowel preparation (rectal filling/enema) or by further optimizing image acquisition.

SS 11.10

Prediction of sphincter preserving by MRI: accuracy and reproducibility between a radiologist and a surgeon

J. Krdzalic[1], M. Maas[2], S. Engelen[2], J.J.M. Van Griethuysen[3], D.M.J. Lambregts[3], G.L. Beets[3], R.G.H. Beets-Tan[3]; [1]Heerlen/NL, [2]Maastricht/NL, [3]Amsterdam/NL

Purpose: Feasibility of sphincter-preserving surgery in low rectal tumours (<5 cm from anorectal junction) is based on the exact distance from the anorectal junction (ARJ), rigidity upon digital rectal examination and presence of sphincter invasion. Aim was to evaluate whether a radiologist and a surgeon can predict feasibility of sphincter-preserving surgery at T2W-MRI.

Material and methods: 44 patients with a rectal tumour <5 cm from the ARJ that did not undergo CRT were included. T2W-MRI in 3 directions was evaluated by a specialized radiologist and a specialized surgeon for feasibility of sphincter-preservation. Distance from ARJ (mm) and confidence level scores for sphincter-preserving surgery and sphincter invasion were scored. Reference standard was type of surgery combined radicality of the resection.

Results: Both the radiologist and surgeon could predict sphincter preservation accurately with AUC 0.81 (radiologist) and 0.82 (surgeon). Sensitivity and specificity are 75% and 83% (radiologist) and 50% and 87% (surgeon), respectively. Height was predictive of sphincter preservation for both readers with AUC of 0.90 (radiologist) and 0.88 (surgeon), with optimal cut-off at 18 and 26 mm, respectively. Interobserver reproducibility of height was ICC 0.70 (0.51-0.82) and of confidence level scores for sphincter preservation was k0.53 (0.31-0.76).

Conclusion: Sphincter preservation can accurately be predicted with T2W-MRI by both specialized radiologists as well as specialized surgeons. Height is the most accurate predictor with a cut-off of approximately 18-26 mm.

11:00 - 12:30 **Congress Hall**

Scientific Session SS 12

Rectum: new paradigms for evaluating tumour response

SS 12.1

Assessment of the IMV diameter and IMV:CIV ratio on computed tomography in response to adjuvant radiotherapy for locally advanced rectal adenocarcinoma

J.A. Stephenson, C. Ivan, J. Mullineux, B. Billimoria, R. Verma, V. Shah, A. Rajesh, M. Elabassy; Leicester/GB

Purpose: Neoadjuvent chemo-radiotherapy for locally advanced rectal cancer (LARC) aims to downstage prior to definitive management. Radiological reassessment of the tumour post-therapy has implications for treatment. Various methods of assessing tumour response exist including TNM stage, RECIST and TRG-score.

Material and methods: We assessed the inferior mesenteric vein diameter (IMV) and the IMV:common iliac vein ratio (IMV:CIV) pre and post-radiotherapy of 100 patients with LARC to ascertain if these are surrogate markers of tumour response. IMV measurements were performed by two radiologists and MRI response assessed by two radiologists blinded to CT measurements.

Results: At baseline IMV diameter was significantly higher for cases with local lymphadenopathy - N0 = 5.2 mm vs N1/2 =6 mm (p=0.0059) - and lymphovascular invasion (LVI) – –ve 5.4 mm vs +ve 6.4 mm (p=0.0001). Post radiotherapy there was a significant decrease in the IMV diameter and IMV:CIV in cases with treatment response compared to non-responders - percentage change IMV:CIV = -16.46% vs +1.18% (p=0.0002). These results were reproduced between TRG groups using ANOVA (p=0.0001). There was also a significant decrease in IMV when assessing lymph-node and LVI response versus non-responders (p=0.0001 and 0.0001 respectively).

Conclusion: We confirm that IMV diameter and IMV:CIV are surrogate markers of lymph-node status and LVI at baseline. IMV diameter and IMV:CIV are also a markers of tumour , LN and LVI response to chemo-radiotherapy.

SS 12.2

withdrawn by the authors

SS 12.3

Dynamic contrast-enhanced MRI: use in predicting pathological complete response to neoadjuvant chemoradiation in locally advanced rectal cancer

T. Tong, Y. Sun, Y. Gu; Shanghai/CN

Purpose: To determine the ability of dynamic contrast enhanced (DCE-MRI) to predict pathological complete response (pCR) before preoperative chemoradiotherapy (CRT), in locally advanced rectal cancer.

Material and methods: In a prospective clinical trial, 38 enrolled patients underwent pre- and post-CRT DCE-MRI at 3.0T. The tumor length and the following perfusion parameters (Ktrans, kep, ve) were measured for the tumor and compared between the pCR group and the non-pCR group, as well as before and after CRT. For categorical variable comparison, the Kruskal–Wallis test was used. P<0.05 was considered significant.

Results: No difference in tumor length was found between pCR and non-pCR group pre-and post-CRT (P=0.26, 0.35, respectively). Before CRT, the mean tumor Ktrans in the pCR group was significantly higher than in the non-pCR group (P=0.01). A Ktrans of 0.66 emerged as the best cut-off for distinguishing pCR from non-pCR. Regarding kep and ve, significant differences were also observed between pCR and non-pCR groups (P=0.02, 0.01, respectively). The mean Ktrans, kep and ve values post-CRT were not significantly different between pCR and non-pCR groups (P=0.10, 0.12, 0.08, respectively).

Conclusion: Before neoadjuvant chemoradiotherapy in rectal cancer, DCE-MRI can distinguish between complete and incomplete response using a Ktrans threshold of 0.66 with a sensitivity of 100%.

SS 12.4

Standardized index of shape (DCE-MRI) and standardized uptake values (PET): two quantitative approaches to discriminate chemo-radiotherapy locally advanced rectal cancer responders under a functional profile. Two biological sides of the same coin?

A. Petrillo, M. Petrillo, R. Fusco, A. Avallone, S. Lastoria; Naples/IT

Purpose: We investigated the potential use of dynamic contrast-enhanced MRI (DCE-MRI) to discriminate responder from non-responder patients after neoadjuvant chemo-radiotherapy (CRT) for locally-advanced rectal cancer (LARC) in comparison with [18F]2-fluoro-2-deoxy-D-glucose positron emission tomography (FDG-PET/CT).

Material and methods: 75 consecutive patients with LARC were enrolled in a prospective study. Each patient gave written informed consent to participate in the trial. Pathological TNM and tumor regression grade (TRG) were estimated. DCE-MRI analysis was performed by measuring SIS value before start and at the end of therapy as well as maximum SUV (SUVmax) by FDG-PET/CT. Non-parametric sample tests, ROC analysis and diagnostic performance were performed.

Results: Fifty-five patients (73.3%) with TRG 1-2 were classified as responders, while 20 subjects (26.7%) with TRG 3-4 were considered non responders. Assessment via ΔSIS reached a sensitivity of 92.7%, a specificity of 80.0% and an accuracy of 89.3% using a cut-off of 6.0% while ΔSUVmax reached a sensitivity of 67.3%, a specificity of 75.0% and an accuracy of 69.7% using a cut-off of 59.7%.

Conclusion: Pre-surgery assessment of CRT response by ΔSIS showed a higher predictive ability than ΔSUVmax in LARC, increasing sensitivity and negative predictive value. SIS percentage change could play a relevant role in LARC management improving the ability to identify complete pathological response, allowing for conservative strategy or for a “wait and see” policy, reducing significant morbidity and functional complications related to total mesorectal excision.

SS 12.5

Diagnostic accuracy of magnetic resonance imaging in predicting response to neoadjuvant therapy in patients with locally advanced rectal cancer

J. Munir, I. Niazi, R. Sayyed, S. Hasan Raza, M. Hussain, S. Khattak, A. Syed; Lahore/PK

Purpose: Magnetic Resonance Imaging of pelvis is the imaging modality of choice for preoperative staging in rectal cancer. We aim to look at the accuracy of MRI in evaluating response to neoadjuvant therapy.

Material and methods: Medical records of patients undergoing surgery for rectal cancer following neoadjuvant therapy at our institution in year 2014 were reviewed. Data was collected regarding T, N stage on MRI at presentation, after neoadjuvant therapy and on histopathology of resected specimen. Concordance of post-treatment MRI and histopathology was evaluated. Factors that might affect this concordance were assessed in univariate analysis.

Results: A total of 108 patients underwent surgery for rectal cancer after neoadjuvant therapy in 2013-14. Most of these had T3 or above tumor (97%) or nodal involvement (95%) on MRI at presentation. Post neoadjuvant therapy MRI scan was able to predict a negative circumferential resection margin, however it was not able to predict complete pathological response. The post treatment MRI scan couldn’t accurately differentiate T3-T4 tumors from T1-T2 tumors or node positive from node negative tumors. No specific factor could be identified to be significantly associated with this concordance. The diagnostic accuracy of MRI for predicting a negative CRM was 84.54%.

Conclusion: Although post treatment changes result in limitation of MRI to evaluate response to treatment, MRI shows acceptable diagnostic accuracy in predicting a negative circumferential resection margin.

11:00 - 12:30 **Forum Hall**

Scientific Session SS 13

Non-cirrhotic liver: focal lesions

SS 13.1

Liver MRI for colorectal cancer liver metastasis: comparative effectiveness research for the choice of contrast agents

N. Seo, M.-S. Park, K. Han, Y.E. Chung, J.-Y. Choi, J. Lim, M.-J. Kim, K.W. Kim; Seoul/KR

Purpose: To compare the diagnostic performance for evaluating hepatic lesions between gadoxetic acid-enhanced MRI (Gd-EOB-MRI) and MRI using extracellular contrast agent (ECA-MRI), and to determine whether the type of contrast agent affects early intrahepatic recurrence.

Material and methods: Between January 2005 and December 2010, 418 colorectal cancer patients who underwent both preoperative CT and liver MRI were retrospectively reviewed. Image interpretation was based on initial radiologic reports and all focal hepatic lesions were confirmed by pathology or follow-up imaging. The diagnostic performance was assessed by the area under the receiver operating characteristic curve (AUROC) and the rate of indeterminate lesions on each MRI. For patients who underwent curative liver surgery, early intrahepatic recurrence rate within 6 months were evaluated.

Results: Total 291 and 127 patients underwent Gd-EOB-MRI and ECA-MRI, respectively. In per-patient analysis, AUROCs of both MRI groups were not significantly different between Gd-EOB-MRI (0.990; 95 % confidence interval, 0.980-0.999) and ECA-MRI (0.985, 0.968-1.000) (P=0.836). The rates of indeterminate lesions on MRI were 6.98 % (30/430) for Gd-EOB-MRI and 4.88 % (10/205) for ECA-MRI, which did not reach significant difference (P=0.309). Early recurrence rate in ECA-MRI group (28.6 %) was significantly higher than that in Gd-EOB-MRI group (11. 6%) (P=0.031).

Conclusion: Gd-EOB-MRI and ECA-MRI showed comparable excellent diagnostic performance in colorectal cancer patients. Further study comparing survival outcome between Gd-EOB-MRI and ECA-MRI should be followed.

SS 13.2

Gd-EOB-DTPA-enhanced magnetic resonance imaging (MRI) for detecting colorectal hepatic metastases in patients who have not previously undergone treatment: a meta-analysis

Y. Liu[1], L. Li[2], Z. Huang[2], H. Tang[2], B. Song[2]; [1]Chongqing/CN, [2]Chengdu/CN

Purpose: To perform a meta-analysis to obtain the diagnostic value of gadoxetic acid (Gd-EOB-DTPA)-enhanced magnetic resonance imaging (MRI) for detecting colorectal hepatic metastases (CRLM) in patients who have not previously undergone treatment.

Material and methods: A comprehensive search was performed in databases including MEDLINE, EMBASE, and Cochrane Library for studies, published from January 2000 to December 2015, evaluating the diagnostic performance of Gd-EOB-DTPA-enhanced MRI in detecting CRLM. We determined sensitivities and specificities across studies, calculated positive and negative likelihood ratios, and constructed summary receiver operating characteristic curves.

Results: Across 7 studies (410 patients, 1809 hepatic metastases), the pooled sensitivity of Gd-EOB-DTPA-enhanced MRI for detecting CRLM was 0.94 (95% CI, 0.92-0.95), and the pooled specificity was 0.88 (95% CI, 0.86-0.91). Overall, the positive likelihood ratio was 8.22 (95% CI, 4.09-16.51), and the negative likelihood ratio was 0.07 (95% CI, 0.04-0.13). The area under the curve was 0.971. Also, among these studies, six of them combined Gd-EOB-DTPA-enhanced MRI with diffusion weighted imaging (DWI). The sensitivity and specificity of Gd-EOB-DTPA-enhanced MRI combined with DWI were 0.94 (95% CI, 0.92-0.95) and 0.91 (95% CI, 0.88-0.93).

Conclusion: Gd-EOB-DTPA-enhanced MRI has good diagnostic performance in the detection of CRLM. Moreover, DWI sequence combined with Gd-EOB-DTPA-enhanced MRI may improve the diagnostic accuracy of CRLM compared with Gd-EOB-DTPA-enhanced MRI alone.

SS 13.3

CAIPIRINHA-VIBE in contrast-enhanced MRI of focal liver lesions: impact on interobserver agreement in comparison with conventional VIBE sequences

D. Leithner, J.L. Wichmann, S.S. Martin, B. Bodelle, P. Dewes, A.M. Bucher, R.W. Bauer, S. Zangos, T. Vogl, M.H. Albrecht; Frankfurt am Main/DE

Purpose: To evaluate the effect of controlled aliasing in parallel imaging results in higher acceleration (CAIPIRINHA) sequences on image quality and interobserver agreement in contrast-enhanced volumetric interpolated breath-hold examination (VIBE) MRI of liver lesions in comparison with standard VIBE sequences.

Material and methods: Twenty-three patients underwent abdominal contrast-enhanced MRI on a 3-T system and were included in this intra-individual comparison study. Each patient underwent both CAIPIRINHA-VIBE and conventional VIBE within 3 months showing stable disease. The sequences were reviewed by two blinded radiologists (A+B) using a 5-point rating scale for liver lesions and affected segments and with regard to overall image quality and sharpness of intrahepatic vessels. Cohen's analysis and Wilcoxon matched pairs tests were performed.

Results: Superior interobserver agreement was observed for CAIPIRINHA-VIBE for both per-lesion and per-segment analysis (per-lesion, κ=0.18, $p<0.04$; per-segment κ=0.47, $p<0.01$) compared to conventional VIBE (per-lesion, κ=0.16, $p<0.03$; per-segment, κ=0.38; $p<0.001$). CAIPIRINHA-VIBE series received better scores (image quality: A=4.8, B=3.7; sharpness of intrahepatic vessels: A=4.2, B=3.7) compared to standard VIBE (image quality: A=4.0, B=3.0; sharpness of intrahepatic vessels A=3.5, B=3.0) from both reviewers ($p<0.01$).

Conclusion: CAIPIRINHA-VIBE sequences facilitate superior image quality and consequently improved inter-observer agreement regarding dignity and allocation of focal liver lesions compared to standard VIBE sequences.

SS 13.4

Liver metastases detection using sparsity-based learned dictionaries

E. Klang[1], A. Ben-Cohen[2], I. Diamant[2], E. Konen[1], H. Greenspan[2], M.-M. Amitai[1]; [1]Ramat Gan/IL, [2]Tel Aviv/IL

Purpose: Automatic liver lesions detection in CT examinations is an ongoing task for the computer vision community. Sparse classification has lately been proved to be powerful algorithms for data analysis. We evaluated sparse based learned dictionaries approach for the liver detection task.

Material and methods: This study included CT examinations of twenty patients with 68 metastases, segmented in 2D. The published SLIC algorithm was used to divide 2D liver images into 500 "super pixels". Each "super pixel" is a homogeneous region that includes neighboring pixels with similar Hounsfield units. Several features sets were extracted from each "super pixel" (grey level histogram, acutance and others), and using this features a dictionary of "super pixels" was created. Sparsisty classification was used to optimize the dictionary, limiting its number of words, creating "super pixels" groups of metastases, normal parenchyma, blood vessels and others, thus, effectively detecting the "super pixels" of metastases. The sensitivity and specificity of the sparse based approach were compared to that of the state of the art "random forests" classification algorithm.

Results: The sensitivity and specificity to detect liver metastases were 71% and 98% for the sparse based algorithm and 66% and 99% for the "random forests" algorithm.

Conclusion: Sparse based approach to detect liver metastases showed promising results in comparison to "random forests" algorithm, with better sensitivity but slightly worse specificity.

SS 13.5

Preoperative staging of colorectal liver metastases after chemotherapy: assessment with diffusion-weighted MR imaging and Gd-EOB-DTPA-enhanced MRI at 3T

P. Boraschi, F. Donati, L. Urbani, M. Castagna, F. Pacciardi, R. Gigoni, M.C. Della Pina, S. Salemi, D. Caramella, F. Falaschi; Pisa/IT

Purpose: To evaluate the diagnostic performance of diffusion-weighted MR imaging (DW-MRI) and Gd-EOB-DTPA-enhanced MRI at 3T-device in the preoperative staging of colorectal liver metastases in patients previously undergone chemotherapy.

Material and methods: Fifty patients with colorectal cancer and focal liver lesions underwent MR imaging at 3T-device (GE DISCOVERY MR750;GE Healthcare) after preoperative chemotherapy. After preliminary acquisition of axial T1w (in/out of phase) and T2w (propeller and SS-FSE) images, DW-MRI was performed using an axial spin-echo echo-planar sequence with multiple b-values (150,500,1000,1500 sec/mm^2) in all diffusion directions. Gd-EOB-DTPA-enhanced MRI was performed using a 3D breath-hold fat-suppressed T1w LAVA-flex sequence including both dynamic and hepato-biliary phase. MR images were reviewed by two observers in conference in order to detect and characterize (benign/malignant) focal liver lesions. MRI findings were correlated with surgery and histopathology, which was our gold standard. Only clear benign lesions at intraoperative ultrasound remained unresected. Statistical analysis was performed on a per-lesion basis.

Results: A total of 306 hepatic lesions were detected; of these, 220 were metastases (72%), whereas the remaining 86 (28%) were characterized as benign lesions (hemangiomas, cysts and nodular regenerative hyperplasia). The sensitivity, specificity, PPV, NPV and diagnostic accuracy of the reviewers for the detection and characterization of focal liver lesions were 98%,93%,97%,95% and 97%, respectively.

Conclusion: The combination of DW-MRI with Gd-EOB-DTPA-enhanced MRI at 3T-device is particularly effective in preoperative staging of colorectal liver metastases after chemotherapy.

SS 13.6

Hepatocellular carcinoma in non-fibrotic liver

M. Wagner[1], P.-A. Lampson[1], M. Ronot[2], G. Hayek[1], A. Bardier[1], V. Paradis[2], V. Vilgrain[2], O. Lucidarme[1]; [1]Paris/FR, [2]Clichy/FR

Purpose: To assess clinical and radiological patterns of hepatocellular carcinoma (HCC) in non-fibrotic liver.

Material and methods: Between 2007 and 2014, all resected HCC, in a non-fibrotic liver (METAVIR F<2), with preoperative CT/MRI, were retrospectively included. Demographics, clinico-biological and pathological data, including alpha-fetoprotein level, differentiation, and presence of steatosis/NASH were recorded. Images were analysed by 2 radiologists in consensus. Presence of an arterial enhancement, a portal or delayed washout, and a capsule were assessed.

Results: Forty-five patients (30 males, mean 60 yo), with 46 HCC (mean 10cm [1-30]) were included. Fourteen patients (31%) had abdominal pain, 3 (8%) a palpable mass and 3 (7%) a haemorrhagic syndrome. Alpha-fetoprotein was increased in 14 patients (31%). The liver was classified F0 and F1 in 24 (53%) and 21 (47%) patients. Significant steatosis and NASH were observed in 13 (29%) and 6 patients (13%). Eleven (24%), 32 (71%) and 2 (4%) tumors were well-, moderately, and poorly differentiated. One was completely necrotic. Forty-five HCC (98%) showed arterial enhancement, 40/46 (87%) showed a washout either on the portal venous or the delayed phases. A capsule was present in 61% (28/46). 40 HCC met the AALSD criteria and 39 were classified as LI-RADS 5.

Conclusion: At the time of diagnosis, HCC in non-fibrotic liver are large and show typical enhancement pattern in most cases.

SS 13.7

DWI in paediatric liver MRI

E. Petrash, E. Mikhaylova, D. Sevrjukov; Moscow/RU

Purpose: The purpose of this study was to find out whether apparent diffusion coefficient (ADC) can enable differentiation of benign and malignant focal liver lesions (FLL) in children.

Material and methods: 39 patients (male-22, female-17) with 66 FLL in total underwent MRI of the liver including DWI. The age of patients ranged from 5 months to 17 years. Inclusion criteria: the presence of newly diagnosed FLL, size of lesions more than 1 cm. Liver lesions were divided into benign (28) and malignant (38). Benign: focal nodular hyperplasia (7), regenerating nodules (11), haemangiomas (9), malignant-hepatoblastoma (15), hepatocellular carcinoma (4), cholangiocarcinoma (3), metastases (17). Diagnosis was confirmed histologically, by contrast-enhanced MRI (including hepatobilliary MRIcontrast agents) and using dynamic control (for benignFLL).

Results: It was found that malignant tumors in the liver have a lower ADC (1.038±0.185*10-3 mm2/sec) than benign (1.372±0.383*10-3 mm2/sec) (p=0.0000136). ADC of malignant FLL was in the range 0.838 – 1.223 * 10-3 mm2/sec, benign - 0.989-1.755 * 10-3 mm2/sec. It was suggested that FLL with ADC 0.989 * 10-3 mm2/sec and lower can be attributed to malignant, above 1.223 * 10-3 mm2/sec - benign. Neoplasms with ADC in the range of 0.989- 1.223 *10-3 mm2/sec should be additionally examined and needs morphological verification.

Conclusion: Though differences in mean ADC values of benign and malignant FLL were significant, confidence intervals indicate their large overlap, so ADC can't be the main differential diagnostic criterion. Analysis of DWI images can help in difficult diagnostic cases, but should only be used in conjunction with standard MRI, including contrast-enhanced MRI.

SS 13.8

Therapy response assessment of colorectal liver metastases after preoperative chemotherapy: diagnostic performance of diffusion-weighted MR imaging at 3T device

F. Pacciardi, F. Donati, P. Boraschi, M. Castagna, L. Urbani, R. Gigoni, D. Caramella, F. Falaschi; Pisa/IT

Purpose: To assess the value of diffusion-weighted MR imaging (DW-MRI) at 3T-device in evaluating therapy response of colorectal liver metastases after preoperative chemotherapy.

Material and methods: Our study group included thirty-two patients with colorectal liver metastases undergone MR imaging at 3T-device (GE DISCOVERY MR750; GE Healthcare) after preoperative chemotherapy. DW-MRI was performed using a spin-echo echo-planar sequence with multiple b-values (150,500,1000,1500 sec/mm^2), obtaining an ADC map. Fitted ADC values were calculated by two observers in conference for each liver lesion (more than 1 cm of diameter) drawing a ROI around the entire tumor and another one at the tumor periphery. All MRI findings were correlated with histopathology after surgery. Hepatic metastases were pathologically classified into three groups on the basis of tumor regression grading (TRG): MHR (major histological response,TRG 1-2), PHR (partial histological response,TRG 3), and NHR (no histological response,TRG 4-5). Statistical analysis was performed on a per-lesion basis.

Results: A total of 104 colorectal liver metastases were analyzed. MHR, PHR and NHR were observed in 18%, 38% and 44% of lesions, respectively. Periphery ADC value was significantly different in the three groups (p<0.01) and was significantly higher in MHR than in NHR (p<0.01). However, ADC value of the entire tumor was not significantly different in the three groups.

Conclusion: DW-MRI, using ADC map and value, can be useful to assess the efficacy of preoperative chemotherapy in colorectal liver metastases.

SS 13.9

Entropy from preoperative CT texture analysis: a potential imaging biomarker of early recurrence after resection of colorectal liver metastases

M. Kudzmaite[1], K.W. Brudvik[1], K. Skogen[1], A. Bethke[1], K.J. Labori[1], B. Ganeshan[2], J.B. Dormagen[1], A. Schulz[1]; [1]Oslo/NO, [2]London/GB

Purpose: To determine the value of entropy, a CT texture analysis (CTTA) parameter, for preoperative prediction of recurrence after resection of colorectal liver metastases (CRLM).

Material and methods: Forty-four patients who underwent resection of CRLM between 2007-2009 were retrospectively included and followed-up until December 2015. CTTA was performed of the largest CRLM on contrast-enhanced CT using a research software TexRAD. Entropy was evaluated with different spatial scale filters (ssf2-6) corresponding to fine to coarse textures. A chemo-naïve group (n=41) and a chemo-exposed group (n=20) were evaluated. TexRAD identified optimal threshold-values for entropy to divide the groups into poor/good prognosis. ROC and Kaplan-Meier/multivariate Cox analyses were performed.

Results: In the chemo-naïve group, the overall time-to-recurrence was 37.3 months and the threshold-value 4.9 (filter ssf2). Below the threshold-value the overall time-to-recurrence was 46.7 months and above 21.7 months (p=0.008). Sensitivity and specificity for recurrence was 54.2% and 82.4%, respectively (p=0.447). In the chemo-exposed group, the overall time-to-recurrence was 19.2 months and the threshold-value was 4.7 (filter ssf3). Below the threshold-value the overall time-to-recurrence was 33.1 months and above 5.2 months (p=0.007). Sensitivity and specificity for recurrence was 62.5% and 100%, respectively (p=0.001).

Conclusion: Entropy derived from preoperative CTTA may have the potential to predict early recurrence, especially in patients treated with preoperative chemotherapy. In practice, this may allow improved selection for resection or focused postoperative follow-up in high-risk patients.

SS 13.10

Assessment of portal venous phase in dual-energy CT of the liver: initial experience with multiple monoenergetic levels and advanced monoenergetic reconstructions

D. Caruso[1], C.N.N. De Cecco[1], A. Laghi[2], A. Schaefer[3], D. Sheafor[3], A.D. Hardie[3]; [1]Rome/IT, [2]Latina/IT, [3]Charleston, SC/US

Purpose: To assess Dual Source Dual-Energy CT (DECT) of the liver for image quality and diagnostic performance for liver lesions following intravenous contrast on the portal venous phase (PVP).

Material and methods: This prospective study included subjects who underwent PVP DECT for assessment of liver lesions. From this data, linear-blended (LB) poly-energetic equivalent datasets and multiple monoenergetic reconstructions from 40-190 keV were performed. Standard virtual monoenergetic images (VMI) and advanced image-based virtual monoenergetic images (VMI+) were performed. Quantitative and qualitative image quality were assessed. An assessment of diagnostic accuracy was performed against Magnetic Resonance, as a reference standard. Direct comparisons were assessed by using repeated measure of variance.

Results: In 29 subjects with 49 liver lesions, the highest peak CNR for liver parenchyma and hyper-vascular liver lesions was achieved for VMI+, although for hypo-vascular liver lesions both VMI+ and VMI had lower CNR than LB. However, qualitative image quality assessments revealed a higher diagnostic quality and also reader preference for VMI+ over LB or VMI. There was also a trend toward higher diagnostic performance and confidence with VMI+ over the other two reconstructions: 83.7 % on LB, 75.5 % on the best VMI keV level (75 keV), and 95.9% on the best VMI+ keV level (50 keV)

Conclusion: Low keV VMI+ may improve detection of liver lesions on PVP despite a lack of clear improvement in measured CNR for hypo-dense lesions.

11:00 - 12:30 **Meeting Hall V**

Scientific Session SS 14

Pancreas and biliary tree: imaging and intervention

SS 14.1

Autoimmune pancreatitis: MRI-MRCP characteristics

G. Avesani, R. Negrelli, E. Boninsegna, L. Frulloni, R. Manfredi, R.M. Pozzi Mucelli; Verona/IT

Purpose: To better delineate the MRI-MRCP findings in a large group of patients with AIP, as up to now the characteristics of autoimmune pancreatitis (AIP) have been evaluated on a restricted population.

Material and methods: We retrospectively evaluated the MR-MRCP performed before therapy in 112 patients diagnosed with AIP between 2001 and 2014. Image analysis included T1- and T2- signal intensity, DWI, pattern of enhancement, extra-pancreatic involvement and main pancreatic duct (MPD) characteristics.

Results: 61 patients showed a diffuse enlargement of pancreas and 51 patients demonstrated a focal pancreatic involvement. The affected parenchyma was hypointense on T1-WI in 110/112 (98.2%) patients, hyperintense on T2-WI in 77/112 (68.8%) and isointense in 30/112 (26,8%). DWI was available in 52 patients and showed restricted diffusion in 36/52 (69.2%). After contrast injection, during the pancreatic phase it appeared hypointense in 104/112 (92.9%). During the delayed phases, 95/112 (84.8%) patients showed delayed enhancement. The MPD was normal in 7/112 (6.3%) patients, while ductal narrowing was observed in 44/112 (39.2%) and complete stenosis in 61/112 (54.5%); multiple stenoses were detected in 51/105 (48.6%). Dilation of side-branch ducts was observed in 47/112 patients (42%). The median value of stricture length was 19 mm and of the caliber of upstream duct was 3 mm. Biliary involvement was observed in 32/112 (28.6%) patients and renal involvement in 23/112 (20.5%).

Conclusion: Our data confirm the characteristic pattern of AIP described in literature, although the prevalence of some findings are quite different from some other published papers.

SS 14.2

Focal and diffuse autoimmune pancreatitis: MRI-MRCP findings and comparison of focal-type of the head and of the body-tail

G. Avesani, R. Negrelli, E. Boninsegna, L. Frulloni, R. Manfredi, R.M. Pozzi Mucelli; Verona/IT

Purpose: To evaluate the MRI-MRCP findings of focal-type and diffuse autoimmune pancreatitis (AIP) and to compare, among focal-types, involvement of the head and the body-tail.

Material and methods: We retrospectively evaluated the MR-MRCP examinations performed before therapy in 112 patients with diagnosis of AIP. Image analysis included signal intensity on T1- and T2-WI, DWI, enhancement pattern, extra-pancreatic involvement and main pancreatic duct(MPD) characteristics.

Results: 61/112 (54.5%) patients had diffuse enlargement of pancreas and 51/112 (45.5%) focal involvement. The signal intensity of affected parenchyma on T1-WI, T2-WI and DWI was not significantly different. The lesions were hypointense in arterial phase (93.4% vs 92.2%) with delayed enhancement (88.5% vs 80.4%) (p=NS). During venous phase, 39.2% of focal-type and 14.7% of diffuse AIP showed hyperintensity (p=0.003). Prevalence of stenosis, side-branch involvement and extra-pancreatic disease did not differ significantly. The caliber of the upstream MPD was higher in focal-type (3.1 mm vs 2.4 mm, p=0.017). Among patients with focal AIP, 21/51 (41.2%) showed involvement of the head and 30/51 (58.8%) of the body-tail. In 42.8% of head involvement and in 16.7% of body-tail there was a multifocal stenosis of MPD (p=0,03); 42.8% and 16.7% respectively demonstrated stenosis of main bile duct (p=0.03). Caliber of upstream duct was higher in AIP of the head (4 mm vs 2 mm, p=0.03).

Conclusion: Focal-type AIP showed an earlier delayed enhancement and a greater dilation of upstream MPD. Head involvement demonstrated a higher frequency of multifocal stenosis of MPD and a greater caliber of it.

SS 14.3

Usefulness of three-dimensional magnetic resonance cholangiopancreatography with partial maximum intensity projection for diagnosing autoimmune pancreatitis

S. Yanagisawa, Y. Fujinaga, M. Maruyama, T. Muraki, M. Takahashi, A. Fujita, S. Fujita, M. Kurozumi, K. Ueda, H. Hamano, S. Kawa, M. Kadoya; Matsumoto/JP

Purpose: To evaluate the usefulness of 3D magnetic resonance cholangiopancreatography (MRCP) with/without partial maximum intensity projection (MIP) in patients with autoimmune pancreatitis (AIP).

Material and methods: 3D MRCP and endoscopic retrograde cholangiopancreatography (ERCP) images were retrospectively analyzed in 24 patients with AIP. Three types of pancreatic duct findings, length of the main pancreatic duct narrowing (NR-MPD), multiple skipped MPD narrowing (SK-MPD) and side branches arising from the narrowed portion of the MPD (SB-MPD) were evaluated on four sets of MRCP images, MIP with 5–7.5 mm (MIP5), 10–15 mm (MIP10), 72–90 mm thickness (full-MIP), and the three data sets combined (a-MIP) were scored using a three- or five-point scale. The scores in the four MRCP data sets were statistically analyzed, and the positive rate of each finding was compared in the MRCP data sets and ERCP.

Results: Scores on NR-MPD and SK-MPD did not differ significantly among the four MRCP data sets. However, full-MIP yielded a significantly lower score on SB-MPD than the other three data sets ($P < 0.05$). NR-MPD and SK-MPD positivity rates were higher in all MRCP data sets than in ERCP ($P < 0.05$), whereas the SB-MPD positivity rate was similar in three MRCP data sets, excluding full-MIP, and ERCP.

Conclusion: 3D MRCP shows NR-MPD and SK-MPD better than ERCP. Partial-MIP MRCP allows good evaluation of SB-MPD, comparable to ERCP.

SS 14.4

Type 1 and type 2 autoimmune pancreatitis: is there any difference in MRI?

R. Negrelli, G. Avesani, E. Boninsegna, L. Frulloni, R. Manfredi, R.M. Pozzi Mucelli; Verona/IT

Purpose: To evaluate the MRI-MRCP findings of autoimmune pancreatitis (AIP) to find radiological patterns which could differentiate type 1 and type 2 AIP.

Material and methods: 84 patients with AIP were included in this retrospective study, who satisfied ICDC criteria for type 1 (n=66) and type 2 (n=18) AIP and performed MR-MRCP before treatment. Image analysis included: signal intensity abnormalities, pancreatic enhancement, biliary and extrapancreatic involvement, main pancreatic duct (MPD) stenosis, presence of upstream MPD dilation.

Results: Pancreatic parenchyma resulted hypointense on T1-WI in 65/66 (98%) cases in type 1 and in 17/18 (94%) in type 2; hyperintense on T2-WI in 41/66 (62%) cases in type 1 and in 15/18 (83%) in type 2 (p=NS). The lesions were hypovascular in 64/66 (97%) cases in type 1 and in 16/18(89%) in type 2 with delayed contrast retention in 56/66 (85%) and in 17/18 (94%) respectively (p=NS). Autoimmune cholangitis was found in 29/66 (44%) patients with type 1 AIP and in 3/18 (16%) with type 2 (p=0,02); renal involvement was found in 20/66 (30%) and 1/18 (6%) respectively (p=0,02). The mean number of stenoses was 1,8 in type 1 AIP and 1,4 in type 2 (p=NS). Mild dilation of the upstream MPD was significantly more frequent in type 1 AIP than in type 2 (p=0,01).

Conclusion: MR-MRCP is useful to detect extra-pancreatic involvement, typically seen in type 1 AIP. The presence of a mild dilation of the upstream MPD suggests type 1 AIP.

SS 14.5

Role of imaging for procedural risk factor assessment in post-ERCP iatrogenic pancreatitis

Z. Verdina, M. Radzina, L. Skrule; Riga/LV

Purpose: To analyze post ERCP iatrogenic pancreatitis risk factors related to invasive procedure parameters by imaging.

Material and methods: We retrospectively studied 677 patients post ERCP from January 2014 to December 2015. Out of selected patients 143 were scanned by CT or MRI after the procedure due to alterations in clinical and laboratory data. Procedural ERCP parameters (manipulation time, ductus choledochus size, papillotomy, contrast and basket usage, balloon dilatation) were correlated to radiological criteria to assess their role in development of pancreatitis.

Results: After ERCP procedure 143 patients were scanned by CT or MRI (21.1%), 86 were female (60.1%) and 57 male (39,9%) with median age 63 ±13.85 years. Iatrogenic pancreatitis diagnosis was proved for 11 patients (7.7%): 8 patients with 3 times elevated serum alpha amylasis ($p<0.001$) and leucocytosis ($p<0.003$), 10 patients had specific radiological signs (edema, infiltration, ascites) and 2 patients had lethal outcome. We found no correlation between ductus choledochus enlargement, procedure time and iatrogenic pancreatitis (p=0.72). We found significant statistical difference between contrast use ($p<0.001$), cannulation ($p<0.001$), basket use ($p<0.004$) and papillotomy ($p<0.001$) in the development of pancreatitis, but there was no significant risk found with stent placement and balloon dilatation (p=0.41).

Conclusion: Imaging may provide additional value in detection of post ERCP iatrogenic pancreatitis. Main procedural risk factors for development of complications are basket and contrast usage, cannulation and papillotomy.

SS 14.6

Are PanIN pancreatic lesions detectable with imaging? A retrospective study upon 99 MRI

L. Menassa[1], T. Ibrahim[1], V. Vilgrain[2], M.-P. Vullierme[2]; [1]Beyrouth/LB, [2]Clichy/FR

Purpose: To retrospectively find imaging signs of PanIN on abdominal CT scans and MRIs of patients being operated on.

Material and methods: 2 independent reviewers, blind to the diagnosis, reviewed retrospectively a series of 99 operated pancreas for NET (n=44, 14 of them having fatty pancreas), solid and pseudopapllary tumor (n=16), and IPMN (n=39), 77% having PanIN at pathology (only one patient having PanIN 3). All patient had an MRI including 2D MRCP, 74 having performed also a CT. Parameters included parenchymal abnormalities (Fibrous foci), and presence of microcyst (<5mm, without communication with pancreatic duct).

Results: Concordance Kappa between reviewers was 0.71. Among elementary findings, microcyst detection by MRI was the only factor found to have a significant discriminatory capacity for PanIN detection with specificity 92.16%, sensitivity 26.9 %, NPV 21.56% and PPV 94%. Furthermore in the head of the pancreas such pattern had an AUC of .651, and p = 0.04. The others signs studied at MRI had no statistical value and CT revealed no significant pattern. One weakness of our study was the very few patients with PanIN 3.

Conclusion: Presence of microcysts detected with MRI could be associated with PanIN 1 or PanIN 2 lesions. These results are to be used with caution, as the consequence of such diagnosis, including patients with family history of pancreas adenocarcinoma, are not established.

SS 14.7

Biliary strictures after orthotopic liver transplantation: can Gd-EOB-DTPA-enhanced 3T MR cholangiography provide additional information?

S. Salemi, P. Boraschi, F. Donati, R. Gigoni, M.C. Della Pina, F. Pacciardi, D. Caramella, F. Falaschi; Pisa/IT

Purpose: To determine whether Gd-EOB-DTPA-enhanced 3T MR Cholangiography may provide additional information in the evaluation of biliary strictures after orthotopic liver transplantation.

Material and methods: Fifty-two liver transplant patients with clinical-echographical suspicion of biliary strictures underwent MR imaging at 3T device (GE-DISCOVERY MR750; GE Healthcare). After acquisition of T1w/T2w images and conventional T2-weighted MR Cholangiography (image set 1), a 3D T1-weighted fat-suppressed LAVA sequence was performed before and 20-120 minutes after intravenous administration of 10 ml Gd-EOB-DTPA (Primovist®, Bayer HealthCare) (image set 2). The diagnostic value of Gd-EOB-DTPA-enhanced MR Cholangiography in the assessment of biliary strictures was tested by separate analysis results of image set 1 alone and image set 1 and 2 together. MRI results were correlated with direct cholangiography, surgery and/or clinical-radiological follow-up.

Results: The level of confidence in the assessment of biliary anastomotic and non-anastomotic strictures was significantly increased by the administration of Gd-EOB-DTPA ($p<0.05$). Particularly, contrast-enhanced T1-weighted LAVA sequences tended to out-perform conventional T2-weighted MR Cholangiography in the visualization of the extra-hepatic biliary system and in the grading and extension of non-anastomotic strictures. Functional information provided by Gd-EOB-DTPA biliary excretion was especially helpful in patients previously undergoing biliary-enteric anastomosis with not or poorly dilated biliary system.

Conclusion: Gd-EOB-DTPA-enhanced MR Cholangiography may improve the level of diagnostic confidence provided by conventional T2-weighted MR Cholangiography at 3T device in the evaluation of biliary strictures in liver transplant recipients.

SS 14.8

Biliary stricture: benign or malignant? Percutaneous transhepatic intraductal biopsy for differentiation

D. Frantsev, M.A. Shorikov, O. Sergeeva, E. Virshke, V. Panov, E. Moroz, O. Chistyakova, B. Dolgushin; Moscow/RU

Purpose: The majority of biliary strictures are attributed to bile duct malignancy. Surgical exploration is usually performed for exception of benign conditions. Pictorial essay of percutaneous transhepatic intraductal biopsy (PTIB) assessment in biliary stricture differentiation is the point of the paper.

Material and methods: Since 2007 224 patients have undergone percutaneous transhepatic biliary drainage (PTBD) for obstructive jaundice causing by biliary strictures without evident periductal mass lesion. PTIB was performed in all cases. Biopsy devices (brush and forceps) were delivered to biliary stricture through thin-walled tube (9-10 Fr) inserted in the biliary drainage channel. Histology and cytology studies of obtained material were performed. The PTIB was repeated at least three times in cases of non-neoplastic pathologist findings.

Results: Ten out of 224 patients (4.5%) demonstrated absence of malignancy in the obtained by PTIB tissue. The following diagnostic work-up identified the nature of non-neoplastic biliary strictures: IgG4-related cholangiopathy in 4, dominant stricture in primary sclerosing cholangitis in 2, biliary papillomatosis in 1, penetrating to hepatoduodenal ligament duodenal ulcer causing biliary stricture in 1, cicatrical biliary strictures of unknown aetiology in 2 patients, respectively. Nobody required surgical exploration. In 8 cases specific treatment was performed followed by patient status improvement. Biliary drainages were removed in 3 patients.

Conclusion: Biliary neoplastic–mimicking lesions still remain diagnostic dilemma frequently require unnecessary surgery. PTIB is easy and effective intervention differentiating benign and malignant biliary strictures without surgery.

SS 14.9

Bile leaks after hepatic surgery and liver transplantation: usefulness of Gd-EOB-DTPA-enhanced MR cholangiography

S. Salemi, P. Boraschi, F. Donati, R. Gigoni, F. Pacciardi, D. Caramella, F. Falaschi; Pisa/IT

Purpose: To determine the usefulness of Gd-EOB-DTPA-enhanced MR cholangiography in the diagnosis of bile leaks after hepatic surgery and liver transplantation.

Material and methods: Twenty-six patients with previous hepatic resection (n=16) or liver transplantation (n=10) underwent MRI at 1.5T/3T-device due to strong suspicion of bile leak, based on a combination of clincal, laboratory and imaging findings. After acquisition of axial T1w/T2w images and conventional MRC (thin-slab 3D FRFSE and thick-slab SSFSE T2w sequences), a 3D fat-suppressed LAVA sequence was performed before, 20 minutes and between 25 and 120 minutes after intravenous administration of 10ml Gd-EOB-DTPA (Primovist®, Bayer HealthCare). Two radiologists in conference evaluated all the images for the presence or absence of bile leak, and its location when present. Imaging results were correlated with direct cholangiography, percutaneous drainage of fluid collection and/or imaging follow-up.

Results: A well-defined collection containing extravasated Gd-EOB-DTPA was detected in 11 out of 26 patients (one false negative case on MRI). Gd-EOB-DTPA enhanced MRC yielded an overall sensitivity of 92%, specificity of 100% and accuracy of 96% for the diagnosis of an active bile leak. The sensitivity of 20 minutes delayed MR images was 42%.

Conclusion: Gd-EOB-DTPA-enhanced MR cholangiography utilizing delayed phase images is a highly reliable technique for the detection of active bile leaks after liver transplantation and hepatic surgery. The images acquired 25-120 minutes after injection significantly increased the dentification of leakages.

SS 14.10

CT and MR findings in xanthoganulomatous cholecystitis: retrospective analysis of pathologically proven 30 cases - tertiary care experience

B. Sureka, V.P. Singh, S. Rajesh, K. Bansal, C. Bihari, A. Rastogi, S.K. Sarin; New Delhi/IN

Purpose: To study the CT and MR findings in histopathologically confirmed cases of xanthoganulomatous cholecystitis - masquerader of gallbladder carcinoma. Approach to management of these two entities differ and so the outcome. Preoperative imaging diagnosis can help the treating surgeons plan their treatment accordingly.

Material and methods: Retrospective analysis of histpathologically confirmed 30 cases of xanthoganulomatous cholecystitis was done (17-CECT; 13-MR). The following features were analysed-wall thickness, intramural nodules,pericholecystic fat stranding, pattern of wall thickness, THAD,fat within the gallbladder wall, cholelithiasis, infiltration into adjacent structures, biliary dilatation, lymph nodes, complications.

Results: Discontinuous mucosal lining was seen in 22 (73.3%) and continuous mucosal lining in 8 cases. Discontinuous mucosal lining was seen in 100% cases with wall thickness >10mm and this was statistically significant (p=0.03). Diffuse wall thickening was seen in 23, focal 3 and polyploidal in 2 cases. Cases which showed polyploidal thickening had coexisting carcinoma gallbladder. Intramural nodules were present in 87.5% cases with discontinuous mucosal lining. Pericholecystic fat stranding was seen in 19. Biliary dilatation was seen in 12, liver infiltration in 13 and intramural fat in 7 cases. 4 cases showed drop in signal in the intramural nodules on out-of-phase image.

Conclusion: Coexistence of five features - diffusely thickened wall, wall thickness > 3mm, intramural hypodense nodule, discontinuous mucosal lining, cholelithiasis may suggest xanthoganulomatous cholecystitis. Correlating with the pathophysiology, we conclude that discontinuous mucosal lining is not so uncommon in xanthoganulomatous cholecystitis especially with delayed hospital presentation.

11:00 - 12:30 **Chamber Hall**

Scientific Session SS 15

Colon: new imaging perspectives

SS 15.1

Computer-aided detection for CT colonography: an evaluation of the optimal reader paradigm using evidence-based medicine methodology

C.E. Redmond, D. Malone, S.J. Skehan; Dublin/IE

Purpose: Computer-aided detection (CAD) software for CT colonography (CTC) interpretation, which can be used in various reader paradigms, is widely available. The aim of this project was to establish the optimal reader paradigm in terms of per-polyp sensitivity (≥ 6mm) and reporting time, based on the current best available evidence.

Material and methods: Evidence-based medicine (EBM) methods were used to retrieve and appraise studies published on the use of CAD for CTC. Appraisal was performed using the Oxford Centre for Evidence Based Medicine (CEBM) tools for diagnostic studies.

Results: No studies were retrieved from the secondary literature. From the primary literature, 9 relevant studies were identified, analysed and ranked in a "hierarchy of evidence". When compared to unassisted interpretation, using CAD as a second reader was associated with a higher per-polyp sensitivity (77.1% vs. 81.5%, respectively, p=0.001). Using CAD as a concurrent reader has a statistically significant shorter reporting time (p <0.001) and equivalent per-polyp sensitivity when compared to CAD as a second reader. The use of CAD as a first reader is controversial, however it appears to have similar per-polyp sensitivity levels.

Conclusion: The best current evidence indicates that CAD for CTC as a second reader results in higher per-polyp sensitivity when compared to unassisted interpretation (grade B recommendation). Using CAD as a concurrent reader is more time efficient and has a similar sensitivity (grade C recommendation).

SS 15.2

Participation to sequential fecal immunochemical test of non-responders to CT colonography and colonoscopy in a randomized screening trial (SAVE)

L. Sali[1], M. Mascalchi[1], L. Ventura[1], M. Falchini[1], S. Delsanto[2], A. Borgheresi[1], G. Gabbani[1], G. Grazzini[1], G. Scarpini[1], M. Zappa[1]; [1]Florence/IT, [2]Turin/IT

Purpose: To evaluate if sequential invitation to fecal immunochemical test (FIT) might improve participation in colorectal cancer screening in subjects refusing CT colonography (CTC) or colonoscopy as primary tests.

Material and methods: Citizens of a district of Florence, Italy, aged 54-65, were allocated (8:2.5:2.5:1) with simple randomization to be invited by mail to one of four screening interventions: 1) biennial FIT for 3 rounds; 2) reduced preparation CTC (r-CTC); 3) full preparation CTC (f-CTC); 4) optical colonoscopy (OC). Non-responders to r-CTC, f-CTC and OC were invited to FIT, realizing a combined strategy (r-CTC+FIT, f-CTC+FIT, OC+FIT). Outcome was participation rate.

Results: 16087 randomized subjects were invited to the assigned screening test. Participation rates were 50.4% (4677/9288) for first-round FIT, 28.1% (674/2395) for r-CTC, 25.2% (612/2430) for f-CTC, and 14.8% (153/1036) for OC. Participation rates to sequential FIT were 20.2% (347/1721) in non-responders to r-CTC, 21.4% (389/1818) in non-responders to f-CTC, and 25.8% (228/883) in non-responders to OC. Overall participation rates to combined screening strategy were 42.6% (1021/2395) for r-CTC+FIT, 41.2% (1001/2430) for f-CTC+FIT and 36.8% (381/1036) for OC+FIT, compared to 50.4% (4677/9288) for first-round FIT alone. All differences between groups were significant (p<0.01), but not between r-CTC+FIT vs. f-CTC+FIT (p=0.32).

Conclusion: Sequential invitation to FIT catches up at least one-fifth of non-responders to screening CT colonography or colonoscopy.

SS 15.3

Colorectal cancer outcomes in a large negative CT colonography screening cohort

D.A. Mccomiskey, K. Mckay, E. Sala; St. John's, NL/CA

Purpose: Computed tomography colonography (CTC) is an efficient method for detecting overt colorectal cancer, serving as a viable alternative to colonoscopy. This study conducts an average 6.63 year follow-up of patients undergoing CTC. Those receiving negative results were followed for the occurrence of incidental colorectal cancers, allowing for the determination of CTC screening efficacy and providing valuable and practical data for the assessment of current colorectal cancer screening guidelines.

Material and methods: Negative CTC screening patients (n=509) in the Newfoundland & Labrador Eastern Health system over a 15-month period were included. A comprehensive electronic medical record review was undertaken, encompassing provider, colonoscopy, imaging, and histopathology reports. Subjects were also cross-validated through the Newfoundland Cancer Clinic Registry Database. Incident colorectal cancers were recorded.

Results: The study population (n=509) was followed for an average of 6.63 years. One incident colorectal adenocarcinoma represented a crude cancer incidence of 0.31 cancers per 1000 patient years, and a rate of 0.2% following a normal CTC.

Conclusion: Colorectal cancer presenting clinically is rare in the 6.63 years following a negative CTC screen, suggesting CTC is an equally effective method for colorectal screening compared to OC. These results also indicate that the 6 mm threshold for clinically significant polyps in CTC is appropriate. Furthermore, current guidelines recommending interval CTC screening every 5 years is conservative, and interval screening can be recommended over a longer time period.

SS 15.4

Bowel preparation in CT colonography: is diet necessary? (DIETSAN) A randomized trial

D. Bellini, D. De Santis, T. Biondi, R. Ferrari, M. Rengo, A. Laghi; Latina/IT

Purpose: To investigate whether diet restriction affects the quality of colon cleansing during reduced bowel preparation for CT colonography.

Material and methods: This pragmatic single-centre randomized trial recruited asymptomatic and symptomatic patients aged 45 years or older and referred by clinicians for CT colonography. Patients were randomly assigned in a 1:1 ratio, in block of ten, to receive a reduced bowel preparation with diet restriction or the same reduced bowel preparation without diet restriction. All investigators were masked to treatment allocation. The primary endpoint, analyzed by ITT, was a composite of indices describing the quality of large bowel cleansing.

Results: 100 patients were randomly allocated to treatments (50 with diet restriction; 50 without diet restriction) and were included in intention-to-treat analysis. Six patients withdrew consent, leaving for analysis 46 assigned to reduced bowel preparation with diet restriction and 48 assigned to reduced bowel preparation without diet restriction. The mean residual stool (0.22 of three, 95%CI 0.00-0.44) and fluid burden (0.39 of three, 95%CI 0.25-0.53) scores for patients underwent diet restriction were similar to those for patients did not follow any diet restriction (0.25, 95%CI 0.03-0.47 [P = .82] and 0.49, 95%CI 0.30-0.67 [P = .38], respectively). Both bowel preparations resulted in optimal colon cleansing. Serious adverse events were absent.

Conclusion: A reduced bowel preparation in association with faecal tagging and without any diet restriction demonstrated optimal colon cleansing effectiveness for CT colonography.

SS 15.5

Straight to test CT colonography in the English two-week wait cancer referral system for investigation of symptomatic patients

J.A. Stephenson, J. Mullineux, B. Billimoria, S.L. Jepson, V. Shah, R. Verma, K. Mulcahy, M. Elabassy; Leicester/GB

Purpose: Due to the over-whelming burden on local colonoscopy services for bowel cancer exclusion we developed a straight to test pathway for patients with iron deficiency anaemia (IDA) and change in bowel habit (CIBH). Referrals from both primary and secondary care with a local population of one million attend directly for CTC with subsequent triage to cancer services or return to referrer dependent on findings.

Material and methods: We aim to present information on the referral pathway, inclusion and exclusion criteria, in built quality assurance mechanisms, reporting proformas, report outcome codes and initial results from prospective audit – to include pathway times, cancer detection, polyp detection and incidental findings.

Results: The first 2 months have seen >400 referrals, 31% for IDA and 66% for CIBH, with 58% females and a mean age of 72. 78% of referrals are from primary care. Referral to scan has a mean time of 12 days, with scan to report taking 2 days. There has been a 9% patient non-attendance rate. Colon cancer diagnosis rate is 5%, with 10% polyp, 4% non-colon cancer and 5% significant incidental finding detection rate. 3% rate of diverticulitis and 43% rate of diverticulosis.

Conclusion: We believe this is the first straight to test CTC service in the UK for symptomatic patients and initial results of this streamlined pathway are promising.

SS 15.6

Conspicuity of important extracolonic pathology at CT colonography without intravenous contrast enhancement

M. Thorley[1], A. Bandara[2], S. Fernando[1], J. Nanayakkara[2], H. Stunell[2], D. Boone[2]; [1]Norwich/GB, [2]Colchester/GB

Purpose: To evaluate conspicuity of important extracolonic pathology at low dose, unenhanced CT colonography.

Material and methods: Two experienced GI radiologists retrospectively reviewed 808 contrast-enhanced CT colonography (CTC) studies carried out on symptomatic patients between 20/10/2011-19/10/2014. Both observers categorised extracolonic findings according to C-RADS criteria and discrepancies were resolved by consensus. For all patients with likely important extracolonic findings (C-RADS E4), histopathological and clinicoradiological outcomes were established by querying relevant databases and examining case-notes. For all patients with confirmed important pathology identified at contrast-enhanced CTC, the low-dose, pre-contrast, prone acquisitions were re-read by a resident, blind to the contrast-enhanced imaging, reports, outcomes and study purpose. Results were compared to the reference standard and descriptive statistics produced.

Results: In total, 94 (12%) studies were classified C-RADS E4, for which follow-up data were available for 87 (median 24 months; range 14-48). One patient refused investigation and 6 had died. 24 were ultimately considered incorrectly classified (12 metastatic disease from colorectal primary; 12 pre-existing pathology). Of 46 potential new extracolonic cancers, 29 were benign; of the 17 confirmed malignancies, 100% were identified at unenhanced CT. Of 7 aortic aneurysms and 10 further important, non-neoplastic findings, all were conspicuous on the pre-contrast acquisition.

Conclusion: All important extracolonic pathology was demonstrated at review of the low-dose, unenhanced CTC studies. The clinical benefit, cost efficacy and safety of routine iodinated contrast enhancement at CTC requires further evaluation.

SS 15.7

CT colonography: a tool to determine favorability for complete optical colonoscopy?

L. Sammut, N. Bonanno, P. Ellul, K. Micallef; Msida/MT

Purpose: CT colonography (CTC) is extremely valuable in patients who had an incomplete colonoscopy. Our aim was to assess the anatomical factors predictive of an incomplete/failed conventional colonoscopy based on CTC findings.

Material and methods: Patients who had undergone a CTC between January 2015 and December 2015, in which the indication was an incomplete colonoscopy, were evaluated retrospectively. The examinations were reviewed by a gastrointestinal radiologist and the parameters assessed were age, gender, total colon length, tortuosity of the colon (that is the number of acute angle flexures), extensive diverticular disease, previous surgery, presence of strictures, adhesions and hernias.

Results: 60 patients (mean age 62.6 years) were recruited. The majority, 68.3%, were females. Mean colon length was 176.6cm; mean number of acute angle flexures was 10.4. Extensive diverticular disease was present in 55% of patients. This was found mainly in the descending and sigmoid colon. 10% of the patients had previous abdominal or pelvic surgery. Colonic strictures were present in 8.3% of patients. 1.67% had adhesions secondary to endometriosis, 1.67% had a spigelian hernia containing a loop of sigmoid colon and 1.67% had large bowel malrotation.

Conclusion: By assessing certain anatomical features, CTC can be used as a tool to determine favorability for performing a complete colonoscopy. This factor is especially important when optical colonoscopy is required as to provide a histological diagnosis.

SS 15.8

Polyp detection rates at CT colonography progressively reduce during the day and over the course of a reporting session

M. Almarashi, A. Plumb, G. Bhatnagar, S.A. Taylor, S. Halligan; London/GB

Purpose: To determine if (a) time of day and (b) number of cases reported each day affects the detection rate of 6mm+ polyps and cancers at CT colonography (CTC).

Material and methods: Single centre retrospective study (January 2013-August 2015) of 1766 CTC examinations reported by one of four radiologists. Each report was categorised as positive or negative for 6mm+ polyps/cancer. The time of day at which the report was issued was extracted from the hospital Radiology Information System (RIS), as was the number of CTC reported by each radiologist on that particular day. Logistic regression models were constructed to assess the statistical significance of (a) time of day and (b) number of prior cases reported that day by a given radiologist on 6mm+ polyp/cancer detection.

Results: The detection rate of 6mm+ polyps/cancer dropped from 20.6% (for scans reported between 08:00am and 09:00am) to only 15.3% (for the 17:00pm to 18:00pm period), p=0.048. The detection rate also progressively declined over the course of a reporting session (from 22.2% to 15.3%, p=0.0123). Radiologists reporting their first CTC study on a given day had a detection rate of 22.5% whereas later scans had progressively lower detection, falling to 10.8% by their 5th scan of the day (p=0.0013).

Conclusion: Detection rates at CTC progressively decline during the day (mirroring previous findings for colonoscopy), raising the possibility of clinically significant reporting fatigue for radiologists.

SS 15.9

Diagnostic performance of MR imaging in local staging of primary colon cancer patients

E. Nerad[1], M.J. Lahaye[2], D.M.J. Lambregts[3], E.L.J. Kersten[1], H.C.M. Van Den Bosch[1], F.C.H. Bakers[3], G.L. Beets[2], H. Grabsch[3], R.G.H. Beets-Tan[2]; [1]Eindhoven/NL, [2]Amsterdam/NL, [3]Maastricht/NL

Purpose: Currently the FOXTROT trial is investigating the benefits of neo-adjuvant treatment for colon cancer. Imaging plays a crucial role, selecting patients for neo-adjuvant treatment. CT shows a questionable performance. Although MRI is standard in rectal cancer staging, only one small study is published concerning colon cancer staging with MRI. Therefore the aim of this study was to evaluate the diagnostic performance of MRI for staging of colon cancer.

Material and methods: 55 colon cancer patients underwent MRI(1.5T; T2TSE/DWI) of the abdomen and were retrospectively analysed by two blinded, independent readers and compared with histopathology after resection, evaluating; invasion through bowel wall (T3/T4 tumours), invasion beyond bowel wall of ≥5mm and/or invasion of surrounding organs(T3cd/T4), serosal involvement, extramural vascular invasion(EMVI) and malignant lymph nodes(N+). Inter-observer agreement was compared using Kappa(κ) statistics.

Results: The sensitivity/specificity detecting T3/T4 tumours (35/55), T3cd/T4 tumours (15/55), fascia involvement (8/55), EMVI (17/55) and nodal involvement (19/55) for reader 1 were; 91%/84%, 40%/88%, 88%/74%, 100%/62% and 47%/86% and for reader 2: 72%/89%, 60%/75%, 75%/72% 88%/70% and 68%/64% respectively. Interobserver agreement between both readers were good to moderate: 0.72, 0.55, 0.62, 0.60 and 0.60 respectively.

Conclusion: MRI seems to be able to select high-risk colon cancer patients with a good sensitivity for tumour invasion through the bowel wall, EMVI and serosal involvement. Together with its well-known superiority in detecting/characterizing liver lesions, MRI might become the most optimal primary staging modality for colon cancer.

SS 15.10

Clinical impact of MRI vs computed tomography in the diagnostic work-up of colon cancer patients

M.J. Lahaye[1], D.M.J. Lambregts[1], E. Nerad[2], G.L. Beets[1], F.C.H. Bakers[3], R.G.H. Beets-Tan[1]; [1]Amsterdam/NL, [2]Eindhoven/NL, [3]Maastricht/NL

Purpose: Traditionally, colon cancer patients are mainly staged with CT. However, MRI is superior to CT for detecting hepatic disease. Preliminairy reports indicate that MRI is able to stage colon tumors and as such may replace CT for integrated local and liver staging. Aim of this study was to evaluate the clinical impact of replacing CT for MRI in abdominal staging of colon cancer patients.

Material and methods: Sixty colon cancer patients were included: 30 underwent abdominal CT (including 4-phase liver scan) and 30 patients underwent abdominal MRI (including 4-phase liver sequences and DWI). Both groups were retrospectively assessed regarding: primary tumour stage, presence of liver metastases and the need for additional imaging in inconclusive results. Histology/clinical/imaging follow-up was the reference standard.

Results: All colon tumors (100%) were detected and staged in both groups. 4/30 patients in the CT-group and 3/30 in the MRI-group presented with liver metastases at primary staging; 2 additional patients from the CT-group developed metastases within 1 year (versus none in the MRI group). In the CT-group 8/30(27%) had inconclusive results concerning hepatic disease; in 5/8 patients additional imaging was performed in the MRI group no inconclusive results occurred and no additional imaging was needed.

Conclusion: Simultaneous staging of hepatic disease and the colon tumor with MRI is feasible and has a clear clinical impact. As such MRI could become a valuable integrated staging tool for colon cancer.

11:00 - 12:30 **Meeting Hall IV**

Scientific Session SS 16

Abdominal imaging: new post processing techniques

SS 16.1

Optimization of the window/level settings for virtual monoenergetic imaging in dual-energy CT of the liver: a multi-reader evaluation of standard monoenergetic and advanced imaged-based monoenergetic data-sets

C.N.N. De Cecco[1], D. Caruso[2], A. Laghi[3], D. Sheafor[1], A. Schaefer[1], A.D. Hardie[1]; [1]Charleston/US, [2]Rome/IT, [3]Latina/IT

Purpose: To evaluate the optimal window settings for displaying and reading virtual monoenergetic reconstructions in third-generation dual-source, dual-energy computed tomography (DECT) of the liver.

Material and methods: Twenty-nine subjects with liver lesions were prospectively evaluated with DECT in the arterial (AP) and portal venous (PVP) phases. Three reconstructed datasets were calculated: standard linearly-blended (LB120), 70-keV standard monoenergetic (M70), and 50-keV advanced image-based virtual monoenergetic (M50+). Two readers determined the optimal window (width and length, W/L) settings and the mean of their assessment was defined as the optimal W/L setting. The optimal settings for each reconstruction were then used for a blinded assessment of liver lesions.

Results: The optimal W/L settings for M50+ were significantly higher for both the AP (W=429.3±44.6HU, L=129.4±9.7HU) and the PVP (W=376.1±14.2HU, L=146.6±7.0HU) than for LB120 (AP, W=215.9±16.9HU, L=82.3±9.4HU; p<0.001) (PVP, W=173.4±8.9HU, L=69.3±6.0HU; p<0.001) and M70 (AP, W=247.1±22.2HU, L=72.9±6.8HU; p<0.001) (PVP, W=232.0±27.9HU, L=91.6±14.4HU; p<0.001). Use of the optimal window settings for M50+ vs. LB120 resulted in higher sensitivity for liver lesion detection (AP, 100% vs. 86%; PVP, 96% vs. 63%).

Conclusion: Application of optimized window settings results in improved liver lesion detection rates in advanced image-based virtual monoenergetic DECT when customized for arterial and portal venous phases.

SS 16.2

CT Perfusion for early response assessment after radiofrequency ablation of focal liver lesions

H.P. Marquez Masquiaran, G.D. Puippe, T. Pfammatter, R.P. Mathew, H. Alkadhi, M.A. Fischer; Zurich/CH

Purpose: To evaluate the feasibility and diagnostic performance of perfusion-CT (P-CT) for early assessment of treatment response in patients undergoing radiofrequency ablation (RFA) of focal liver lesions.

Material and methods: 20 patients (14men; mean age 64±14) undergoing RFA due liver metastases (N=10) or HCC (N=10), were prospectively included. P-CT was performed within 24 hours after RFA. Two readers determined arterial-liver-perfusion (ALP,mL/min/100mL), portal-venous-perfusion (PLP,mL/min/100mL) and hepatic-perfusion-index (HPI,%) in all 20 lesions by placing a freehand volume-of-interest (VOI) in the necrotic central (CZ), transition (TZ) and surrounding parenchymal (PZ) zones. Patients were classified in responders (no residual-tumor) and non-responders (residual/progressive-tumor) using imaging follow-up with contrast-enhanced CT or MRI after a mean of 139±70 days. Prediction of treatment response was evaluated using receiver-operating-characteristics.

Results: Mean ALP/PLP/HPI of both readers was 4.89/15.44/61.25 for the CZ, 9.98/16.88/66.35 for the TZ and 20.70/29.09/61.87 for the PZ. Interreader agreement of HPI was good for the CZ (ICC=0.875) and the TZ (ICC=0.857) zone, and high for the PZ (ICC=0.920). For both readers there was significant difference in PVP/HPI of the CZ and HPI of the TZ (all, P<0.03) between responders and non-responders. HPI of the TZ showed the highest area under the curve (0.90) for prediction of residual tumor, suggesting a cut-off value of 73%.

Conclusion: Increased arterial perfusion of the transition zone assessed directly after RFA might be an early biomarker for residual tumor/tumor recurrence in patients with focal liver lesions.

SS 16.3

CT with 3D reconstruction for planning of staged "in situ split" hepatectomy (ALPPS)

A. Kaprin, N. Rubtsova, D. Sidorov, L. Petrov, M. Lozhkin, A. Isaeva, K. Puzakov; Moscow/RU

Purpose: To evaluate the role of CT volumetry with 3D liver reconstruction in planning of ALPPS for liver malignancies.
Material and methods: Volumetric measurements of FLR using CT with 3D liver reconstruction were obtained in pre- and post-first stage of ALPPS. CT scans were performed with a 80-section Aquilion PRIME Toshiba MS scanner, with 1 mm slice thickness, reconstruction interval 0,5mm, pitch factor 1.8, voltage 120 kV, 100 mA, tube rotation time 0.35 s. As a CT-contrast agent we used omnipack 350 (Iohexol) 200 ml, injection speed 5 ml/s. We used standard liver multiphase bolus contrast enhancement program. The circumscribed areas were then automatically multiplied by the CT section thickness, yielding an approximate volume for each liver section, and the volumes of all sections were summed to give the selected liver volume. The critical minimum FLR has been estimated to be approximately 25-30% in normal liver, and 35-40% in liver after chemotherapy.
Results: Between January 2013 and September 2015 in 15 patients FLR ratio were < 26%, determining the indication for ALPPS. CT scans were performed on postoperative day 8, after liver transection and portal vein ligation. All patients have had significantly increases in FLR (195,1%) and extended right hepatectomies were successfully performed in all cases.
Conclusion: CT-volumetry with 3D reconstructions allows to increase the safety of major liver resections for primary and metastatic liver cancer.

SS 16.4

Is a CT unique portal phase enough for causal diagnosis of non traumatic abdominopelvic emergencies?

G. Herpe, M. Verdier, G. Vesselle, J.P. Tasu; Poitiers/FR

Purpose: Computed tomography (CT) is widely used in the management of acute non traumatic abdominal emergencies (ANTAE). The aim of this study is to evaluate if a reduced CT protocol including a unique portal phase (Pp) is as accurate than a protocol including pre-contrast and post-contrast phases (Pc).
Material and methods: A retrospective study included adults undergone pre-contrast and post-contrast abdominopelvic CT for ANTAE was conducted. Suspected haemorrhagic and/or ischemic disease were excluded. Two blind CT readings were carried out, one using only Pp, the second all phases of the Pc. In case of reading discrepancy, a third reading was performed, by an abdominal imaging expert. The final diagnosis obtained by consulting the clinical report of the patient was considered as the gold standard for the diagnosis. Total radiation dose was compared for each CT protocol.
Results: 196 patients were included. There was no statistically significant difference in term of diagnosis between Pp and Pc (concordance ratio 98.5%; CI95% = 95.6% - 99.7%). Three errors due to an inappropriated protocol were observed (1.5%), Two of them were related to biliary tract obstruction causes. The use of single portal phase led to a 61% decrease of the global radiation dose.
Conclusion: Using a single portal phase in cases of ANTAE, CT accuracy remains the same and radiation dose decreases by 61%. Precontrast phase should be nevertheless added in suspicious biliary tract pathologies.

SS 16.5

Prognostic significance of PET texture analysis in oesophageal cancer staging

K.G. Foley, B. Berthon, C. Parkinson, C. Marshall, W.G. Lewis, E. Spezi, S.A. Roberts; Cardiff/GB

Purpose: Texture analysis is a rapidly evolving field, in which potentially significant additional prognostic data are extracted from radiological staging investigations. This study aims to determine the prognostic significance of PET texture variables when incorporated into a model predicting overall survival in patients with oesophageal cancer (OC).
Material and methods: Consecutive OC patients were staged with PET/CT between October 2010 and December 2014. PET-defined tumour variables were obtained using PET-STAT, software developed and written in the Matlab-based open source software CERR (Computational Environment for Radiotherapy Research). The tumour was outlined with ATLAAS, a learning algorithm for optimised automatic segmentation developed at Cardiff University. A Cox regression model, stratified by treatment and including age, TNM stage, tumour length (TL) and 12 novel texture variables, including Entropy (a measure of the uniformity of grey-levels derived from a histogram) was developed. Primary outcome measure was overall survival (OS).
Results: 264 patients [median age 67 (range 38-83), 196 adenocarcinoma, 198 male] were included. Multivariate analysis demonstrated three variables that were significantly and independently associated with OS; Age (HR 1.028, 95% CI 1.010 - 1.046, p=0.002), SUVmax (HR 1.000, 95% CI 1.000 - 1.000, p=0.011) and Entropy (HR 0.157, 95% CI 0.042 – 0.585, p=0.006).
Conclusion: Age, SUVmax and Entropy are important prognostic indicators in OC. This study demonstrates the additional benefit of texture analysis in OC staging compared to the current TNM system.

SS 16.6

Can CT histogram texture analysis help in the differential diagnosis between pancreatic neuroendocrine tumours and pancreatic metastasis of kidney clear cell carcinoma?

N. Cardobi, G.A. Zamboni, F. Lombardo, M.C. Ambrosetti, R.M. Pozzi Mucelli; Verona/IT

Purpose: To evaluate the differences at CT histogram texture analysis between pancreatic neuroendocrine tumours (PNETs) and pancreatic metastasis of renal clear cell carcinoma (PMRCCCs).
Material and methods: We selected 28 patients (15 PNETs and 13 PMRCCCs) with a CT with baseline and arterial phase scans, and histologically proven lesions. The DICOM files of each patient were loaded in a texture analysis freeware software (MaZda 4.6), then lesions were selected by manually drawing a Region of Interest (ROI). Since lesions were not always clear on unenhanced CT, ROIs were drawn on the arterial CT scan and then copied to the unenhanced CT. Mean, variance, skewness and kurtosis histogram values were extracted for each ROI in both unenhanced and enhanced CT images. Mean and standard deviation were calculated for each parameter and an unpaired t-test was used to compare PNETs and PMKCCCs.
Results: No significant difference was observed between PNETs and PMRCCCs for all the analyzed parameters, both for the unenhanced and arterial phases. Kurtosis and skewness extracted from the unenhanced CT phase showed a trend to significance (respectively p = 0.056 and p = 0.072).
Conclusion: From our preliminary results, a differentiation between PNETs and PMRCCCs by means of CT histogram texture analysis parameters does not appear feasible.

SS 16.7

Multi-slice accelerated EPI diffusion-weighted imaging versus conventional diffusion-weighted imaging in the upper abdomen: influence of acceleration factor on image quality

C.S. Reiner, B.K. Barth, L. Filli, D. Kenkel, M. Piccirelli, A. Boss; Zurich/CH

Purpose: To optimize a diffusion-weighted (DWI) echo-planar-imaging (EPI) sequence capable of simultaneous multi-slice (SMS) excitation in liver and pancreas regarding acquisition time (TA), signal-to-noise ratio (SNR), and image quality (IQ).

Material and methods: Ten volunteers underwent DWI of the upper abdomen in a 3T MR-scanner with an 18-channel body-coil. A SMS-DWI sequence using blipped CAIPIRINHA technique (b-values 0/50/400/800 s/mm2, acceleration factors (AF) 2 and 3) was compared to a standard EPI (AF1). Three schemes were evaluated: (i) reducing TA, (ii) keeping TA identical with increasing averages, (iii) increasing number of slices with identical TA. All acquisition schemes were evaluated qualitatively (IQ) and quantitatively (SNR).

Results: In scheme (i), no differences in SNR were observed (p=0.321-0.038) with reduction in TA from 5:23min to 2:55min (AF2, increase in SNR/time 75.6%) and 2:14min (AF3, increase SNR/time 102.4%). Comparable image quality was obtained for AF1 and AF2, whereas AF3 resulted in image degradation. No improvement in SNR was obtained in scheme (ii). Increased SNR/time could be invested in acquisition of more and thinner slices (30 slices, 5mm; 40 slices, 4mm; 50 slices 3mm) without significant reduction in SNR (p=0.083-0.702). Image quality scores were stable for AF2 but decreased for AF3.

Conclusion: SMS-DWI of the liver and pancreas provides substantially higher SNR/time, which may be used for shorter scan time or higher slice resolution. Optimum acceleration factor is AF2 as higher acceleration results in increased artifacts.

SS 16.8

The 3D Bag of Visual Words (3D-BoVW) algorithm for classification of liver lesions

E. Klang[1], I. Diamant[2], A. Ben-Cohen[2], E. Konen[1], H. Greenspan[2], M.-M. Amitai[1]; [1]Ramat Gan/IL, [2]Tel Aviv/IL

Purpose: To evaluate the improved performance of 3D-BoVW over the typical-BoVW algorithm for automatic classification of liver lesions in multi-phase CT images.

Material and methods: This study included multi-phase CT images of 134 liver lesions: 22 cysts, 35 metastases, 32 hemangiomas, 16 FNH and 29 HCC (2011-2013). Radiologist circumscribed the lesions margins in one slice per CT phase (2D). The typical-BoVW algorithm classifies images by treating image-features as “words in a dictionary”. Images are divided to small patches (“words”), and “dictionaries” are created, that are used to classify new lesions. In multiphase CT studies, dictionaries are built from each phase. Our 3D-BoVW algorithm is a refinement of the typical-BoVW. Instead of using data from only one slice in each phase, as was done before, the 3D-BoVW automatically propagates the 2D segmentation of each lesion in the z-direction to several neighboring slices, thus, extending data to 3D. Sensitivity and specificity of the 3D-BOVW and the typical-BoVW were compared.

Results: The 3D-BoVW showed an overall improvement of sensitivity from 71.6% to 76.1% and specificity from 91.9% to 93.4%, compared to the typical-BoVW. Best performances were shown for hemangioma (sensitivity from 62.5% to 81.3%) and FNH (sensitivity from 56.3% to 68.8%).

Conclusion: Extending BoVW classifier from 2D to 3D showed promising results in the multi-phase CT liver lesions classification task. Implementation of this algorithm in other medical imaging problems should be considered.

SS 16.9

Fusion of real-time ultrasonography with CECT by navigation system for CECT indeterminate focal liver lesions

H. Petrasova, J. Foukal; Brno/CZ

Purpose: Aim was to find out, if fusion of US and CECT,in patients with indeterminate focal liver lesion by navigation system, is a feasible method and to calculate statistic analysis of fused US/CECT in determination of lesions’ etiology.

Material and methods: Prospective study has covered 30 indeterminate hypoattenuating liver nodule found on CECT. Fused real-time US/CECT was performed within the same day by navigation system Percunav. Reconstructed images of CECT- porto-venous phase, slice thickness 2mm, were used as a data source for the fusion. Registration process for seeing fused images was done manually (3 points match). US was performed with 1-5MHz probe. All US modes were used in area of interest (B-mode, color Doppler, power Doppler, CEUS- application of 2.4 ml of sulfur hexafluoride intravenously). The biological nature of all lesions was proved in time by follow up (for period at least 1 year).

Results: The fusion of US with CECT was possible in all our patient with high spatial accuracy. All lesions were detectable in fused US, determination of nature was based on features in all US modes. Statistic analysis of our data brings following results: sensitivity of fused US/CECT on regard of the evaluation of malignant etiology was 83%, specificity 100%, PPV 100%, NPV 96%, AAC 96,67%.

Conclusion: The navigation systems for ultrasound represent News in radiology. We have found fusion of US/CECT very helpful, feasible, just slightly operator depended and highly accurate.

SS 16.10

Metal implants on CT: comparison of iterative reconstructions algorithms for reduction of metal artifacts with single energy versus spectral CT scanning in a phantom model

J. Fang, D. Zhang, B. Heidinger, V. Raptopoulos, A. Brook, O.R. Brook; Boston, MA/US

Purpose: To assess single energy metal artifact reduction (SEMAR) and spectral energy metal artifact reduction (MARS) algorithms in reducing artifact generated by different metals.

Material and methods: Phantom was scanned with and without SEMAR (Aquilion One, Toshiba) and MARS (Discovery CT750 HD, GE), with various metal implants. Images were evaluated objectively by measuring standard deviation and subjectively by two independent reviewers grading on a scale of 0 (no artifact) to 4 (severe artifact). Reviewers graded new artifacts introduced by metal artifact reduction algorithms.

Results: SEMAR and MARS significantly decreased variability of the density measurement adjacent to the metal implant, with median SD (standard deviation) of 52.1HU without SEMAR, vs. 12.3HU with SEMAR, p<0.001. Median SD without MARS of 63.1HU decreased to 25.9HU with MARS, p<0.001. Median SD with SEMAR is significantly lower than with MARS (p=0.0011). SEMAR improved subjective image quality with reduction in overall artifacts grading from 3.2±0.7 to 1.4±0.9, p<0.001. Improvement of overall image quality by MARS has not reached statistical significance (3.2±0.6 to 2.6±0.8, p=0.088). There was introduction of artifacts introduced by metal artifacts reduction algorithm for MARS with 2.4±1.0, but minimal with SEMAR 0.4±0.7, p<0.001.

Conclusion: CT iterative reconstruction algorithms with single and spectral energy are effective in reduction of metal artifacts. Single energy algorithm provides better image quality than spectral CT algorithm. Spectral metal artifact reduction algorithm introduces mild to moderate artifacts in the far field.

11:00 - 12:30 **Panorama Hall**

Scientific Session SS 17

Contrast media: optimising abdominal protocols

SS 17.1

High concentration (400 mgI/mL) versus low concentration (320 mgI/mL) iodinated contrast media in multi detector computed tomography of the liver: comparison between 100 kV and 120 kV acquisition protocol

S. Picchia, M. Rengo, D. De Santis, D. Bellini, D. Caruso, A. Laghi; Latina/IT

Purpose: To compare Iodixanol 320mgI/mL and Iomeprol 400mgI/mL in terms of liver enhancement in MDCT at 100kV and 120kV.

Material and methods: 110 patients were prospectively randomized into three groups. Group A received 637.5mgI/kg LBW of Iodixanol 320 and images were acquired at 120kV. Group B received 637.5mgI/kg LBW of Iodixanol 320 and images were acquired at 100kV. Group C received 750mgI/kg LBW of Iomeprol 400 and images were acquired at 120kV. Attenuation values were measured on pre-contrast and portal-venous phase. Contrast Enhancement Indexes (CEI) were calculated subtracting basal densities from post-contrast acquisitions. Means were compared with paired T-test. A blinded independent reader evaluated image quality.

Results: Mean CEIs for groups A, B and C were respectively 49.37, 58.04 and 54.55 HU. Liver enhancement achieved injecting Iodixanol320 was significantly higher at 100kV compared to 120kV (P=0.0369). Liver enhancement achieved injecting Iodixanol320 at 100 and 120kV was not significantly different from that achieved injecting Iomeprol400 at 100 and 120kV, respectively (P=0.4183 and P=0.0526). No significant differences were observed in terms of image quality among the three groups.

Conclusion: Similar liver enhancement values were observed injecting a lower amount of Iodixanol 320 compared to the ones achieved injecting Iomeprol 400. Values were even more similar when images obtained at 100kV with Iodixanol 320 were compared to the ones obtained at 120kV with Iomeprol 400 with no significant differences in terms of image quality.

SS 17.2

Iodine quantification in an ex-vivo calf liver model with simulated lesions using a single source dual energy CT (ssDECT) and three segmentation methods: inter-reader agreement and reproducibility.

A. Agostini, U. Mahmood, D. Ryan, P. Sawan, L. Mannelli; New York, NY/US

Purpose: To evaluate inter-reader agreement and reproducibility of iodine quantification using a single source dual energy CT (ssDECT) and three segmentation methods on an ex-vivo animal model.

Material and methods: A radiologist manually injected different volumes of Iohexol 300 mgI/ml in ten chicken sausages and inserted them in two calf livers, recording injected volumes and positions. Livers were scanned 7 times with a GE Discovery CT750HD (80/140kVp, 260 mA, 0.984 pitch, 0.7s rotation time, and 2.5mm slice thickness). Three other radiologists, blinded to iodine injected and sausage positions, segmented the sausages with three methods (manual, semi-automatic segmentation, and fixed threshold) by using a GE AW VolumeShare 5; iodine concentrations were calculated on iodine (-water) images. The estimated and injected iodine quantities were compared with Bland-Altman plots. Inter-reader agreement and reproducibility were calculated with intra-class correlation coefficients.

Results: 8 sausages were injected with a total of 1590mg of iodine; two sausages were excluded because of macroscopic iodine leakage. Mean errors of estimated iodine quantities were -2.76mg (-2.73%), -3.73mg (-3.27%), and -2.62mg (-2.67%) for manual, semi-automatic segmentation, and fixed threshold. Inter-reader agreements were respectively 0.9998, 0.9951, and 0.9883, while intraclass correlation coefficients among 7 scans were 0.9993, 0.9977, and 0.9999 respectively for the three segmentation methods.

Conclusion: ssDECT has high inter-reader agreement and reproducibility in iodine quantification.

SS 17.3

Contrast media protocol optimization in MDCT of the liver: advantages of using a bioimpedance device

S. Picchia, M. Rengo, D. Caruso, D. Bellini, D. De Santis, A. Laghi; Latina/IT

Purpose: To compare two different approaches to the quantification of CM volume for MDCT of the liver, in a population of patients with high (>30) BMI, one using nomograms and the second using a bioimpedance device.

Material and methods: 9 patients were prospectively randomized into two groups. In Group A LBW was calculated using nomograms while in Group B using a bioimpedance devices. In both groups patients received 750mgI per Kg of LBW of iodinated contrast medium. Attenuation values were measured on pre-contrast and portal-venous phase. Contrast Enhancement Indexes (CEI) were calculated sottracting basal densities from post-contrast acquisitions. Means were compared with Paired T-test. Image quality was evaluated by a blinded independent reader.

Results: The average amount of iodine administered in group A (41,9g) was significantly higher (p=0,04) than in group B (35,91g). Mean CEIs of the liver in portal-phase for groups A and B were respectively 66,09HU and 58,6HU. A significant greater portal-enhancement of the liver was observed in group A (p=0,03). No significant differences were observed in terms of image quality among the three groups.

Conclusion: In patients with high BMI (>30) a significant higher liver enhancement was achieved using a bioimpedance device for the quantification of CM volume. The use of nomograms for the calculation of LBW in high BMI patients determine an underestimation of the adequate amount of iodine needed to obtain a proper liver enhancement.

SS 17.4

Incidence of acute transient dyspnea (ATD) after administration of gadoxetic acid (EOB) in liver magnetic resonance imaging

L. Grazioli[1], R. Faletti[2], G. Battisti[3], B. Frittoli[1], P. Fonio[2]; [1]Brescia/IT, [2]Turin/IT, [3]Spoleto/IT

Purpose: The aim of the study was the evaluation of the incidence of ATD after administration of EOB and its correlation with motion artifacts during arterial phase.

Material and methods: Two hundred fifty consecutives patients who underwent liver MRI with EOB were prospectively analyzed with multi-arterial CAIPIRINHA algorithm. The incidence of ATD and the breath impairment were evaluated either after the saline flush and the MR scan procedure using a specific questionnaire and a breath hold registration (PACE system). Quality of the images was evaluated with a semiquantitative five-point scale by three different radiologists.

Results: PACE system alterations were recognized in 16/250 patients (6%). Incomplete breath-hold at the end of arterial phase was reported on specific questionnaire in 11/16 patients. Acute transient dyspnea, in agreement with PACE system and questionnaire, was identified in 2/250 patients (0,8%). Motion artifacts are present in 51/250 (20%) and increase from first and second phase to the third in both different administration (saline flush and EOB) using CAIPIRINHA multi-arterial phase technique. Inter-observer concordance by three radiologists was good (k=0.78 with Choen test).

Conclusion: Incidence of ATD after EOB administration was significantly lower than previously reported by literature. Motion-related artifacts incidence increased during third phase independently by saline or EOB administration.

SS 17.5

Gadoxetic acid-enhanced MRI for visual assessment of graft dysfunction in liver transplant recipients

D. Tamandl, N. Bastati-Huber, A. Wibmer, H. Einspieler, S. Poetter-Lang, A. Ba-Ssalamah; Vienna/AT

Purpose: To evaluate whether a qualitative visual scoring system, using specific features of gadoxetic acid-enhanced MRI, could be applied to estimate graft function and survival probability after orthotopic liver transplantation (OLT).

Material and methods: 85 patients, 31 females (36.5%) and 54 males (63.5%) with a median age of 54.6 years were examined on a 3 Tesla MR. Gadoxetic acid was administered using a bolus injection of 0.025 mmol/kg at 1 mL/sec. Dynamic imaging, including a 20 minute hepatobiliary phase (HBP), was subsequently performed. Two readers independently analyzed the unenhanced and HBP-enhanced MR images qualitatively. The degree of parenchymal contrast enhancement (enhancement quality score [EnQS]), biliary excretion (excretion quality score [ExQS]) as well as the persistence of signal intensity (SI) in the portal vein on the HPB (portal vein sign quality score [PVsQS]) was assessed. A quantitative measurement on the unenhanced and HBP-enhanced images was performed as well, to measure the relative liver parenchymal enhancement (RLE) at 20 minutes. Kaplan-Meier survival estimates and Cox proportional hazard regression models was used to calculate the probability of graft survival.

Results: The inter-reader agreement for the qualitative assessment of EnQS, ExQS, PVsQS was very good (k: 0.81). Univariate and multivariate survival analysis showed that the EnQS, ExQS, and PVsQS were independently associated with the probability of graft survival, respectively.

Conclusion: Qualitative assessment using gadoxetic acid enhanced-MRI allows us to estimate graft survival probability after OLT.

SS 17.6

The liver-to-spleen enhancement difference normalized by phantoms (LSED_NP20): a new signal intensity-based index for hepatocellular uptake function of the liver easily available in clinical practice using Gd-EOB-DTPA-enhanced MR imaging

A. Yamada[1], Y. Fujinaga[1], Y. Kitou[1], A. Nozaki[2], Y. Iwadate[2], T. Suzuki[1], D. Komatsu[1], K. Ueda[1], M. Kadoya[1]; [1]Matsumoto/JP, [2]Hino/JP

Purpose: To clarify an optimal signal intensity-based index for hepatocellular uptake function of the liver using Gd-EOB-DTPA-enhanced MR imaging (EOB-MRI).

Material and methods: Consecutive 34 patients with chronic liver diseases who underwent EOB-MRI using Differential Sub-sampling with Cartesian Ordering (DISCO) pulse sequence were enrolled in this prospective study. Plastic bottle phantoms containing several concentrations of contrast media diluted by normal saline were scanned together in order to evaluate contrast enhancement quantitatively. The estimated concentration of Gd-EOB-DTPA in hepatocytes at heaptobiliary phase (eCi20) was determined from compartment model analysis of normalized signal intensities of abdominal aorta, portal vein, and the liver on dynamic EOB-MRI. Previously reported signal intensity-based clinical indices for hepatocellular uptake function, such as the liver-to-spleen contrast ratios (LSC_20) and the normalized liver-to-spleen contrast ratios (LSC_N20), and newly proposed index, the liver-to-spleen enhancement difference normalized by phantoms (LSED_NP20) were obtained from signal intensities of the liver and spleen on hepatobiliary phase of EOB-MRI. The correlation between eCi20 and these indices were statistically evaluated.

Results: Correlation coefficients and its 95% CIs between eCi20 and signal intensity-based clinical indices for hepatocellular uptake function were as follows: LSC_20, r = -0.19 (-0.44, 0.13); LSC_N20, r = 0.23 (-0.25, 0.59); and LSED_NP20, r = 0.90 (0.80, 0.95).

Conclusion: LSED_NP20 is an optimal signal intensity-based index for the hepatocellular uptake function of the liver easily available in clinical practice using EOB-MRI.

SS 17.7

Gadoxetic acid enhanced MR imaging of transient hepatic perfusion disorder: another cause of hypointense observation on hepatobiliary phase

C. Torrisi, D. Picone, M. Midiri, G. Brancatelli; Palermo/IT

Purpose: To describe MR imaging features of transient hepatic perfusion disorders (THPD) in the hepatobiliary phase (HBP) of gadoxetic acid-enhanced MR imaging.

Material and methods: Gadoxetic acid-enhanced MR imaging of 125 patients (91 males; mean age: 68 years; range 26-82 years) with THPD were retrospectively reviewed. 105/125 patients had chronic liver disease. Three readers evaluated in consensus intensity of THPD on HAP and HBP and evolution at follow up. In cases of patients with multiple THPD, largest lesion was selected as being representative for each patient. Fisher's exact test was used for statistical analysis.

Results: THPD were hypervascular on HAP (125 of 125;100%) and hypointense on HBP (17 of 125;14%). Hypointense THPD were observed in patients with previous loco-regional treatment of adjacent tumors (either RFTA, PEI or TACE: n=13), peripheral portal venous branch thrombosis (n=1), biliary obstruction (n=1), previous surgery (n=1), cryptogenic (n=1). Of 108 patients with isointense THPD,63 were cryptogenic, 40 had previous locoregional treatment or were adjacent to hemangioma (n=4) or metastasis (n=1). At Fisher's exact test, hypointense THPD on HBP was associated with previous locoregional treatment (p<0,05). Of seven patients with hypointense THPD who had follow-up MR (range: 3-15 months; mean 7 months), six showed reduction in size.

Conclusion: A hypointense THPD on HBP was observed in 14% of patients, and it was associated with previous locoregional treatment of adjacent tumor.

SS 17.8

Gadolinium-based contrast agent (GBCA) in rectal MRI: could patient care be enhanced?

M. Corines[1], S. Nougaret[2], M. Weiser[1], J.L. Fuqua Iii[1], M.J. Gollub[1]; [1]New York, NY/US, [2]Montpellier/FR

Purpose: To assess if GBCA, including dynamic contrast enhancement (DCE-MRI) changes (1) radiologic stage at baseline (BL) or post neoadjuvant treatment (PNT) MRI and (2) treatment plan

Material and methods: This IRB approved, retrospective study analyzed 100 rectal MRIs from Dec. 2011 to Jan. 2015. Subjects operated by the surgical co-author or with distant metastases were excluded. Two radiologists independently re-interpreted MRI unfamiliar to them. Cases were assessed without (C-) then with GBCA (C+) for tumor stage and location. Differences were analyzed using Student's T-test. Interpretations were presented with clinical histories to 1 experienced surgeon blinded to GBCA use for treatment assessments. Management differences were analyzed descriptively.

Results: With GBCA, T-down-staging occurred in 16% and 4% and T-upstaging in 8% and 4% of BL and PNT, respectively. Mean distances (cm) from tumor to the anorectal junction, anal verge and mesorectal fascia C- and C+ at BL were not statistically different, but were statistically smaller at PNT. Seventeen baseline discordant treatment assessments, included 5 appropriate to changed T-stage and 12 unexplained by radiologic differences. Three PNT cases recommended a different operation despite unchanged radiologic assessment.

Conclusion: In this unique evaluation of GBCA including DCE-MRI in rectal cancer, tumor stage infrequently changed, and did so more often at baseline; resulting in down-staging. Most discrepancies in recommended treatment were unrelated to radiologic stage and may reflect clinical equipoise in rectal cancer management.

SS 17.9

Contrast-enhaced ultrasonography in the evaluation of incidental focal liver lesions: a cost-effective study for three years

M. Šmajerová, T. Andrasina, H. Petrasova; Brno/CZ

Purpose: The purpose was to find out whether contrast-enhanced ultrasonography (CEUS) is a cost-effective method for the first line evaluation of focal liver lesions (FLL) compared to CT and MRI.

Material and methods: The retrospective study included 1058 patients with incidental FLL, examined using CEUS in three years. Where CEUS results were not conclusive, CT or MRI was performed. Some patients with malignant findings on CEUS had additional CT for staging. The costs of this strategy were calculated. Other calculations show potential savings compared to costs if all the patients had been examined by CT or MRI after initial native ultrasound.

Results: The costs for evaluation of these lesions by CEUS (+ additional examinations) were CZK 1,624,314 (approx. €63,600) for three years. If CT or MRI had been used instead it would have been CZK 1,888,255 (€74,000) and CZK 5,141,971 (€200,000), respectively. CEUS was CZK 263,941 (€10,300) (13.98 %) cheaper compared to CT and CZK 3,517,657 (€138,000) (68.41 %) cheaper compared to MRI for all three years together. The average difference in price between CEUS and CT or MR for a year was CZK 87,980 (€3,500) and CZK 1,172,552 (€46,000), respectively.

Conclusion: Costs for evaluation of FLL by CEUS were slightly lower than CT. CEUS is a much more cost-effective method compared to MRI.

SS 17.10

Early clinical experience in the management of post-operative lymphatic leakage using lipiodol lymphangiography and two additional glue embolization techniques

S. Hur; Seoul/KR

Purpose: To evaluate the safety and efficacy of lipiodol lymphangiography and two additional embolization techniques using glue (N-butyl cyanoacrylate) for the management of postoperative lymphatic leakage.

Material and methods: This study included patients with post-operative lymphatic leakage who were referred to the interventional radiology department of two tertiary referral centers for Lipiodol lymphangiography from August 2010 to December 2015. Lipiodol lymphangiography was performed for both diagnostic and therapeutic purposes. Additional embolization using glue was performed as needed using two different techniques: 1) lympho-pseudoaneurysm embolization and 2) lymph node embolization. The safety and efficacy of these techniques were determined.

Results: All 18 patients underwent successful lymphangiography. Fifteen patients were observed for the therapeutic effect of lymphangiography and 7 (47%) recovered without further embolization. Nine patients, including 3 patients who underwent embolization immediately after lymphangiography and 6 patients whose conditions did not respond to lymphangiography, underwent 7 lympho-pseudoaneurysm and 4 lymph node embolizations. The clinical success rate of additional embolization was 89% (8/9) and the overall clinical success rate was 83% (15/18). The median time from initial lymphangiography to recovery was 5.5 days. No major complication related to these procedures were reported other than transient leg edema in 3 patients, all of which could be managed conservatively.

Conclusion: Lipiodol lymphangiography and the two additional embolization techniques using glue are safe and effective for the management of post-operative lymphatic leakage.


European Society
ESGAR
Gastrointestinal and Abdominal Radiology

L

M

N

O

P

European Society
ESGAR
Gastrointestinal and Abdominal Radiology

JUNE 20-23

ESGAR 2017

ATHENS
GREECE

European
Society
of Gastrointestinal
and Abdominal
Radiology

www.esgar.org